CRITICAL REGION BEHAVIOR AND EFFECT OF PRESSURE ON LIQUID VISCOSITY

By

DAVID DUANE MCCOY

Bachelor of Science
Oklahoma State University
Stillwater, Oklahoma
1971

Master of Science
Oklahoma State University
Stillwater, Oklahoma
1973

Submitted to the Faculty of the Graduate College
of the Oklahoma State University
in partial fulfillment of the requirements
for the Degree of
DOCTOR OF PHILOSOPHY
May, 1976

CRITICAL REGION BEHAVIOR AND EFFECT OF

PRESSURE ON LIQUID VISCOSITY

Thesis Approved:

R. N. Maddox
Thesis Adviser

J. K. Norton

John H. Erbar

H. J. Harris

N. D. Durham
Dean of the Graduate College

PREFACE

The effect of transport properties (viscosity, surface tension, density and thermal conductivity) on engineering design calculations has been recognized by the hydrocarbon processing industries and chemical engineers, in general (39). However, the behavior of transport properties under varying conditions of temperature, pressure and composition is only partially understood. Data and predictive correlations are needed to understand the behavior of these properties. An important correlating parameter for liquid viscosity is the critical viscosity. This study presents critical viscosity data for several pure liquids and mixtures.

The effect of pressure on liquid viscosity has been widely studied. However, few researchers have examined the effect by placing compressed gases in intimate contact with the test fluid. This phenomenon was studied at isothermal conditions using hydrogen, helium, nitrogen, argon and methane in contact with n-octane and n-octanol.

I am indebted to Professor R. N. Maddox for the advice and assistance he has provided while serving as my thesis adviser. The entire Faculty of the School of Chemical Engineering has provided assistance in many forms to aid my research and professional development.

The financial assistance provided by the School of Chemical Engineering, Fluid Properties Research, Inc. and the Phillips Fellowship were greatly appreciated.

I wish to thank my family for their encouragement and advice during my years of graduate study. Very special thanks to my wife, Pat, for all the extra duties she performed, in my stead, during this period in our lives.

TABLE OF CONTENTS

LIST OF TABLES

LIST OF FIGURES

LIST OF SYMBOLS

English Letters

F_c	- flow flux through curved tube
F_s	- flow flux through straight tube
g	- acceleration of gravity, cm/sec^2
g_c	- gravitational constant, 32.1740 (lb_m/lb_f) (ft/sec^2)
h	- height of liquid, cm
h_{f_c}	- head loss for sudden contraction of piping
h_{f_e}	- head loss for sudden expansion of piping
K	- viscometer constant, centistokes/sec
K'	- single flow variable
L	- length of capillary tube, cm
L_e	- entrance length, in
m	- mass, gm
P	- pressure, lb_f/in^2
ΔP	- pressure drop, $dyne/cm^2/cm$
Q	- volumetric flow rate, cm^3/sec
r	- radius of capillary tube, cm
R	- radius of curvature, cm
R_e	- Reynolds' number
S	- cross-sectional area, cm^2
t	- efflux time, sec

English Letters

T	- temperature, ^{o}F
V	- volume of fluid, cm^3
$\overline{V}$	- velocity of fluid, cm/sec
w_i	- independent variable
W	- dependent variable

Greek Symbols

∂	- partial derivative
Δ	- finite difference
μ	- absolute viscosity, centipoise
ν	- kinematic viscosity, centistokes
ξ	- kinetic energy correction factor
π	- constant, 3.14159
ρ	- density, gm/cm^3
σ	- deviation of subscripted variable
$\tilde{\rho}$	- correlation coefficient of subscripted variables

CHAPTER I

INTRODUCTION

Viscosity is an important parameter in many scientific and engineering areas such as momentum, heat and mass transfer. Only a small amount of experimental data exists in the literature, especially as a function of temperature and pressure. The more common paraffinic and aromatic hydrocarbons and primary alcohols are the compound types that have been widely studied.

This study was conducted with two specific aims:

1. Measure liquid viscosity in the region of the critical point.
2. Determine the effect of pressure on liquid viscosity.

The pressure effect was further subdivided to compare a back pressure applied directly to a sample liquid and an inert gas atmosphere in contact with a sample liquid. This portion of the study was done at isothermal conditions.

There were two viscometers used during this study. An absolute capillary viscometer was used to determine the effect of back pressure on liquid viscosity. This apparatus was also used for some measurements in the critical region. A relative kinematic viscometer was used to study the effect of an inert gas atmosphere on a sample liquid and for some measurements in the critical region.

The pressure effect was studied using n-octane as the test liquid. The inert gas atmosphere effect was studied using n-octane

and n-octanol in contact with hydrogen, helium, nitrogen, argon and methane.

Critical region data were taken using n-octane, n-propanol, ethanol and ethylene-propylene binary mixtures as test fluids.

CHAPTER II

LITERATURE SURVEY

A literature survey was conducted during the course of this study to determine the amount of experimental work done in the specific areas of this study. The survey was divided into two parts, viscosity measurements in the critical region and the pressure effect on liquid viscosity.

Critical Region

The measurement of fluid viscosities in the region of the vapor-liquid critical point has been recommended for correlation development by various workers. The published results found during this survey are summarized in Table I. Data for mixtures could not be found. The lack of agreement between various works illustrates the difficulty of taking consistent data in the critical region.

Carmichael and Sage (13) studied the viscosity of ethane over the temperature range of $80^{\circ}F$ to $400^{\circ}F$ at pressures up to 5000 psia. The measurements were taken along isotherms at various pressures with a rotating cylinder viscometer. The recommended critical viscosity value was 187 ± 38 micropoise (0.0187 ± 0.0038 centipoise).

Clark (15, 16) studied the viscosity of ethyl ether near the critical point with a torsional viscometer. The main thrust of his work was to determine whether the liquid phase existed at temperatures

TABLE I

CRITICAL VISCOSITY MEASUREMENTS FROM LITERATURE SOURCES

Material	Critical Viscosity (Centipoise)	Method Measurement	Reference
Parahydrogen	0.0355 ± 0.0005	Torsional Crystal	19
Neon	0.0168	Falling Cylinder	50
Xenon	0.0448 ± 0.0005*	Light Scattering	62
	0.05352	Torsional Crystal	55
	0.02235	Transpiration	57
Nitrogen	0.035**	Torsional Crystal	23
	0.0180 ± 0.0002	Oscillating Disc	63
Oxygen	0.060**	Torsional Crystal	23
Chlorine	0.01852	Transpiration	59
Methane	0.00726	Transpiration	58
	0.0249	Falling Cylinder	56
Ethane	0.02002	Torsional Crystal	55
	0.00935	Transpiration	58
	0.0187 ± 0.0038	Rotating Cylinder	13
	0.0210 ± 0.0002	Capillary	53,54
Propane	0.00990	Transpiration	58
	0.0240 ± 0.0005	Capillary	53,54
n-Butane	0.0245 ± 0.0005	Capillary	53,54
n-Pentane	0.0235**	Falling Object	26
iso-Octane	0.025**	Transpiration	30
Ethylene	0.02465	Oscillating Disc	36
	0.00962	Transpiration	58
Propylene	0.01050	Transpiration	58
β-Butylene	0.01087	Transpiration	58
Cyclohexane	0.030**	Transpiration	30
Benzene	0.056	Falling Object	25

TABLE I (Continued)

Material	Critical Viscosity (Centipoise)	Method Measurement	Reference
Methanol	***	Capillary	33
n-Propanol	***	Capillary	33
Ethyl Formate	0.0380**	Capillary	31
Methyl Acetate	0.0400**	Capillary	31
Ethyl Acetate	0.0360**	Capillary	31
n-Propyl Acetate	0.0351**	Capillary	31
Ethyl Propionate	0.0291**	Capillary	31
Ethyl Ether	***	Oscillating Pendulum	15,16
	0.0475	Falling Ball	48
Carbon Tetra-Chloride	***	Capillary	33
Carbon Dioxide	0.0345 $\pm$ 0.0002	Oscillating Disc	29
	***	Transpiration	37
	0.03678 $\pm$ 0.0002	Oscillating Disc	40
	0.0321	Falling Object	41
	0.0032	Falling Object	52
Nitrous Oxide	0.01198	Transpiration	60
Hydrogen Iodide	0.01632	Transpiration	59
Nitrosyl Chloride	0.01779	Transpiration	60
Water	0.074	Falling Object	24
	0.0038	Capillary	49

* Kinematic Viscosity
** Read from graphical presentation
*** No value cited or presented

slightly greater than the critical. No value for the critical viscosity was given and the liquid phase existed above T_c only when insufficient time was allowed for attainment of equilibrium.

Diller (19) measured the critical region viscosity of parahydrogen with a torsional crystal viscometer. Experimental runs were conducted isothermally. The recommended value for the critical viscosity of parahydrogen was 355 $\pm$ 5 micropoise (0.0355 $\pm$ 0.0005 centipoise).

Grevendonk, et al. (23) used a torsional crystal viscometer to determine the viscosity of liquid oxygen and nitrogen. The temperature range was between 77°K and the critical temperature at pressures up to 200 kg_f/cm^2 (2842 psia). The data were taken along isotherms and extended to the saturation line. The critical viscosity values were read from the presented graphical results; for oxygen, μ_c = 0.060 centipoise; for nitrogen, μ_c = 0.035 centipoise.

Hawkins, et al. (24) studied the critical viscosity of water using a falling object viscometer. The value for the critical viscosity was found to be 0.074 centipoise at 706°F (T_c). No correlation of the data was presented.

Heiks and Orban (25) used a falling object viscometer to determine the critical viscosity of benzene. The value recommended was 0.056 centipoise at 288,5°C (T_c). There was no correlation tested or recommended.

Hubbard and Brown (26) used a falling ball viscometer to measure the viscosity of n-pentane. The experiment was conducted isobarically at various temperatures. The value for the critical viscosity was read from the graphical presentation. The value for μ_c was 0.235 millipoise (0.0235 centipoise).

Kestin, et al. (29) used an oscillating disk viscometer to measure the viscosity of carbon dioxide in the critical region. The critical point was approached from the vapor region along isochores. A value of 345 $\pm$ 2 micropoise (0.0345 $\pm$ 0.0002 centipoise) was recommended.

Khalilov (30) used a capillary viscometer to determine the saturated liquid and vapor viscosities of iso-octane, cyclopentane, and cyclohexane. The critical viscosity was determined for only iso-octane. The value read from the graphical presentation was 0.025 centipoise.

Khalilov (31) studied the saturated liquid and vapor viscosities of a number of esters at temperatures up to the critical region. The compounds studied in the critical region were ethyl formate, methyl acetate, ethyl acetate, n-propyl acetate and ethyl propionate. The critical viscosity values were read from the graphical presentation. The corresponding critical viscosity values are 0.0380, 0.0400, 0.0360, 0.0351 and 0.0291 centipoise, respectively.

Kopylov (33) determined the critical point viscosities for methanol, n-propanol and carbon tetrachloride using a capillary viscometer. Only smoothed data were presented and the critical point values were not quoted.

Mason and Maass (36) studied the critical region viscosity behavior of ethylene using an oscillating disc viscometer. Measurements were taken along isotherms which traversed the saturation line from both directions, i.e., measurements were recorded in the vapor region and in the liquid or dense fluid region by controlling the system pressure. A minimum value for the viscosity was found at the

critical point. The miminum value for the viscosity was 0.02465 centipoise at 50.0°F.

Michels, et al. (37) used a transpiration method to determine the critical region viscosity behavior of carbon dioxide. Anomalous behavior in the critical region was cited as the reason for no recommendation of a single value for the critical viscosity.

Naldrett and Maass (40) used an oscillating disc viscometer to study the critical region viscosity of carbon dioxide. Values were determined along isochores and isotherms. The recommended value for the critical viscosity was 367.8 $\pm$ 2 micropoise (0.03678 $\pm$ 0.0002 centipoise).

Phillips (41) used a falling object viscometer to determine the viscosity of carbon dioxide in the critical region. The measurements were taken along isotherms from the vapor region to the saturation line. The value cited for the critical viscosity was 0.321×10^{-3} poise (0.0321 centipoise).

Schroer and Becker (48) used a falling ball viscometer to determine the critical region viscosity of ethyl ether. The experiment was conducted along isotherms between 184.5°C and 235°C at pressures between 25 and 75 kg/cm^2 (355 and 1066 psia). The value for the critical viscosity of ethyl ether was 0.000475 poise (0.0475 centipoise).

Sigwart (49) used a capillary viscometer to study the viscosity of water and steam up to the critical region. The experiment was conducted along the saturation line in the liquid region and along isotherms in the vapor region. The value cited for the critical viscosity was 3.85×10^{-6} kg sec/m^2 (0.0038 centipoise).

Slyusar, et al. (50) measured the viscosity of neon along the saturation line in the liquid and vapor phases with a falling cylinder viscometer. The temperature range was between 24.7°F and 300°F. The critical viscosity for neon was 168 x 10^{-6} poise (0.0168 centipoise).

Stakelbeck (52) determined the viscosities of carbon dioxide, ammonia, sulfur dioxide and methyl chloride using a capillary viscometer. The experiment was done isothermally at various pressures. The saturation values were given as well as the values for the subcooled liquids. The only material examined in the critical region was carbon dioxide. The recommended value for the critical viscosity was 3.22 x 10^{-6} kg sec/m^2 (0.0032 centipoise).

Starling, et al. (53,54) used a capillary viscometer to determine the critical viscosities of ethane, propane and n-butane. The recommended values were 210 $\pm$ 2, 240 $\pm$ 5 and 245 $\pm$ 5 micropoise (0.0210 $\pm$ 0.0002, 0.0240 $\pm$ 0.0005 and 0.0245 $\pm$ 0.0005 centipoise), respectively. An evaluation of critical viscosity estimation techniques was made but no firm recommendation resulted.

Strumpf, et al. (55) used a torsional oscillating crystal viscometer to examine the critical point viscosities for ethane and xenon. The critical point was approached along isochores beginning in the vapor region. These workers also studied the critical temperatures and densities. The critical viscosities recommended were 200.2 and 535.2 micropoise (0.02002 and 0.05352 centipoise), respectively. Anomalous behavior was noted in the critical region viscosity.

Swift, et al. (56) used a falling cylinder viscometer to determine the liquid viscosity of methane and propane. The viscosity of methane

was determined between -150°C and the critical temperature. Propane viscosity was determined between -185°C and +90°C. The critical viscosity of methane was found to be 0.0249 centipoise.

Trautz and Heberline (57) used a transpiration method to determine the vapor viscosities of xenon, up to the critical point, and its mixtures with water and helium. The critical viscosity value recommended was 2235 x 10^{-7} poise (0.02235 centipoise).

Trautz and Husseini (58) used a transpiration method to study the vapor viscosities of propylene and β-butylene and their mixtures with helium and hydrogen. The critical viscosity values recommended were 1050 x 10^{-7} and 1087 x 10^{-7} poise (0.01050 and 0.01087 centipoise), respectively.

Trautz and Ruf (59) used a transpiration method to determine the vapor viscosities of chlorine and hydrogen iodide. The main purpose of their study was to find viscometer materials for use with corrosive gases. The critical viscosity values recommended were 1852 x 10^{-7} and 1632 x 10^{-7} poise (0.01852 and 0.01632 centipoise), respectively.

Trautz and Freytag (60) used a transpiration method to determine the vapor viscosities of nitrous oxide, nitrosyl chloride and the reaction products from the reaction, 2 NO + Cl_2 = 2 NOCl. The critical viscosity values recommended for NO and NOCl were 1198 x 10^{-7} and 1779 x 10^{-7} poise (0.01198 and 0.01779 centipoise), respectively.

Zollweg, et al. (62) used light scattering experiments to deduce the critical kinematic viscosity of xenon. The critical kinematic viscosity value recommended was 448 $\pm$ 15 microstokes (0.0448 $\pm$ 0.0015 centistokes).

Zozulya and Blagoi (63) used an oscillating disc viscometer to determine the viscosity behavior of nitrogen up to the critical region. The experiment was conducted in the subcooled liquid and vapor regions with isotherms crossing the phase envelope. The value for the critical viscosity was read from the graphical presentation. The value read from the graph was 180 $\pm$ 2 micropoise (0.0180 $\pm$ 0.0002 centipoise).

Pressure Effect

The effect of pressure on the viscosity of pure liquids and liquid mixtures has been the object of research for many years. Investigators have thought that the knowledge gained from these studies would aid toward understanding liquid phase behavior. Investigations have failed to reach this objective. In fact, these studies have illustrated the degree of difficulty encountered during study of liquid phase behavior. At present, there is no theory that adequately describes the pressure effect on liquid viscosity. The most apparent result has been the dependence, of the viscosity of liquids under pressure, on molecular structure.

This survey covers two areas of pressure effect research. Studies where the pressure was supplied by the fluid under test (hydraulic) and studies where compressed gases were used to supply the system pressure (compression).

Hydraulic Pressure Effects

Agaev and Golubev (1,2) used a falling object viscometer to study the effect of pressure on the liquid viscosity of n-pentane,

n-heptane and n-octane. The temperature range of the study was between 25°C and 275°C at pressures between 1 and 500 atmospheres (14.7 and 7350 psia). The viscosity increased linearly with pressure except in the critical region where some curvature was evident. The data were tabulated as functions of the temperature and pressure.

Babb and Scott (3) used a rolling ball viscometer to determine the viscosity at 30°C for five hydrocarbons and refrigerant R-12 at pressures between 2 and 12 kbars (29000 and 174000 psia). The data were presented with no mathematical model. Within the pressure range of their study, the increase in viscosity with pressure is concave and exponential in shape.

Bicher and Katz (6) used a rolling ball viscometer to study the viscosity of methane, propane and four of their binary mixtures (20, 40, 60 and 80 percent methane). A temperature range of 77°F to 437°F was covered at pressures between 400 and 5000 psi. At pressures significantly removed from saturation, the viscosity behavior became linear with pressure.

Brazier and Freeman (8) used a rolling ball viscometer to determine the pressure effect on the viscosity of seven hydrocarbons. The temperature range covered was 0°C to 60°C at pressures from 1 to 4000 bars (14.5 to 58000 psia). The data were reported as the increase with pressure of the logarithm of the relative viscosity.

Bridgman (9,10) studied the pressure effect on viscosity for 43 pure liquids at temperatures of 30°C and 75°C at pressures up to 12000 kg/cm^2 (170000 psia). A falling object viscometer was used. The behavior of various liquids was a function of molecular structure. Water showed the most anomalous behavior, at low temperatures

decreasing slightly with pressures up to 1000 kg/cm^2, (14200 psia), then increasing. At high temperatures, the viscosity increased across the entire pressure range. For other compounds, the logarithm of viscosity against pressure curves are, at first, concave toward the pressure axis, but above 3000 kg/cm^2 (42600 psia) become very nearly linear, and for some fluids become convex toward the pressure axis. No correlation for the pressure effect was recommended.

Bridgman (11) used an oscillating vane viscometer to study the effect of pressure on the viscosity of liquids. The study was conducted under isothermal conditions at pressures up to 40000 kg/cm^2 (570000 psia). The suggested behavior was not linear with the logarithm of viscosity but somewhat greater increases in viscosity with pressure were noted. No values of absolute viscosity were cited, only relative viscosities as functions of pressure.

Chaudhuri, et al. (14) studied the effect of pressure on the viscosity of liquid aldehydes from atmospheric to 20000 psig. The logarithm of the ratio of the absolute viscosity at a pressure P to the viscosity at atmospheric conditions was found to be a linear relationship with pressure. The expression $\mu = \mu_0 \exp(mP)$ was suggested, where

μ = viscosity at P, centipoise

μ_0 = viscosity at atmospheric conditions, centipoise

P = pressure, psi

m = slope of resulting line when log (μ/μ_0) is plotted against pressure. No attempt was made to verify whether this expression was general.

Dow (20) studied the pressure effect on the viscosity of liquid mixtures at temperatures of 30°C and 75°C at pressures up to 12000 kg/cm^2 (170000 psia). A falling object viscometer was used. The behavior of the viscosity with pressure was approximately linear for nonpolar liquid mixtures. The mixtures of polar and nonpolar compounds behaved very irregularly. The author had great difficulty drawing smooth curves through the data. No correlation was developed or recommended.

Eakin, et al. (21) used a capillary viscometer to study the liquid, gas and dense fluid viscosity of ethane. The temperature range of this study was 77°F to 220°F at pressures from atmospheric to 10000 psia. The isobars showed little curvature until pressures were reduced to values slightly larger than the critical pressure or until temperatures were significantly greater than the critical temperature. No correlation was recommended.

Greist, et al. (22) used a rolling ball viscometer to study the pressure effect on liquid viscosity for seven hydrocarbons with 25 or 26 carbon atoms. The temperatures studied were 37.8°C, 60.0°C, 98.8°C and 135°C at pressures up to 3450 bars (50000 psia). The increase in the viscosity with pressure was found to be dependent on molecular structure. For saturated compounds at constant temperature, an approximately linear relationship was found between log μ and $\left[(v/v_0)^4 - (v/v_0)^2\right]$, where v and v_0 are the specific volumes at pressure P and pressure P_0, respectively.

Isakova and Oshueva (27) studied the pressure effect on the viscosity of methanol at temperatures of 20°C and 160°C at pressures

between atmospheric and 250 kg/cm^2 (3550 psia). A capillary viscometer was used in the study. The effect of pressure on methanol appears to be linear in pressure for the temperatures studied.

Macleod (35) proposed and tested an expression for pure component viscosity as a function of temperature. A modification was proposed for the pressure effect which showed reasonable agreement with experimental results. However, the model was empirical and required regression of six constants from data.

Reamer, et al. (42) studied the effect of pressure on the viscosity of n-pentane from the bubble point to 5000 psi. A linear relationship was illustrated at pressures greater than 1000 psi. Between the saturation curve and 1000 psi, the viscosity - pressure function was, in general, nonlinear. At temperatures below 160^oF ($T_r = 0.73$) the behavior was linear in the pressure range previously mentioned. Above a T_r of 0.73, the region between saturation and 1000 psi shows significant departure from linearity with pressure.

Rein (43) studied the effect of pressure on viscosity for 11 fluids using an oscillating crystal viscometer. The curves of viscosity as a function of pressure were concave as pressure increased. The study was conducted under isothermal conditions. No model for the pressure effect was recommended.

Sage and Lacey (45) used a rolling ball viscometer to determine the pressure effect on liquid n-pentane, gaseous methane and two natural gas mixtures. The temperature range of the n-pentane data was 100^oF to 200^oF at pressures between saturation and 1500 psia. The behavior of each isotherm was linear with slopes that increased with

temperature. All isotherms crossed at approximately 250 psia. No pressure correlation was presented or recommended.

Sage and Lacey (46) studied the effect of pressure on the viscosity of liquid propane with a rolling ball viscometer. Linear behavior of viscosity was observed above the bubble point. The linearity persisted until a reduced temperature of approximately 0.9 was reached. The linearity was evident at pressures above $P_r = 1.6$, even in the critical region. Variations in the viscosity behavior in the critical region were illustrated.

Sage, Yale and Lacey (47) studied the pressure effect on the viscosity of n-butane and isobutane using a rolling ball viscometer. The temperature range covered in their study was between 100°F and 200°F. A slight curvature was illustrated between the saturation locus and 2000 psi for all temperatures.

Smith and Brown (51) used a rolling ball viscometer to study the viscosity of ethane and propane in the temperature range 15°C to 200°C at pressures between 100 and 5000 psi. These workers correlated experimental and literature data through corresponding states techniques. The parameter $\mu/\sqrt{M}$ was plotted as a function of the reduced temperature and pressure. The correlation fit the data reasonably well for members of homologous series.

Compression Pressure Effects

Bagzis (4) used a Zeitfuchs capillary viscometer to study the viscosity of n-decane, n-hexane and a binary mixture of n-butane and n-decane saturated with methane over a pressure range between the solvent vapor pressure and 1200 psia. A system of n-decane saturated

with ethane was also studied. The methane-n-decane binary was studied between 1°F and 130°F at pressures up to 1200 psia. The ethane-n-decane binary was studied between 31°F and 174°F at pressures up to 300 psia. For these systems, the saturated liquid viscosity was more greatly affected at low temperatures than at high temperatures. The isotherms became linear with pressure as temperature increased. The methane-n-hexane binary was studied at 1°F and the isotherm decreased exponentially with pressure. The isotherm of the methane-n-butane-n-decane system increased sharply to a maximum between atmospheric and 200 psia. The isotherm then decreased linearly between viscosities of 0.86 centipoise at 400 psia and 0.75 centipoise at 1200 psia.

Bennett (5) used a Zeitfuchs capillary viscometer to study binary mixtures of n-nonane saturated with methane along isotherms over a temperature range of -30° to 78°F. The pressure range was between the vapor pressure of the solvent to 1200 psia. In general, the isotherms decreased exponentially with pressure at low temperatures and approached linearity at the higher temperatures.

Lewis (34) used a capillary viscometer to study the viscosity of liquids containing dissolved gases. The gases used were sulfur dioxide and chlorine. The concentration of dissolved component was limited by the glass apparatus to a maximum concentration of 30 weight percent. The pressures applied to the systems were not specified. Markedly different viscosity behavior was illustrated depending upon the chemical species of the components in the mixtures.

Rudolf (44) used a Zeitfuchs capillary viscometer to study the effect of methane saturation on the viscosity of lean absorber oils. The oils studied were Mineral Spirits 135, a highly aromatic absorption

oil, a highly naphthenic absorption oil, virgin oil, and a 50/50 mixture of Mineral Spirits 135 and Heavy Solvent No. 1. The temperature range of this study was from -26°F to 77°F at pressures from atmospheric to 1006.7 psia. The systems studied exhibited the same general behavior, i.e., an exponential decrease in viscosity with presure at low temperatures and an approach to linearity at higher temperatures. For further details concerning the characterization of these oils, the reader is referred to Rudolf's thesis.

Kinematic Viscometer

Poiseuille's Law for laminar flow inside tubes for Newtonian fluids was presented by Bird, et al. (7) in the form

$$Q = \frac{\pi (\Delta P) r^4}{8\mu L} \qquad (1)$$

Van Wazer, et al. (61) showed that this relationship could be applied to capillary viscometers provided that the following substitutions were made.

$$\Delta P = \rho g h \qquad \text{and} \qquad Q = V/t$$

In addition, if the effect of kinetic energy is considered in the derivation of the Poiseuille Law, the form of Equation 1 becomes upon substitution and rearrangement:

$$\mu = \frac{\pi r^4 \rho g h t}{8 L V} - \frac{\xi \rho V}{8 \mu L t} \qquad (2)$$

Noting that the kinematic viscosity, ν, is equal to (μ/ρ), the following expression may be obtained:

$$\nu = \frac{\pi r^4 g h t}{8 L V} - \frac{\xi V}{8 \pi L t} \qquad (3)$$

This relationship can be written as

$$\nu = K_1 t - K_2/t \qquad (4)$$

in which K_1 is characteristic of a given viscometer and K_2 is reported by Cannon, et al. (12) to be a function of the Reynolds' number.

The difficulty in the evaluation of K_2 reported by Johnson, et al. (28) suggests that the best solution to the dilemma is to use a viscometer designed to make K_2 as small as possible. These authors found that the Zeitfuchs style capillary viscometer had a value of K_2 small enough to give a correction for kinetic energy of approximately 0.03 percent. Cannon, et al. (12) estimated a maximum value for the kinetic energy correction of 0.07 percent. Ignoring this small correction factor, Equation 4 can be written in the following form:

$$\nu = K_1 t \qquad \text{or} \qquad \nu = K t \qquad (5)$$

Equation 5 served as the basis for the viscosity measurements made with the kinematic viscometer during this study. K was determined by measuring the efflux time, t, of a fluid of known kinematic viscosity, ν. Once K was determined, the kinematic viscosity of a test fluid was found by measuring the efflux time for the test fluid.

Johnson, et al. (28) evaluated the Zeitfuchs capillary viscometer and reported that the cross-arm design of the instrument virtually eliminated errors due to differences in surface tensions of the

calibration and test fluids. The cross-arm design eliminates errors resulting from the liquid clinging to the walls of the vessel from which the liquid is drawn during the flow process of viscosity measurement.

Absolute Viscometer

Poiseuille's Law also applies to the theory of operation of the absolute viscometer. Equation 1 can be solved for the absolute viscosity, μ, which yields the following expression

$$\mu = \frac{\pi r^4}{8 L} \frac{(\Delta P)}{Q} \tag{6}$$

Equation 6 served as the basis for all viscosity measurements made with the absolute viscometer during this study.

The term $\frac{\pi r^4}{8 L}$ was evaluated from the geometric values of the capillary radius, r, and the capillary length, L. The instrumentation of the absolute viscometer gave values for the pressure drop through the capillary, ΔP, and the test fluid flow rate, Q. The calculation of the absolute viscosity was straightforward with no correction terms except the instrument calibrations.

CHAPTER III

EXPERIMENTAL APPARATUS AND PROCEDURE

Experimental Apparatus

There were two types of experimental apparatus used during this study. The two types are differentiated by viscosity measurement technique, kinematic and absolute. Each apparatus will be discussed separately. First, the kinematic viscometer system will be described, followed by the description of the absolute viscometer system.

Kinematic Viscometer

The kinematic viscometer experimental apparatus was basically the same as constructed by Bennett (5). The reader is referred to his thesis for a more detailed discussion. The apparatus consisted primarily of the capillary viscometer, the pressure cell, the constant temperature bath, the flow system used to move the test fluid through the capillary tube, and the instrumentation used to measure temperature, pressure, and efflux time of the test fluid.

Viscometer

A Zeitfuchs cross-arm capillary viscometer (Figure 1) was used to make all kinematic viscosity measurements. Manufactured by the Cannon Instrument Company, the viscometer had a one piece glass body

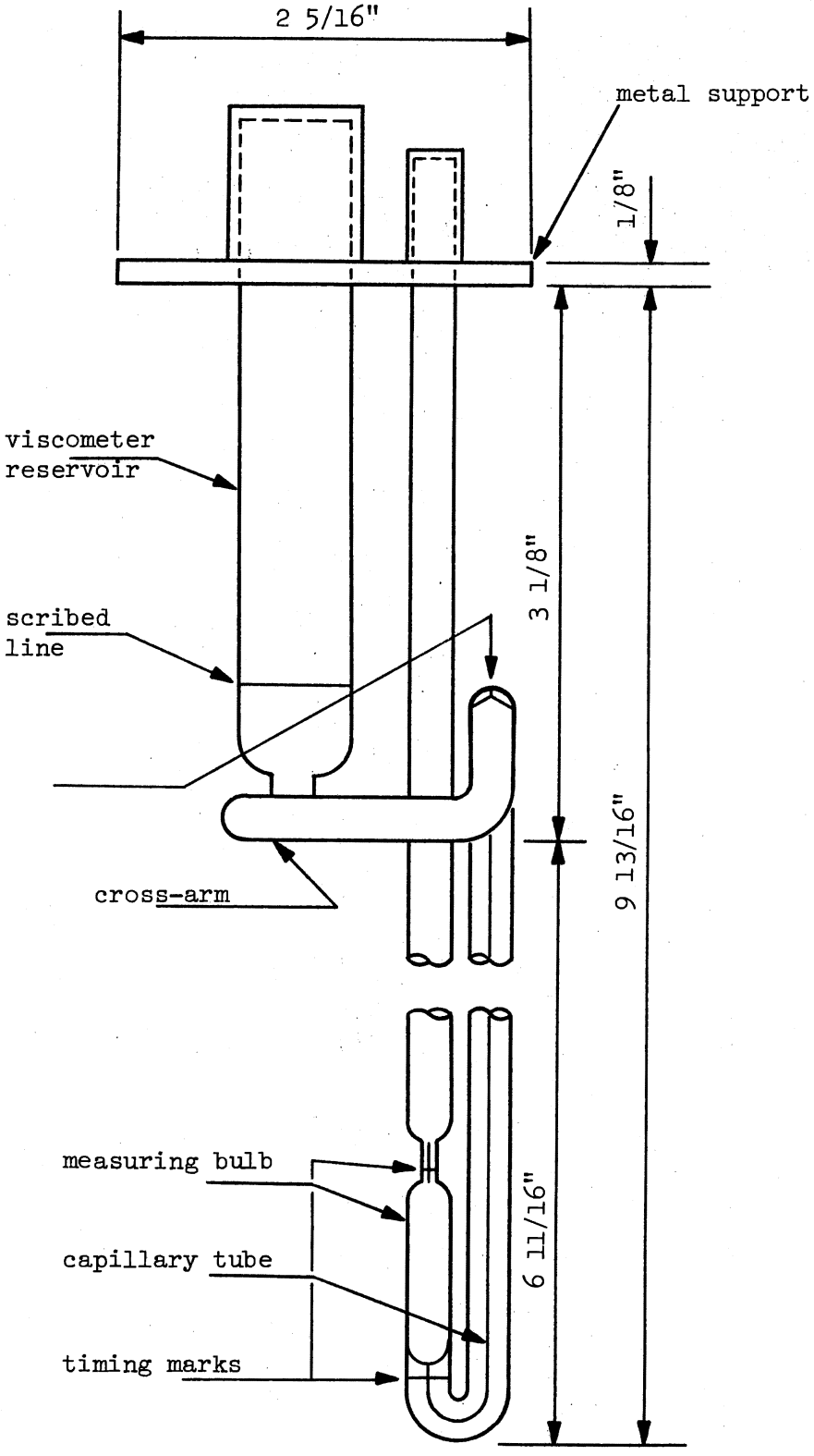

Figure 1. Zeitfuchs Capillary Viscometer

with a stainless steel metal support (Figure 2) attached with Lithargian glue. The viscometer consisted of a reservoir, cross-arm, reverse bend, capillary tube, measuring bulb, and metal support.

The liquid sample was held at a depth specified by the height of the reverse bend prior to entry into the capillary tube. The liquid sample was transported to the capillary tube via the cross-arm. The capillary tube had a measuring bulb with scribed lines above and below the bulb body. These scribed lines served as timing marks for all kinematic viscosity measurements. The metal support served as a mounting bracket to hold the viscometer in place within the pressure cell.

Pressure Cell

The pressure cell (Figure 3) contained the viscometer during operation and allowed observation of the viscometer reservoir and measuring bulb. The pressure cell was used to hold an excess of liquid sample and contain the vapor pressure of the sample fluid. An excess of sample was required to maintain a constant composition during measurements made on mixtures.

Observation of the viscometer inside the pressure cell was through four view ports (Figure 4) installed in the sides of the pressure cell body. The windows in the observation ports were made of fused quartz. All observations were made through a 14 power cathetometer, as recommended by Bagzis (4), to see the fluid movement within the very fine capillary tube.

The pressure cell body and top flange were constructed of 304 stainless steel. A tight seal was made by using "Viton" O-rings in

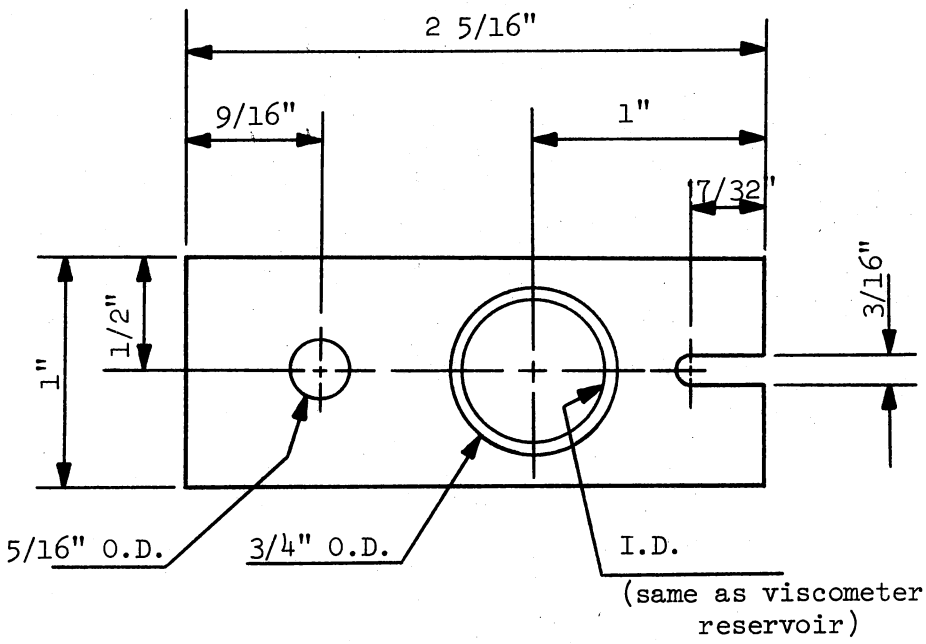

MATERIAL: 304 stainless steel

Figure 2. Support Frame for Zeitfuchs Capillary Viscometer

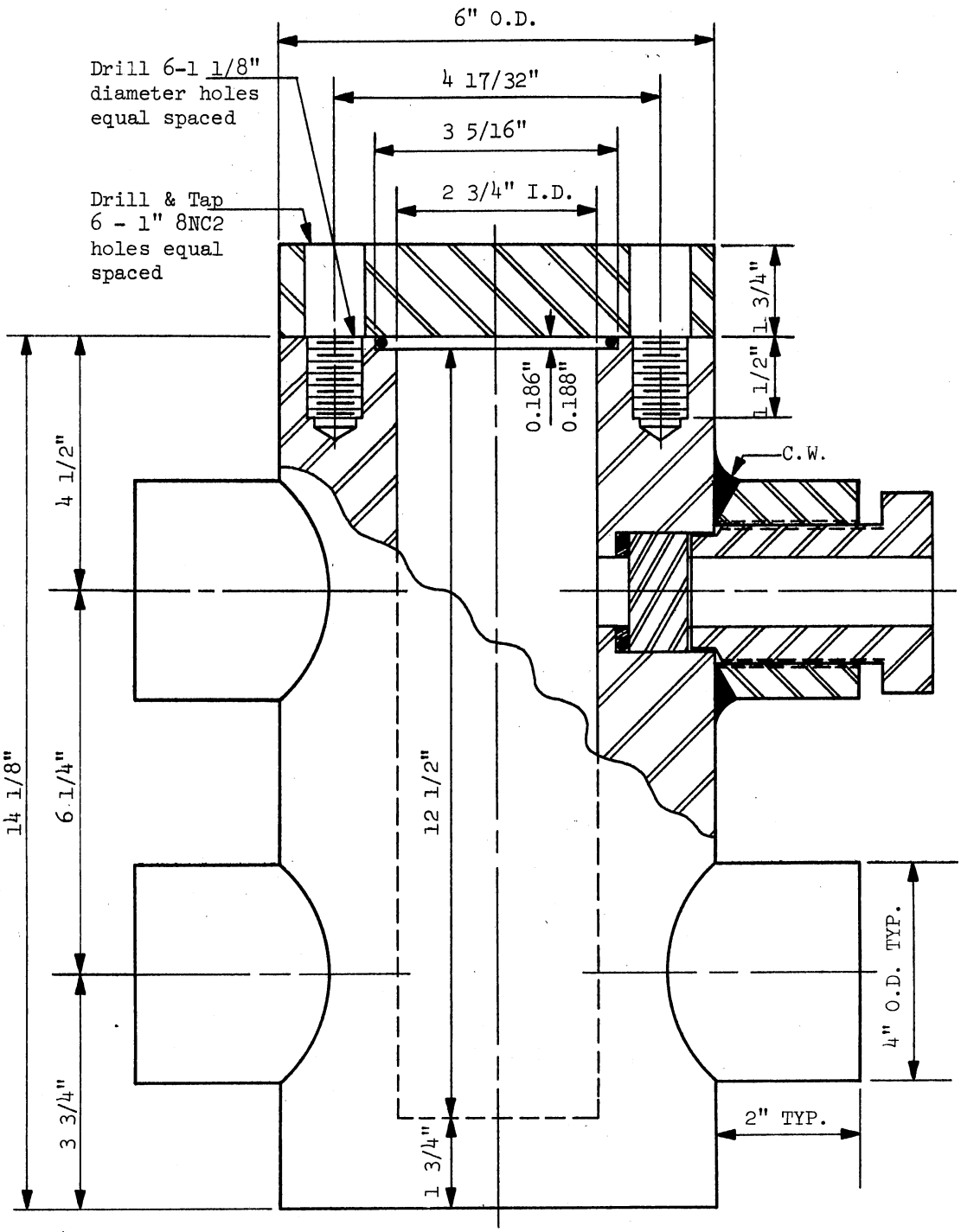

Figure 3. Pressure Cell

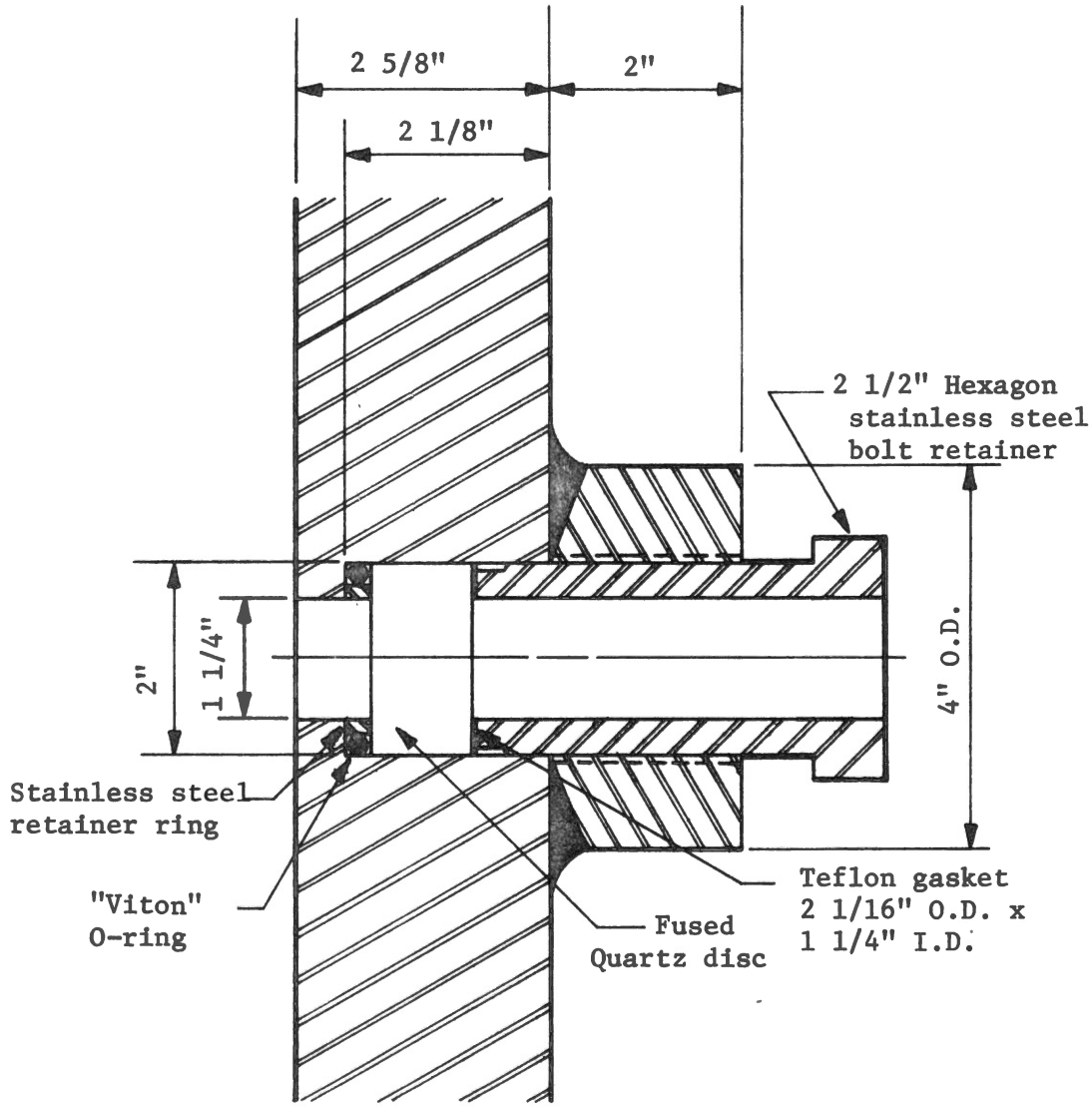

Figure 4. View Port Details

all openings of the pressure cell. Table II illustrates the types and sizes of all O-rings used in the pressure cell. The cell body and top flange assembly are shown in Figure 5. Eight 5/8 inch diameter bolts secured the top flange to the pressure cell body.

Bagzis (4) plugged an exterior liquid injection system opening with a threaded brass plug. To use the equipment with light hydrocarbons, this plug was removed and replaced with a tubing connector. A length of 1/8 inch stainless steel tubing was inserted through the connection. The end of the tubing was cut to coincide to the height of the reverse bend of the viscometer. This tubing served to fill the pressure cell with test fluid and remove excess sample from the viscometer reservoir.

Temperature Control

A constant temperature bath surrounded the pressure cell. Two separate baths were used, a high temperature bath and a low temperature bath. Duplicate temperature baths allowed greater flexibility during this study. A variable speed Lightning, Model F, Serial Number 6014917, mixer motor with a 3 1/2 inch diameter commercial agitator was used as the stirrer for both baths. The two baths and associated temperature control equipment are described in the following paragraphs as hot and cold, respectively.

Hot Bath. The high temperature bath was designed and instrumented to cover a temperature range of $+80^{o}F$ to $\pm 500^{o}F$. A Fisher, Model Number 22, Serial Number 946, proportional temperature controller was used to control the bath fluid temperature. Manufacturer

TABLE II

PRESSURE CELL SEALS

Seal Type	Inside Diameter inches	Outside Diameter inches	Compound	Parker Part No.
O-ring	2.975	3.395	Viton	2-337
O-ring	1.600	2,020	Viton	2-326
Washer	1.500	2.020	Teflon	---

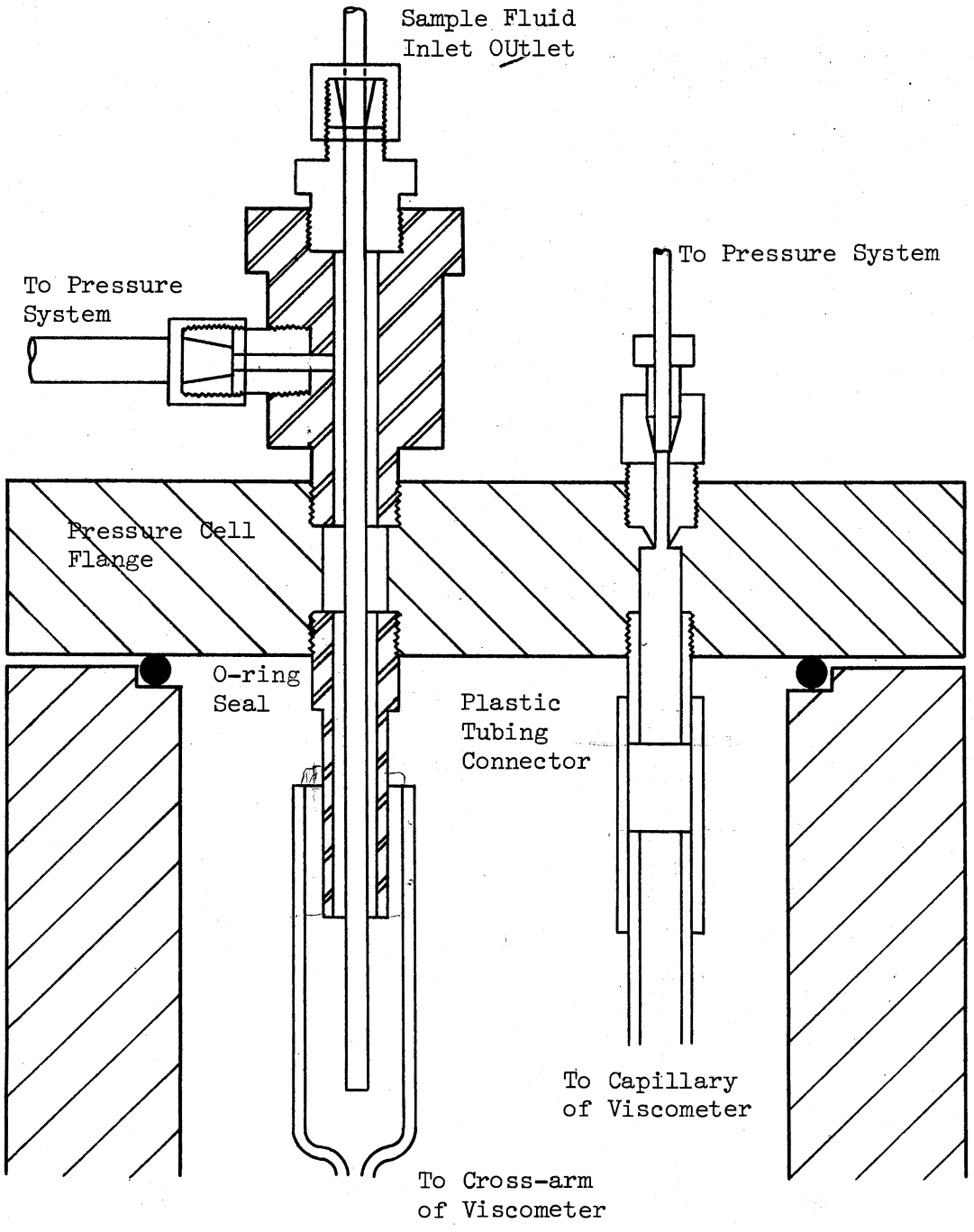

Figure 5. Pressure Cell Top Flange and Viscometer Connections

specifications for the controller are a temperature range of $0^{o}C$ to $250^{o}C$ with a sensitivity of $\pm$ $0.01^{o}C$ assuming adequate agitation and a repeatability of the set point of $\pm$ $0.02^{o}C$. The temperature controller had two controlled electrical outlets each rated for 750 watts capacity. Immersion heaters of 750 and 500 watts were used. The hot bath fluid was General Electric Type SF 1154 silicone oil. This fluid had excellent optical characteristics across a wide temperature range.

Cold Bath. The low temperature bath was designed and instrumented for a temperature range of $-100^{o}F$ to $+80^{o}F$. A Yellow Springs Instrument Company, Inc. temperature controller was used to control the bath fluid temperature. This controller had a manufacturer specification of a sensitivity of $\pm$ $0.05^{o}C$ assuming adequate agitation. A 500 watt immersion heater was used as a trim heater. A cascade refrigeration system (Figure 6) was used to cool the bath fluid. The fluid used in the cold bath was n-propanol. This alcohol has a very low freezing point and a low vapor pressure. The vapor pressure at $50^{o}C$ was 50 mm mercury. This fluid was chosen specifically because of the low vapor pressure to minimize evaporation when the cold bath was not in use. A finned tube heat exchanger was immersed in the cold bath fluid to serve as the bath fluid cooler and the refrigeration unit evaporator.

Pressure Distribution System

The pressure distribution system (Figure 7) provided a means for introducing sample liquid into the pressure cell, controlling the liquid level in the viscometer reservoir, and measuring the pressure exerted by the sample on the pressure cell.

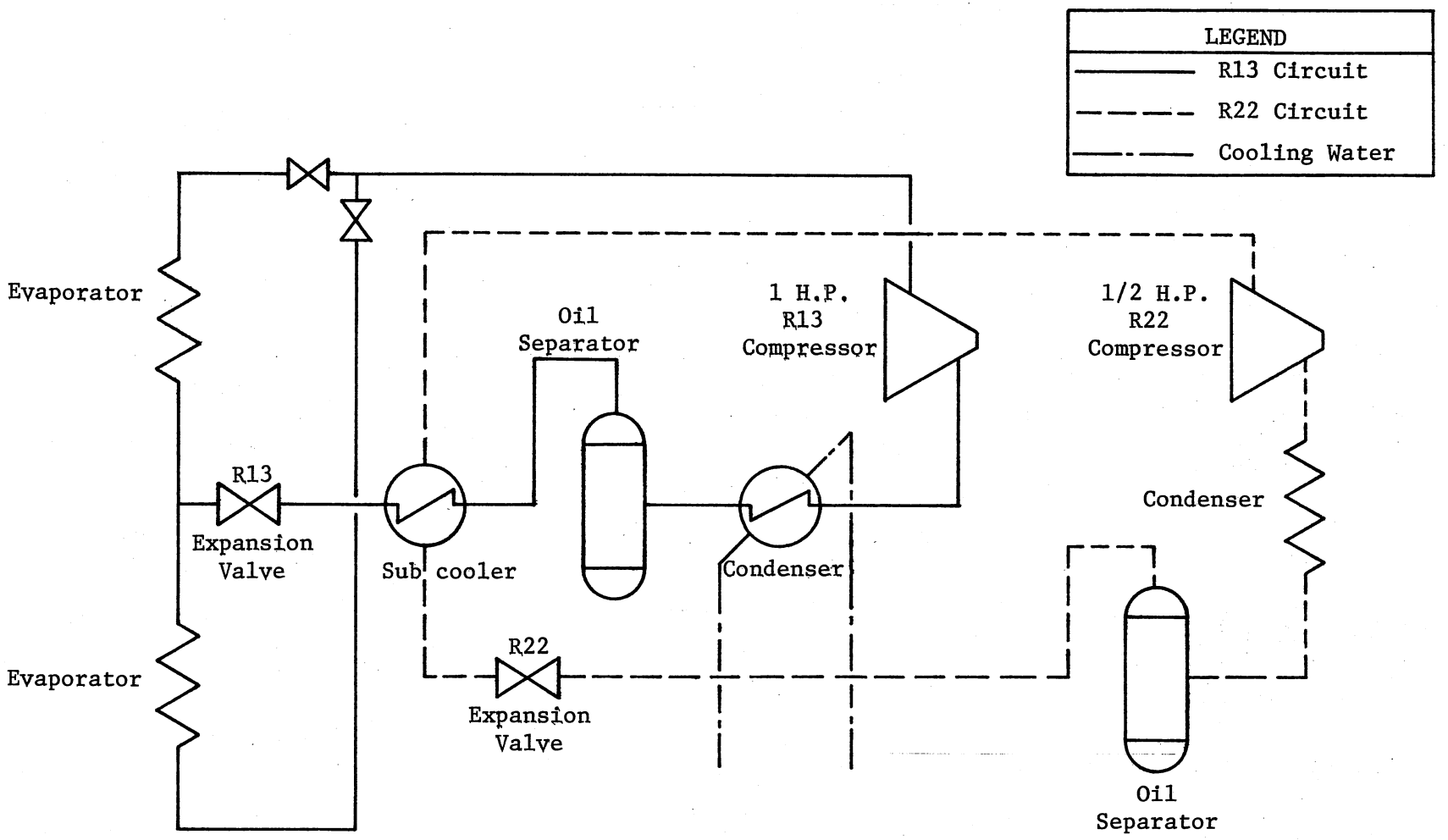

Figure 6. Schematic Flow Diagram of Cascade Refrigeration Unit

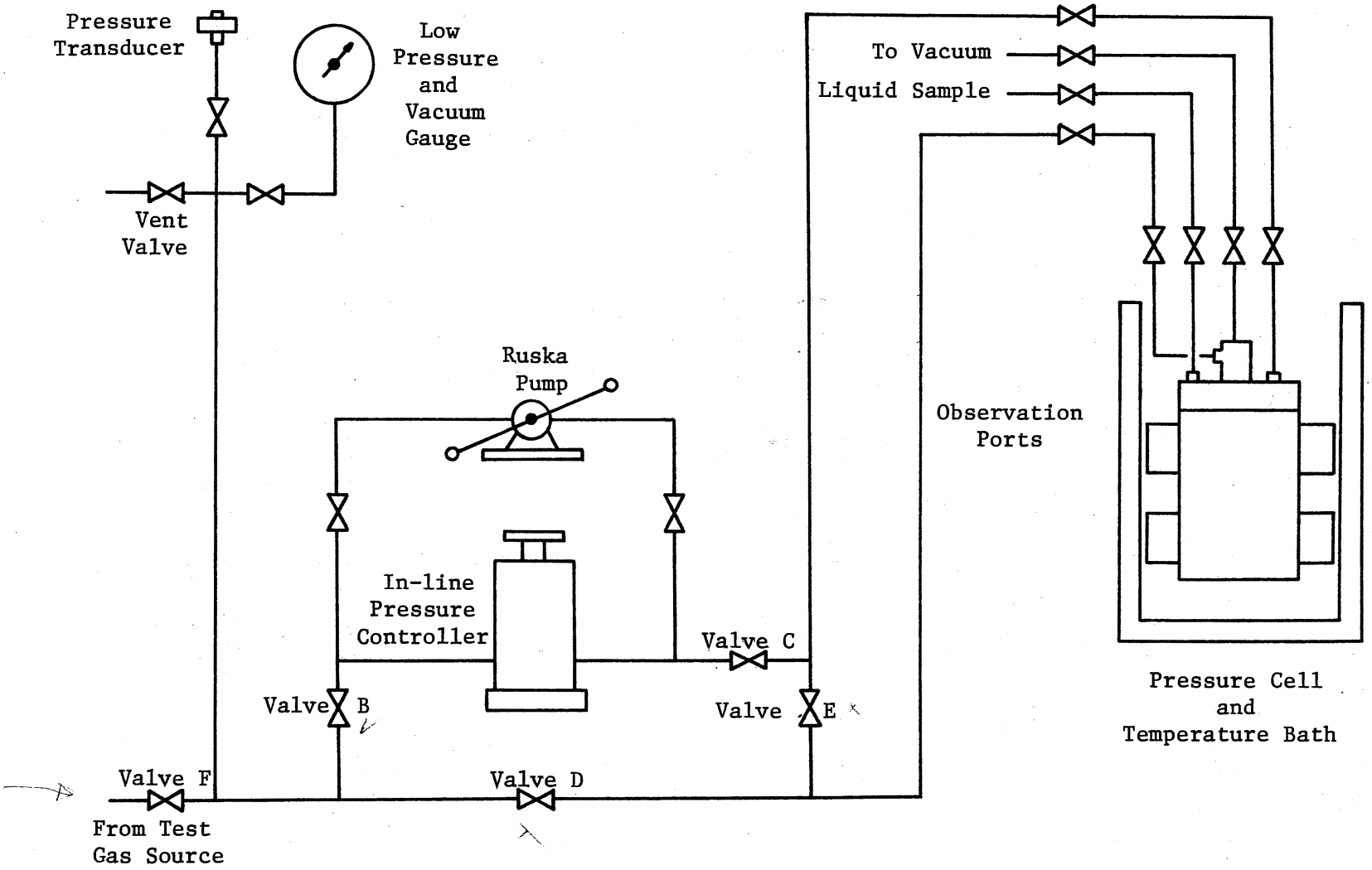

Figure 7. Schematic Flow Diagram of the Kinematic Viscometer Experimental Apparatus

The in-line pressure controller and the Ruska screw pump provided the motive force to move the sample liquid through the cross-arm to the capillary tube of the viscometer. The in-line pressure controller consisted of a cylinder with a piston enclosed. The piston was attached to a screw drive. The Ruska screw pump was used at high system pressures. Adjustment of either screw mechanism changed the system volume and thereby the system pressure. Pressure exerted by the sample liquid was contained in the in-line pressure controller by means of a series of "Viton" O-rings. Table III lists the number, size, and Parker part number of the O-rings.

TABLE III

IN-LINE PRESSURE CONTROLLER SEALS

Number	Inside Diameter inches	Outside Diameter inches	Compound	Parker Part No.
3	1.600	2.020	Viton	2-326
2	1.864	2.004	Viton	2-32

Removal of air from all portions of the pressure distribution system was done with a Duo-Seal vacuum pump prior to filling the pressure cell and viscometer with sample liquid. The vacuum pump was manufactured by the Welch Scientific Company.

Instrumentation

Figure 8 shows the schematic diagram of the instrumentation used during this study. The temperatures of the constant temperature bath and the sample liquid were measured with copper-constantan thermocouples referenced to 32°F. The thermocouples were manufactured by the Conax Corporation (Part No. T-SS12-G-T3-MK125A-24") with lead wires 36 inches long.

The system pressure was measured by a pressure transducer and a compound gauge. A Consolidated Electrodynamics Corporation Model 4-317 pressure transducer was used to measure pressures outside the range of the compound gauge. The range of allowable pressures for the transducer was from 0 to 2500 psig. A five volt direct current was required to excite the transducer. A Hewlett-Packard Model 6204B, Serial Number 1138A01806, power supply was used as the five volt power source. The compound gauge was used to measure low system pressures and vacuum. The Ashcroft gauge had pressure increments of 1/2 psi from 0 psig to 30 psig. The vacuum side had graduations of 1 inch of mercury from 0 to 30 inches of mercury vacuum.

With the exception of the Ashcroft compound gauge, all instruments had millivolt outputs. The output from each sensor was measured by use of a Leeds and Northrup Model 8686 millivolt potentiometer. The potentiometer allowed millivolt readings between -16 mV and +16 mV.

All instrument calibrations are shown in Appendix C.

Absolute Viscometer

The absolute viscometer experimental apparatus consisted of the

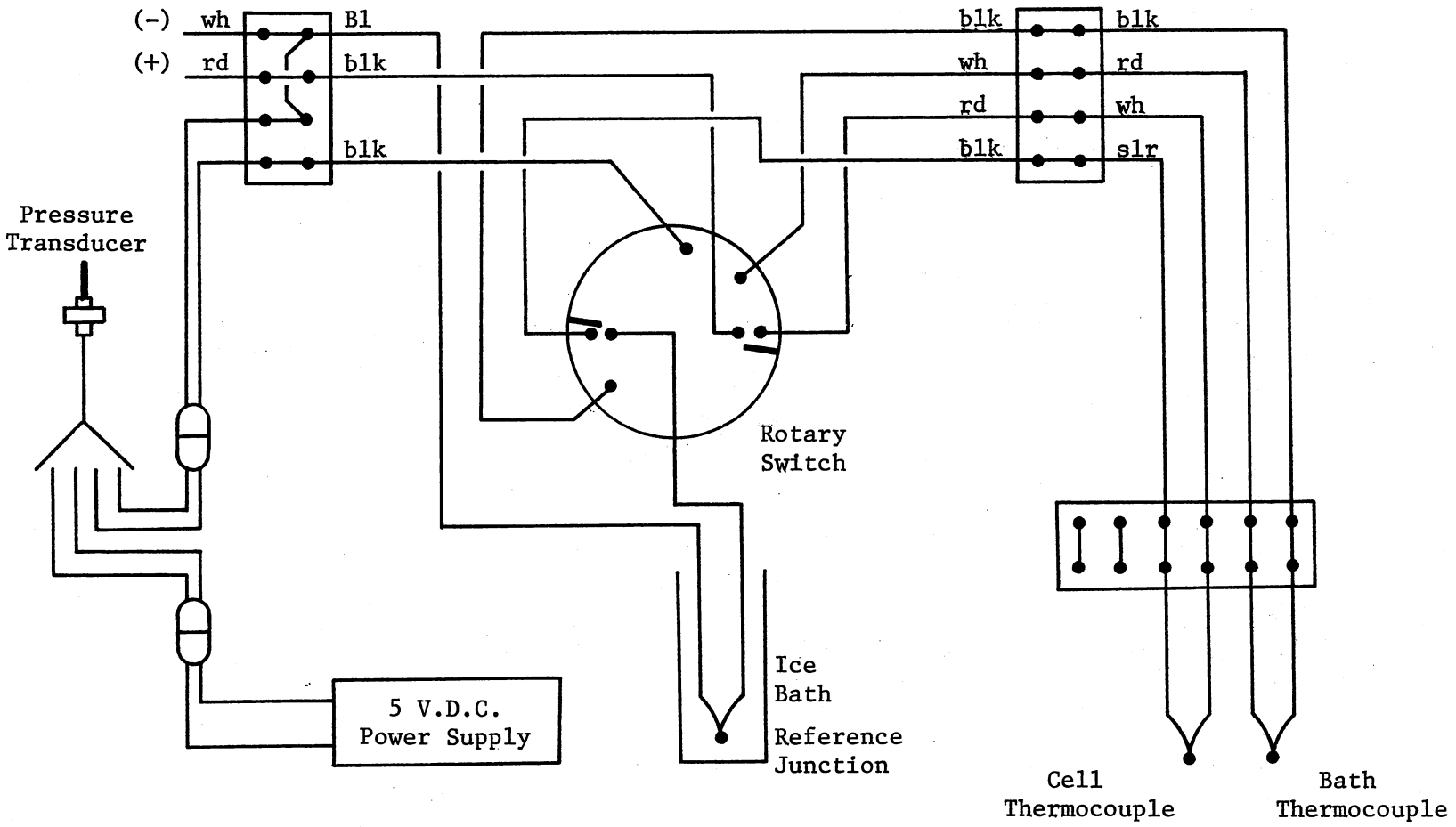

Figure 8. Schematic Diagram of Kinematic Viscometer Apparatus Instrumentation

test capillaries, pump, temperature bath, system pressure gauge, and differential pressure gauges (Figure 9). The viscometer used a positive displacement pump to deliver a steady flow of test fluid through one of the test capillaries. The inlet pressure, temperature, flow rate, and the pressure drop through the capillary were measured. These measurements and the capillary constant allowed the viscosity of the test fluid to be calculated. The components of the viscometer are described in the following sections.

Test Capillaries

The absolute viscometer used three test capillaries. Each capillary was constructed from 304 stainless steel. Table IV lists the capillary dimensions. The test capillaries were manifolded with inlet and outlet valves, pressure taps, and thermocouples.

TABLE IV

CAPILLARY DIMENSIONS

Nominal Outside Diameter inches	Nominal Inside Diameter inches	Length inches
0.0625	0.0065	19.125
0.0625	0.0185	18.250
0.125	0.055	18.4375

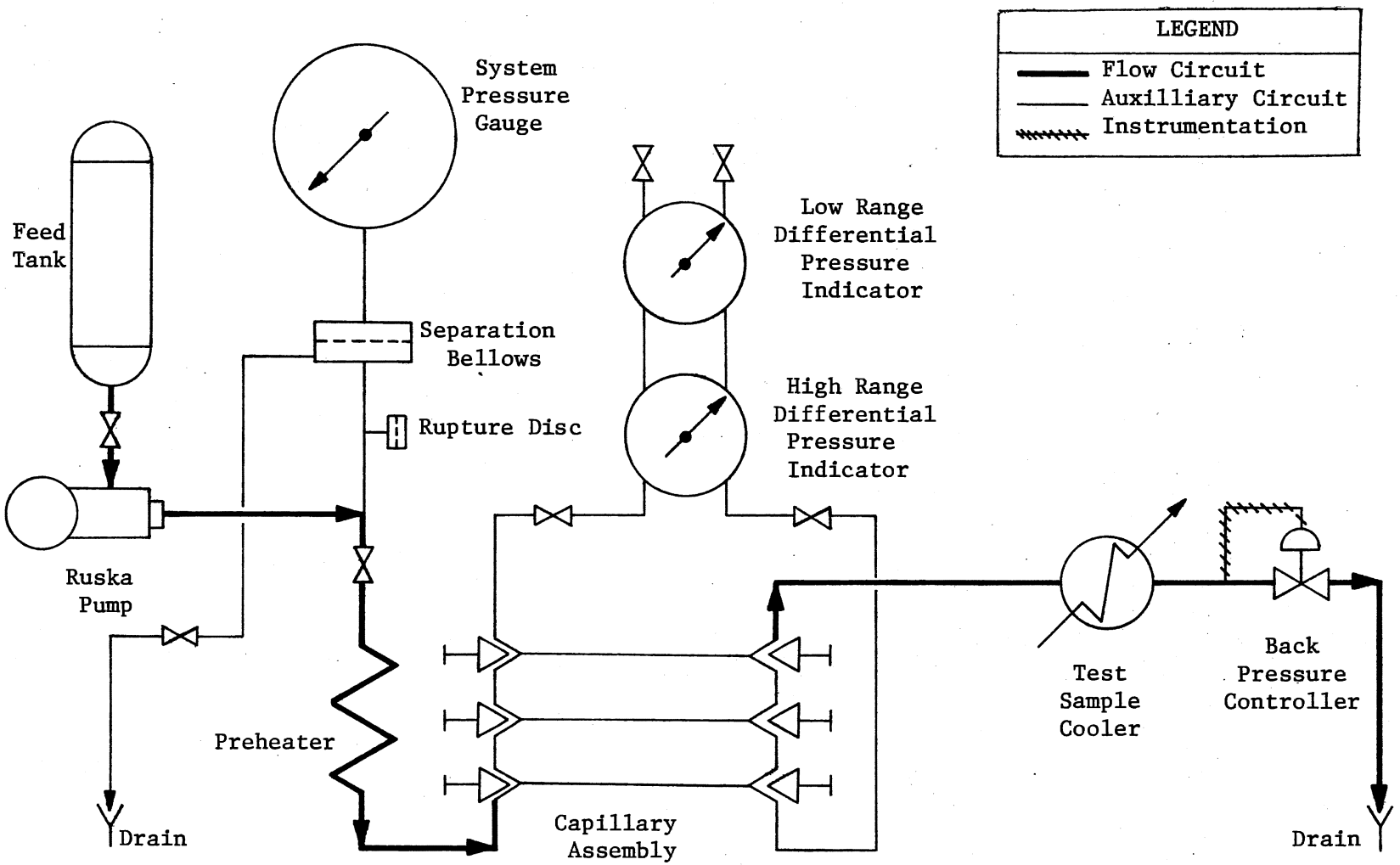

Figure 9. Schematic Flow Diagram of Absolute Viscometer Experimental Apparatus

The manifold blocks, inlet and outlet valves, and the thermocouple assemblies were manufactured by Autoclave Engineers, Inc. The manifold block details are shown in Figure 10. The inlet and outlet valve details are shown in Figure 11. A typical thermocouple assembly is shown in Figure 12.

Positive Displacement Pump

The test liquid was forced through the capillaries by a Ruska Piston Pump, Model Number 2254-803-00, Serial Number 17753. This positive displacement pump could deliver a charge capacity of 250 cm^3 at flow rates between 0.1 and 10 cm^3/min. The pump was driven by a variable speed, direct current electric motor manufactured by the Morse Division of Borg-Warner Corporation. The electric motor was connected to the pump with a chain drive transmission manufactured by Turner Uni-Drive Company, Model Number 2M2-4 RR, Serial Number 70-10077. The transmission had gear ratios of 1:1 and 4:1.

The pump had a slightly varying delivery rate as a function of system pressure. The calibration curves are shown in Appendix C.

Temperature Bath

A fluidized bed sand bath was used to heat and control the temperature of the test liquid. The heating medium, sand, was heated by electric heaters which were controlled by a proportional temperature controller. The sand bath and associated temperature controls were manufactured by Procedyne Corporation. The temperature controller was a Procedyne Thermocal Model TH-050. The bath was fluidized by

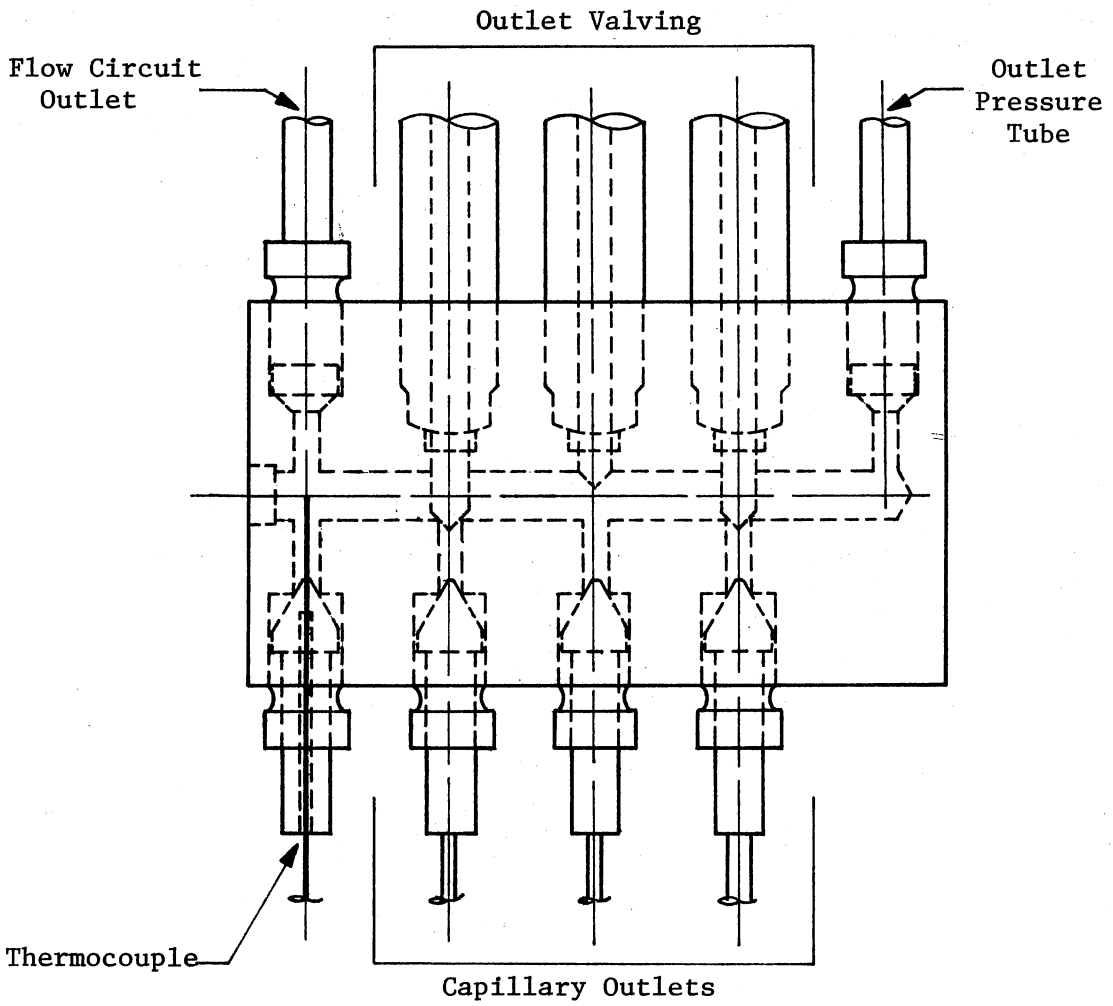

Figure 10. Absolute Viscometer Outlet Manifold Block Details

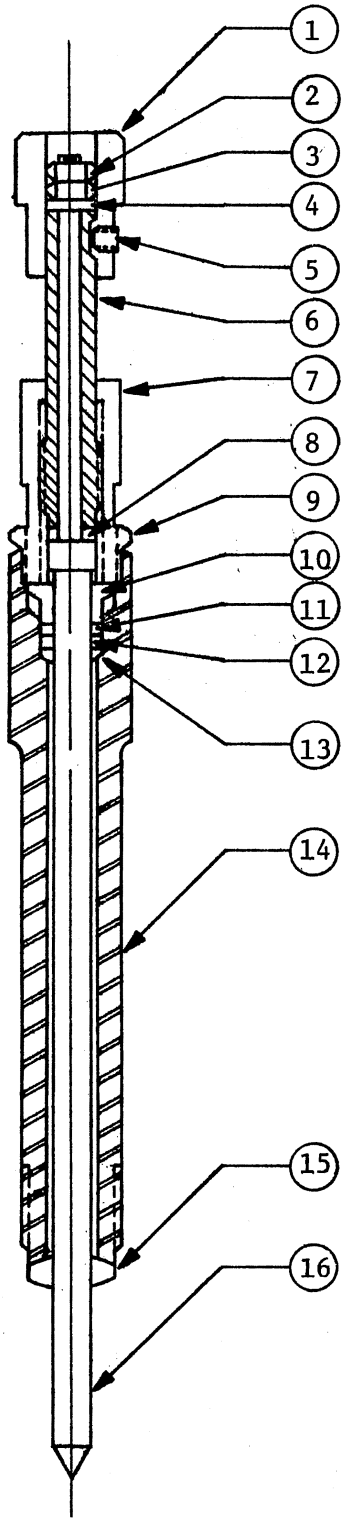

Parts List	
Item Number	Description
1	Stem Drive Adapter
2	Lock Nut
3	Lock Nut
4	Thrust Washer
5	Set Screw
6	Sleeve
7	Gland
8	Thrust Washer
9	Lock Nut
10	Spacer
11	Packing
12	Packing
13	Washer
14	Stem Housing
15	Lens Ring
16	Stem

Figure 11. Absolute Viscometer Inlet - Outlet Valve Details

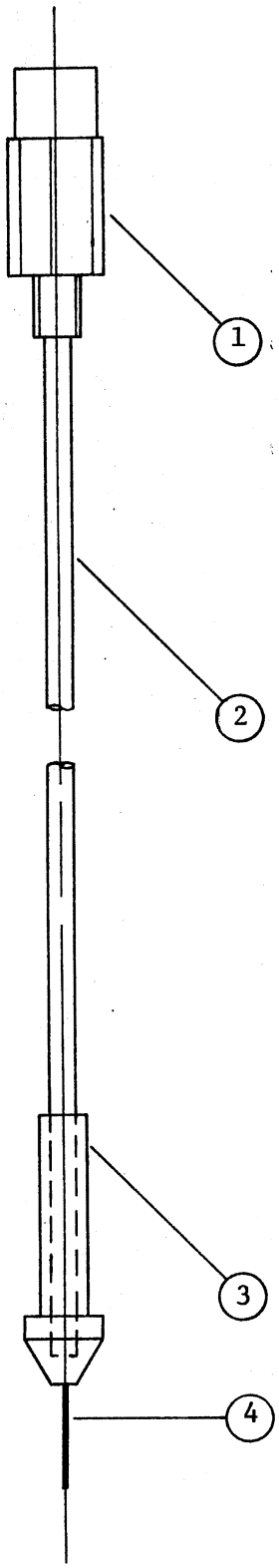

Parts List	
Item No.	Description
1	Electrical Connector QDHT
2	1/8" Stainless Steel Tube
3	Sealant
4	0.020" O.D. Thermocouple

Figure 12. Absolute Viscometer Thermocouple Assembly Details

the flow of compressed air through the sand bed. A rotameter measured the flow rate of the compressed air.

System Pressure Measurement

The system pressure was measured with a Martin-Decker bourdon tube pressure gauge Model Number WA30-0600-1, Serial Number 6540. The gauge had scale divisions of 10 psig from 0 to 6000 psig. The bourdon tube was isolated from the test liquid with an isolation bellows. The system pressure was transmitted to the gauge through the bellows to the bourdon tube. Silicon oil was used to fill the bourdon tube to facilitate ease of cleaning the viscometer between different test samples.

Differential Pressure Measurement

Two different pressure gauges were used to measure the pressure drop across the test capillaries. The gauges were ITT Barton Model 227 differential pressure indicators. The high range gauge, Serial Number 62566, had divisions of 2 inches of water on a scale from 0 to 300 inches of water. The low range gauge, Serial Number 67612, had divisions of 1/2 inch of water on a scale of 0 to 70 inches of water. These differential pressure gauges were connected to the ends of the test capillaries at the manifold blocks. The piping to the gauges required purging to ensure that no gas was trapped in the lines. Trapped gas would give erroneous readings on the differential pressure gauges.

Temperature Measurement

The bath, capillary inlet and outlet, and system outlet temperatures were measured with chromel-constantan thermocouples. The millivolt output from the thermocouples was displayed on a digital voltmeter. The voltmeter was a Newport Laboratories, Inc. Model 2000-1, Serial Number 1376. Thermocouple outputs were displayed to the nearest 1/100 of a volt. All thermocouple readings were referenced to $32^{o}F$.

Experimental Procedure

The experimental procedures for each type of viscometer used during this study are presented in the following sections. The experimental procedure for the kinematic viscometer precedes the procedure description for the absolute viscometer.

Kinematic Viscometer

Zeitfuchs cross-arm capillary viscometers were used for all kinematic viscosity measurements. The viscometer constant was determined by calibration with distilled water. Calibration of the viscometers with a fluid of known viscosity provides a common basis for all viscosity measurements. A change in value of the viscosity of the calibration fluid, supported by new experimental evidence, would alter the calibration constant. The experimental data could easily be updated by use of the new value for the calibration constant.

Calibration of Viscometer

The viscometer was first cleaned thoroughly by three alternating

washings with absolute ethanol, distilled water, and acetone. The viscometer was dried by flowing dry, filtered air through the viscometer. The viscometer reservoir was filled to the prescribed level and secured to the pressure cell top flange. After the pressure cell top flange had been bolted to the pressure cell body and the external connections made, the constant temperature bath was filled with bath fluid. A slight suction was applied to the capillary exit tube to start the calibration fluid flowing down the capillary tube. After flow had been initiated, the flow would continue due to siphon action. Two coupled electric timers were used to measure the time necessary to fill the measuring bulb from the lower to the upper timing marks on the viscometer. The electric timers were manufactured by The Standard Electric Time Company. One timer had divisions of 1/100 of a second with a total measurable time of 60 seconds. The other timer had divisions of 1/100 of a minute with a total measurable time of 60 minutes. The coupled timers allowed measurement of flow times as long as one hour. After a measurement was completed, a slight pressure was applied to the capillary exit tube and the flow reversed. When the calibration fluid had completely returned to the viscometer reservoir, the measurement process could be repeated.

The first measurement was conducted with a dry capillary and was not recorded. Subsequent measurements were made with the capillary tube wetted from previous measurements. Bennett (5) made an extensive study of viscosity measurements using a wetted Zeitfuchs capillary viscometer and found that the measurements were reproducible. The reader is referred to his work for an elaboration on the subject.

In this study, the viscometer calibration and experimental measurements were made with a wetted capillary viscometer.

Due to the large volume of bath fluid in the constant temperature bath and the ability to hold ambient temperature for a time sufficient to conduct the necessary measurements, a temperature control system was not required for the calibration.

The viscometer measuring bulb and reservoir were illuminated by a 15 watt green fluorescent lamp. Observation of the bulb was made through a 14 power cathetometer. The cathetometer allowed use of a smaller capillary than would be possible with an unaided eye. A viscometer with a smaller capillary tube affords the advantage of longer flow times. For a constant time error, a longer flow time gives a smaller relative error. All calibration measurements were made under conditions identical with experimental techniques. Two series of calibration measurements were made. The flow times and viscometer constants are tabulated in Appendix C. The distilled water density and viscosity data are from the Engineering Sciences Data Unit (64).

Preparation of Experimental Apparatus

While the equipment was dismantled, the viscometer was cleaned in the manner previously described. The viscometer was attached to the pressure cell top flange (Figure 5). The top flange was bolted securely to the pressure cell body and the external piping connections were made. The flow system was checked for leaks with compressed gas. After the system was found to be without leaks, the pressure cell and flow system were vented. The vacuum pump was started and

the system was evacuated to approximately 28 inches of mercury vacuum. The system was pressured to approximately 30 psig with test gas, vented, and evacuated again. This procedure was repeated a total of three times to ensure that air was removed from the system. Bagzis (4) showed that such a sweeping procedure resulted in an evacuation equivalent to 0.11 micron of mercury. The reader is referred to his work for a more detailed discussion.

The procedure for filling the viscometer reservoir and the pressure cell differed for different classes of test fluids. The alternate filling procedures are described in the sections that follow for condensible gases and liquids, respectively.

Condensible Gases. After the sweeping procedure had been completed, the pressure cell was cooled below ambient temperature and the condensible gas was allowed to flow into the flow system. The pressure cell was filled until the system pressure equaled the outlet pressure of the test gas regulator. The filled pressure cell was permitted to reach the temperature for measurement. When the desired temperature had been reached, the level of the liquid in the viscometer reservoir was lowered to the height of the reverse bend of the viscometer. The system was then allowed to attain equilibrium.

Liquids. After the sweeping procedure had been completed, a bottle of test liquid was attached to the pressure cell top flange. The appropriate valves were opened and the test liquid was allowed to fill the viscometer reservoir and the pressure cell by gravity. The temperature controller was set to the desired temperature and the pressure cell was allowed to stand until the desired temperature was

reached. The level of test liquid in the viscometer reservoir was lowered to the height of the viscometer reverse bend. The system was then allowed to attain equilibrium.

Operation

To measure the viscosity, all system valves were closed except valves C and D. The volume of the system was increased by the Ruska screw pump or the in-line pressure controller. The resulting decrease in pressure in the capillary exit tube caused the test fluid to flow into the capillary tube. After flow had been initiated, valve C was closed and valve E was opened to equalize the pressures across the flowing fluid. The flow of the sample fluid continued due to siphon action. Electric timers were used to measure the flow times between the timing marks on the viscometer.

At the conclusion of the measurement, valve E was closed and valve C opened. The pressure on the exit tube was increased by manipulation of the Ruska screw pump or the in-line pressure controller which caused the test fluid to return to the viscometer reservoir. The measurement procedure was repeated to provide reproducibility of the flow times. When the flow times remained consistent for several measurements, equilibrium was assumed. The temperature could then be changed and a new series of measurements taken.

After completing the series of measurements, the bath medium was removed and the cell depressured by opening valves C, D, and A. The apparatus could then be dismantled, cleaned, and recharged for another series of measurements.

Absolute Viscometer

The absolute viscometer was used strictly for saturated and sub-cooled liquid viscosity measurements. The inlet and outlet valves on the manifold blocks allowed selection of capillary sizes. The viscometer constant was found by determination of the geometric quantities, radius and length, for each capillary.

Preparation of Viscometer

The absolute viscometer flow system was drained, flushed with air, filled with a suitable solvent, drained and dryed with air prior to any experimental measurements. The pump was then filled with test liquid and the flow system purged of all air. In general, the purging step required a complete pump charge of test liquid.

The following steps were completed prior to starting an experimental measurement. The flow system was pressure tested for leaks to approximately 3000 psig. The capillary was selected. Temperature and pump speed controls were set to appropriate values. The rotameter was opened to fluidize the sand bath. The differential and system pressure gauges were set to zero after a steady no-flow condition had been attained.

Operation

The operation of the absolute viscometer was not difficult. The most critical requirement was to insure that no air or other non-condensible gas was trapped in the instrument lines.

After preparatory steps were completed, the pump was refilled with test liquid and an experimental run was started. The test section inlet valve was opened after a few milliliters of sample entered the flow system. The back pressure regulator was set to the desired system back pressure. The flow system attained steady state flow conditions after approximately 50 ml of test sample had entered the piping. The following experimental data were recorded: thermocouple readings (T.C. 1, T.C. 2, T.C. 3, and T.C. 4), pump speed, back pressure, atmospheric pressure, and differential pressure.

The readings were checked at equal intervals during each pump charge of test liquid. Four to five data readings would be recorded for each pump charge, temperature, and back pressure. After the pump was empty, the preparatory steps were repeated to do another data run. (The cleaning steps were done when the test liquid was changed.)

Materials Tested

The materials tested, purity and suppliers are listed in Table V. The listed purities are quoted from the supplier specifications.

Composition Analysis

A F & M Scientific Company Model 500 Serial Number 1008 gas chromatograph was used to determine the mixture compositions for the ethylene-propylene binaries during this study. The column was a 1/4 inch diameter copper tube six feet in length packed with 30/60 mesh silica gel. Auxiliary equipment is listed in Table VI.

TABLE V

TEST MATERIAL SPECIFICATIONS

Material	Supplier	Grade	Minimum Purity mol %
Argon	Matheson Gas Products	Matheson	99.9995
Ethanol	U. S. Industrial Chemicals Co.	Absolute	--
Ethylene	Phillips Petroleum Co.	--	99.8
Helium	Linde Specialty Gases	Commercial	99.99
Hydrogen	Linde Specialty Gases	Commercial	99.95
Methane	Phillips Petroleum Co.	Pure	99.0
Nitrogen	Matheson Gas Products	Matheson	99.9995
n-Octane	Phillips Petroleum Co.	Pure	99.0
n-Octanol	Fisher Scientific Co.	A.C.S. Certified	--
n-Propanol	Fisher Scientific Co.	A.C.S. Certified	--
Propylene	Phillips Petroleum Co.	Polymerization	99.0

TABLE VI

AUXILIARY CHROMATOGRAPH EQUIPMENT

Equipment Type	Manufacturer	Model	Serial Number
Integrator	Perkin-Elmer	D2	GC 06053
Printer	Kienzle	D11-E	1719
Isolation Transformer	Kuhnke	150 VA	17243

Helium was used as the carrier gas at a flow rate of approximately 60 ml/min through both ports of the detector block. The bridge current was set at 175 mA. The column and block temperatures were set at 125°C for isothermal operation. A Hamilton Company Model 1725NCH 250 µl gastight syringe was used to inject gas samples. The calibration curve for this equipment for ethylene and propylene binaries is shown in Appendix C.

CHAPTER IV

RESULTS AND DISCUSSION OF RESULTS

Absolute Viscosity Measurements

Absolute viscosity measurements for ethanol, n-propanol and n-octane in the critical region were measured using the absolute capillary viscometer. The apparatus was also used to determine the effect of system back pressure on n-octane and n-octanol.

The viscosity behavior of ethanol and n-propanol in the critical region appeared to be normal. The results are illustrated in Figures 13 and 14. These measurements did not reach the critical temperature because the operation became unstable at higher temperatures. The viscosity of ethanol at the highest temperature point was substantially higher than other measurements. The system pressure was below the saturation pressure (vapor pressure) of ethanol. The low system pressure allowed the fluid to become two phase in the flow system which resulted in an erroneous high viscosity. The low viscosity of n-propanol at the lowest temperature point had no apparent explanation other than error in apparatus operation.

The viscosity of n-octane had a significant decrease in the critical region. This behavior has been observed by Khalilov (30) for isomers of n-octane and monocyclic hydrocarbons. Points that deviate from the curve shown in Figure 15 resulted from either operational errors or measurements taken in the two phase region.

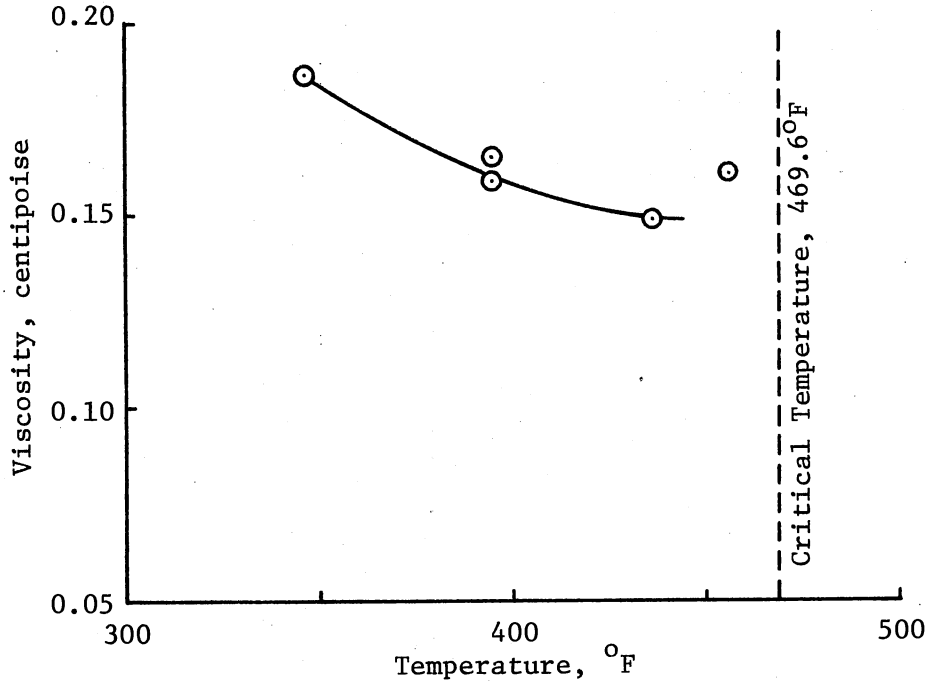

Figure 13. Absolute Viscosity of Ethanol Near the Critical Temperature

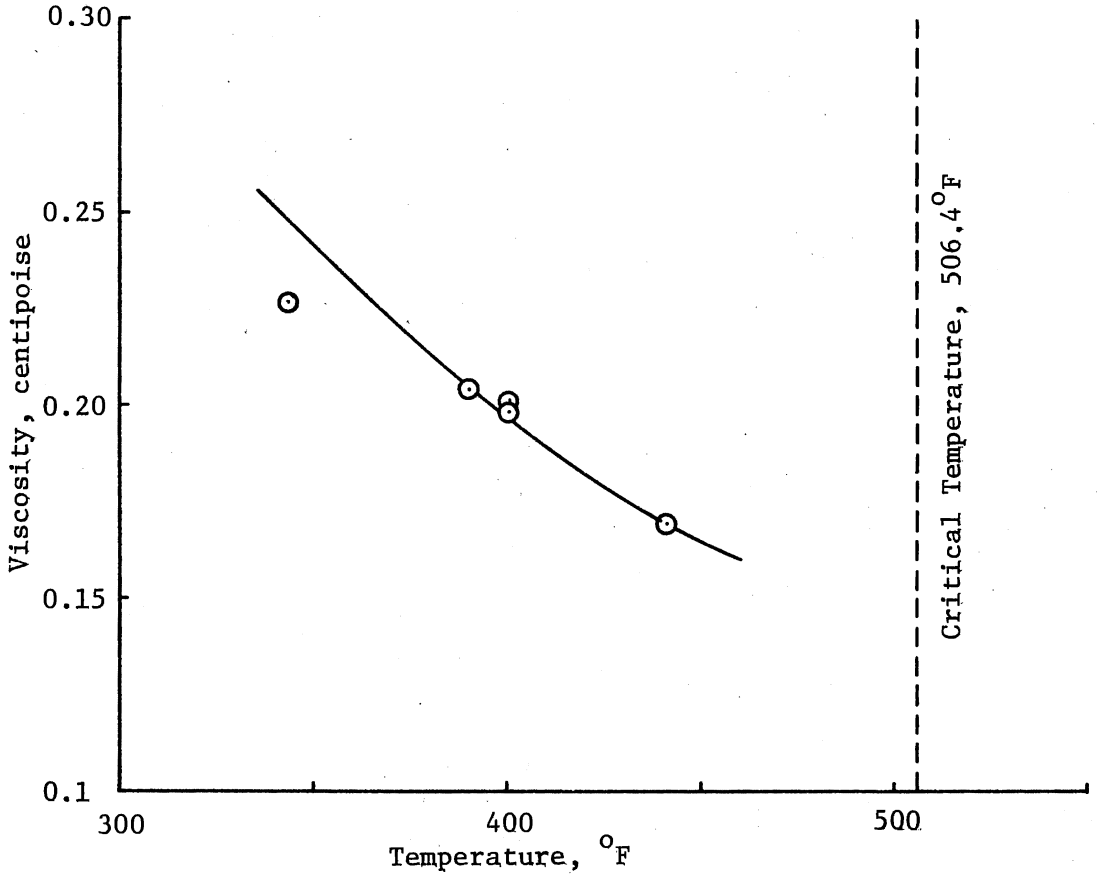

Figure 14. Absolute Viscosity of n-Propanol Near the Critical Temperature

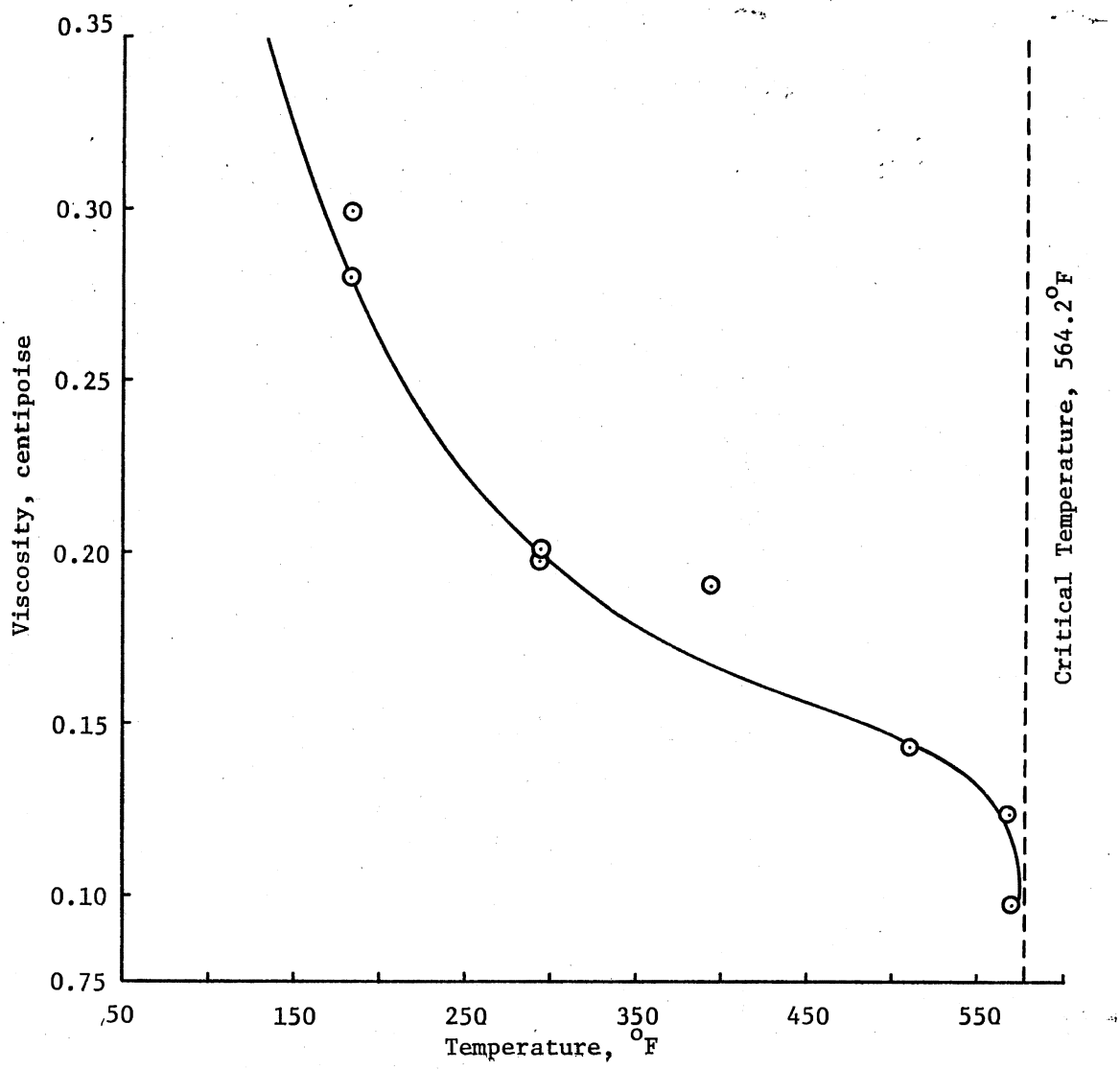

Figure 15. Absolute Viscosity of n-Octane Near the Critical Temperature

The viscosities of n-octane and n-octanol under back pressures up to 1000 psi are illustrated in Figures 16 and 17, respectively. The two materials show similar pressure effects - the isotherms are linear over the pressure range of this study. The slope of the isotherms for both materials decrease as the temperature increases. Extension of these results to higher pressures is not recommended because other workers (10,45) have published results showing non-linear behavior for fluids at higher pressures.

Kinematic Viscosity Measurements

The viscosity of n-octane under gas blankets of argon, helium, hydrogen, methane, and nitrogen was measured using the kinematic viscometer. The isotherms for each mixture are non-linear for gas pressures up to 1000 psia. The results are shown in Figure 18.

The argon - n-octane isotherm was concave in shape and approached linearity at high pressure. The isotherms of n-octane with helium, hydrogen, and nitrogen were convex but approached linearity at pressures greater than 500 psia. The nitrogen - n-octane isotherm showed an initial decrease with pressure then increased rapidly at the higher pressures. The methane - n-octane isotherm showed a very sharp decline then appeared to asymptotically approach a constant viscosity value.

The saturated liquid densities for the n-octane mixtures with hydrogen, methane, and nitrogen were calculated using the G.P.A. K&H computer program (65). The absolute viscosity values for these mixtures are shown in Figure 19. The isotherms are similar in shape to the kinematic viscosity isotherms but show slight decrease in curvature.

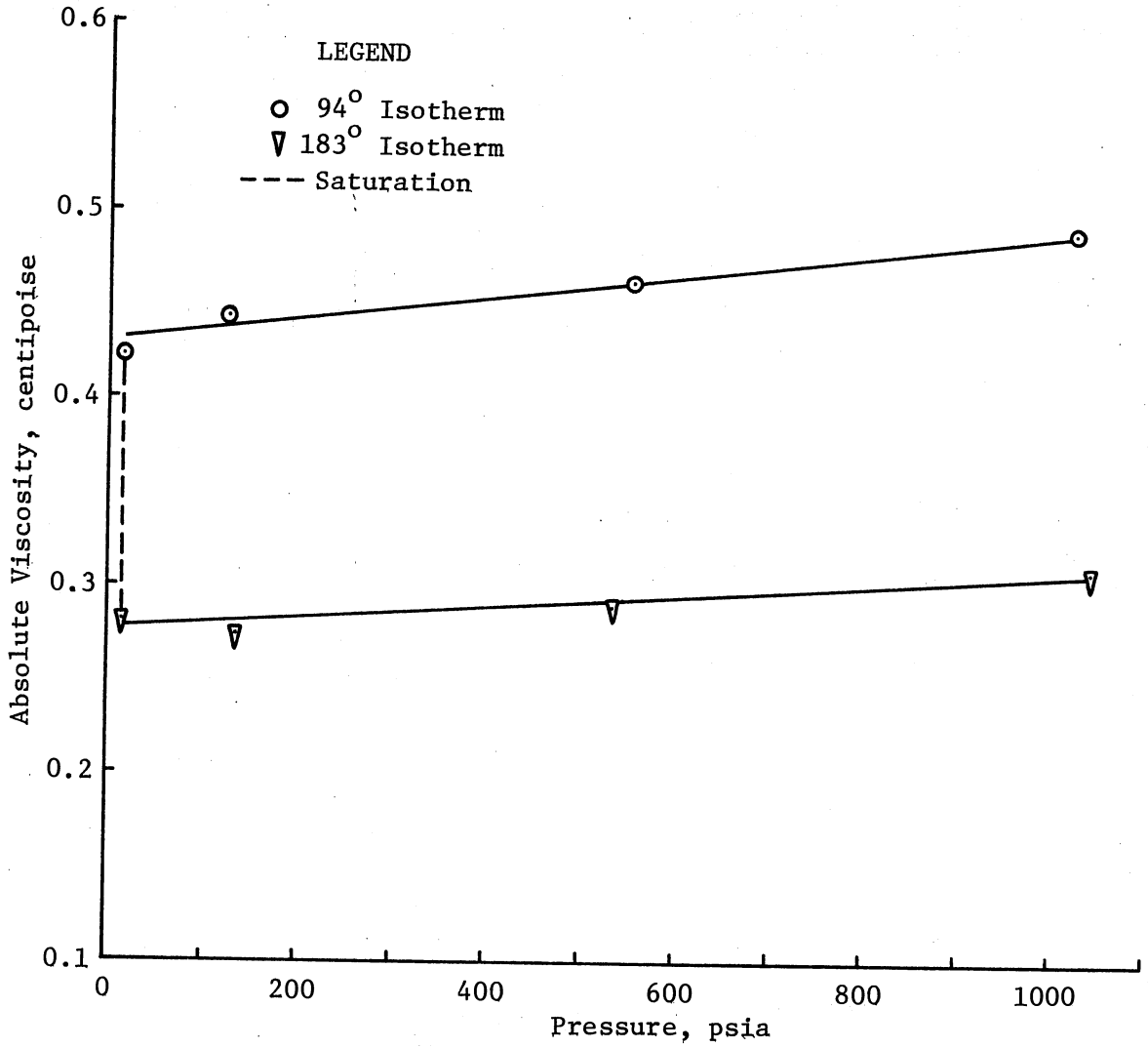

Figure 16. Absolute Viscosity of n-Octane Under Pressure

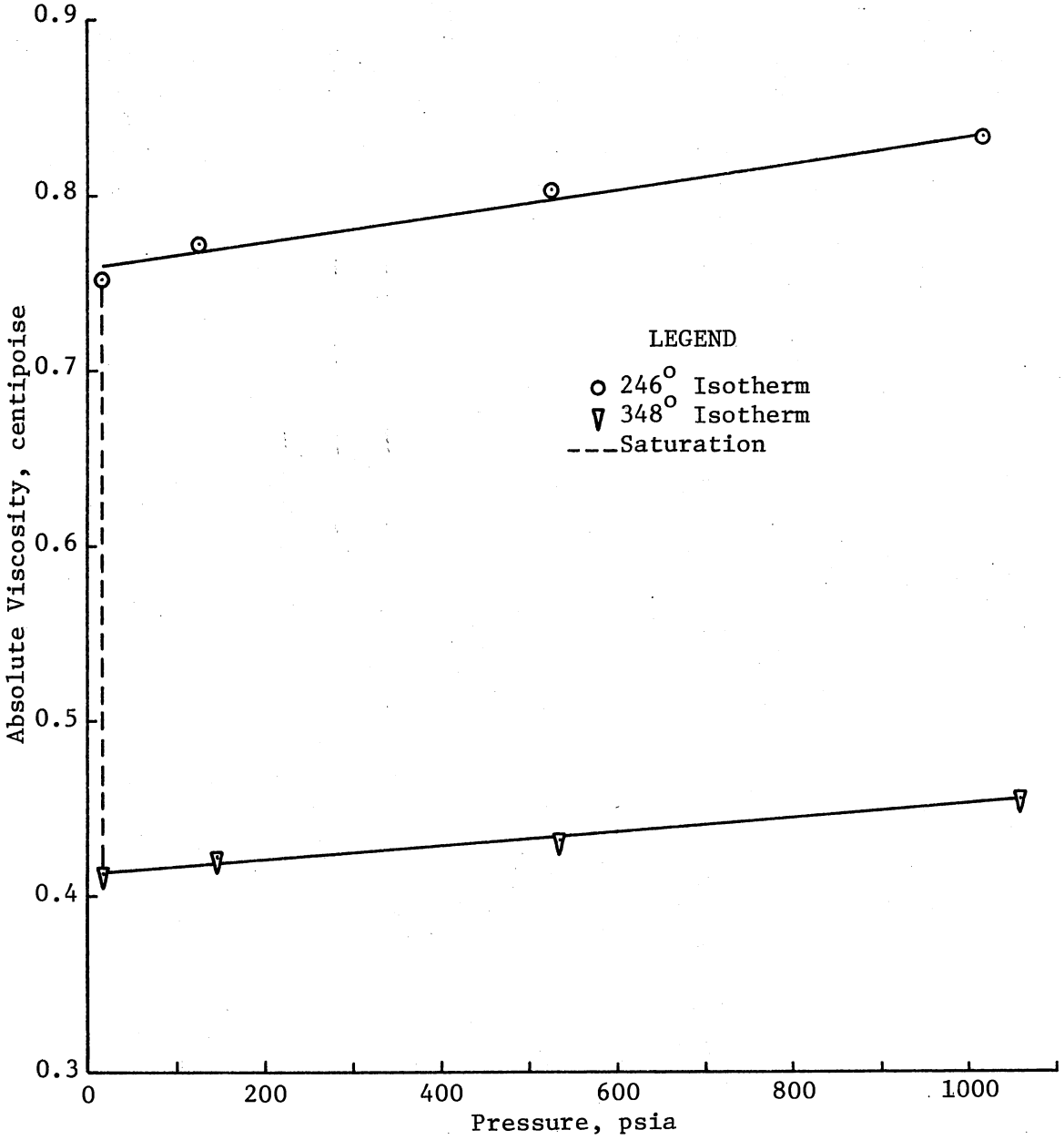

Figure 17. Absolute Viscosity of n-Octanol Under Pressure

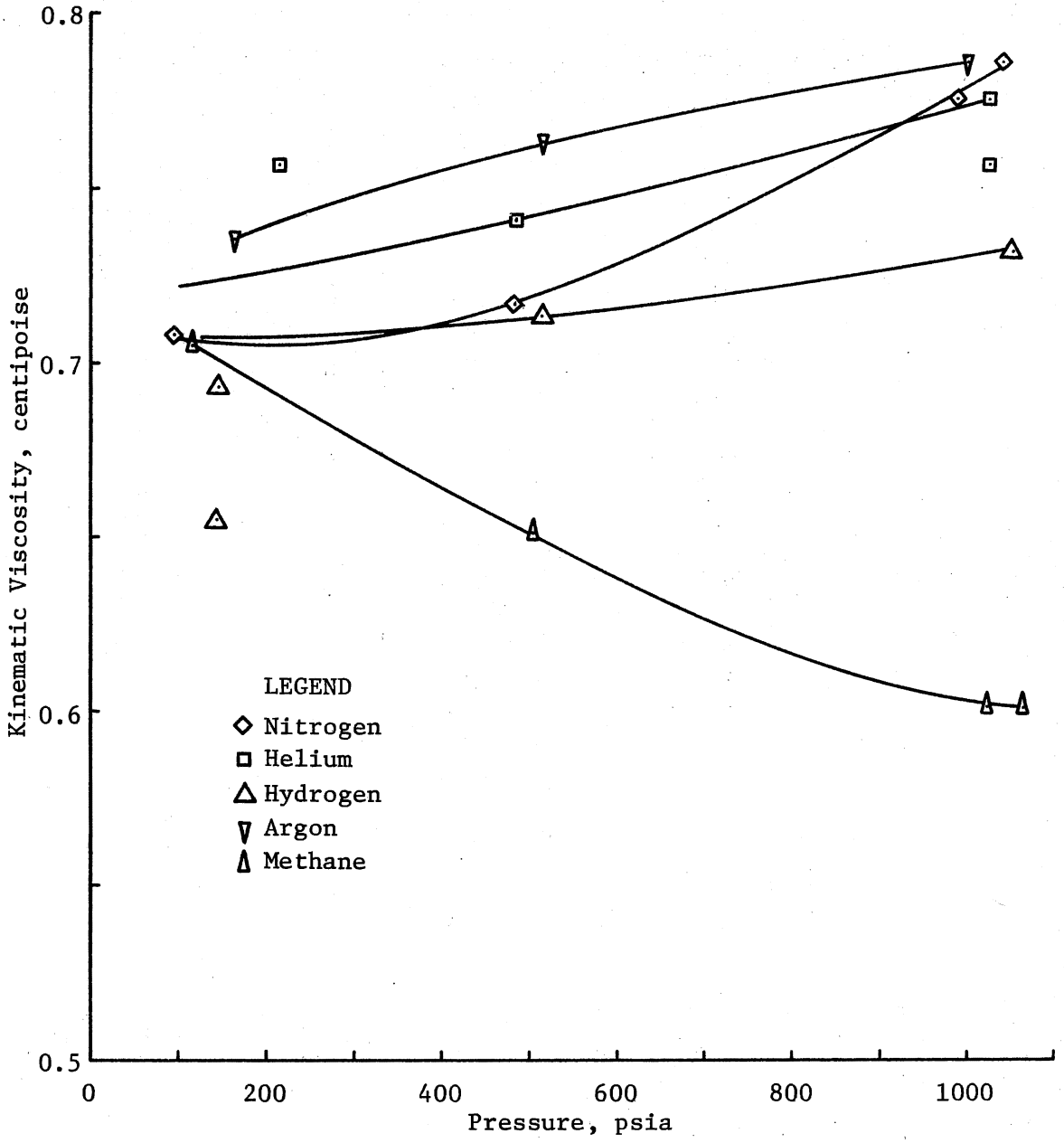

Figure 18. Kinematic Viscosity of n-Octane Under Various Gas Blankets

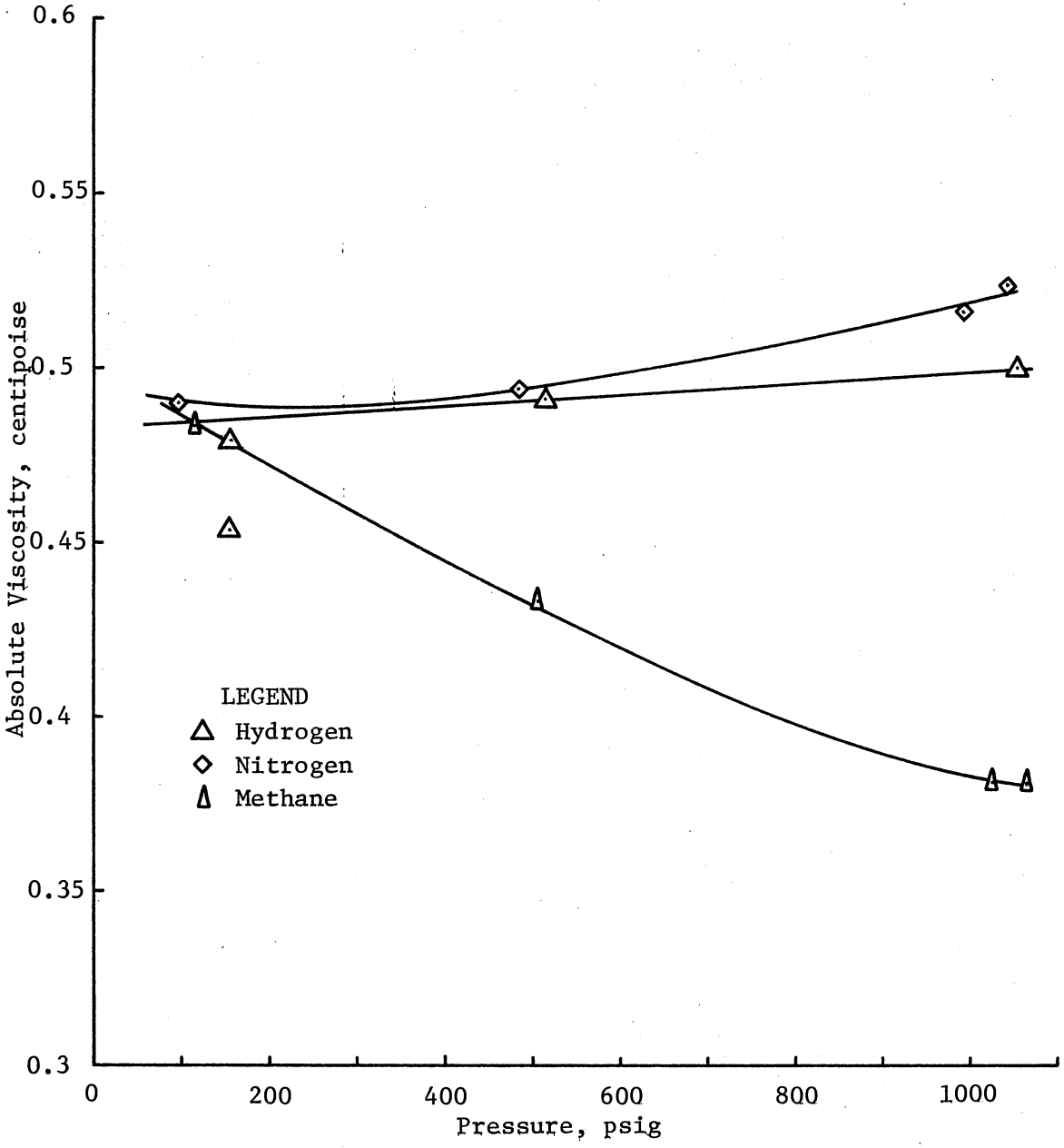

Figure 19. Absolute Viscosity of n-Octane Under Various Gas Blankets

The saturated liquid densities changed with mixture composition which resulted from the increasing gas blanket pressure. The densities and liquid compositions are tabulated in Appendix B.

The kinematic viscosity of n-octanol was measured at saturation conditions at temperatures between 98°F and 155°F. The kinematic viscosity decreased rapidly with increasing temperature. The saturated liquid density of n-octanol was not available for calculation of the absolute viscosity. The kinematic viscosity behavior of n-octanol is illustrated in Figure 20.

The kinematic viscosity of n-octanol under gas blankets of argon, helium, hydrogen, methane, and nitrogen was measured with the kinematic viscometer. The isotherms were convex in shape with the exception of the nitrogen - n-octanol curve which was concave. The mixtures of n-octanol with argon and hydrogen decreased with low pressure initially then increased with pressure. The methane - n-octanol isotherm decreased throughout the pressure range. Figure 21 illustrates these results.

The saturated liquid densities and mixture compositions could not be estimated or measured with analytical equipment presently available. Therefore, the absolute values for the viscosity of these mixtures are not presented.

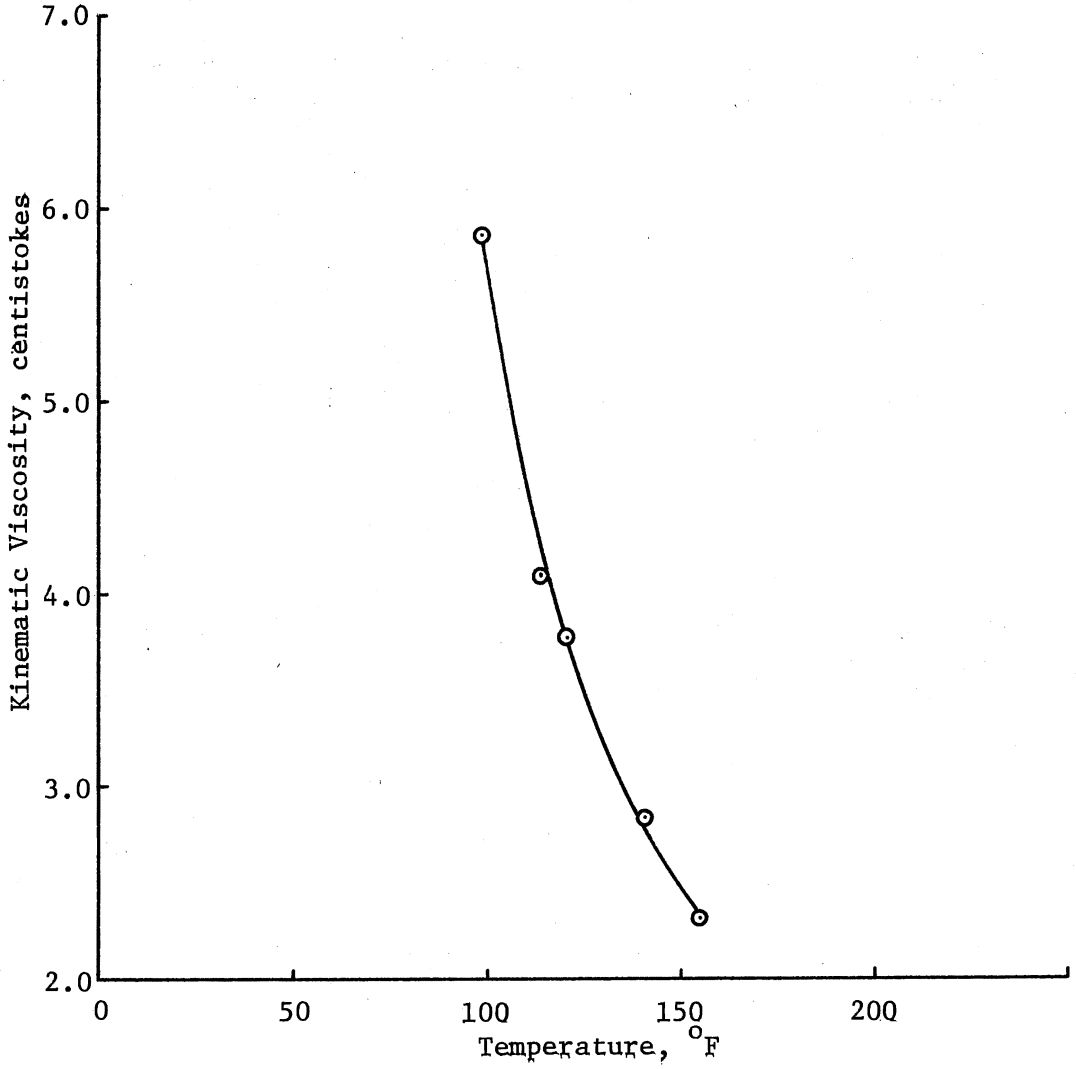

Figure 20. Kinematic Viscosity of n-Octanol at Saturation Conditions

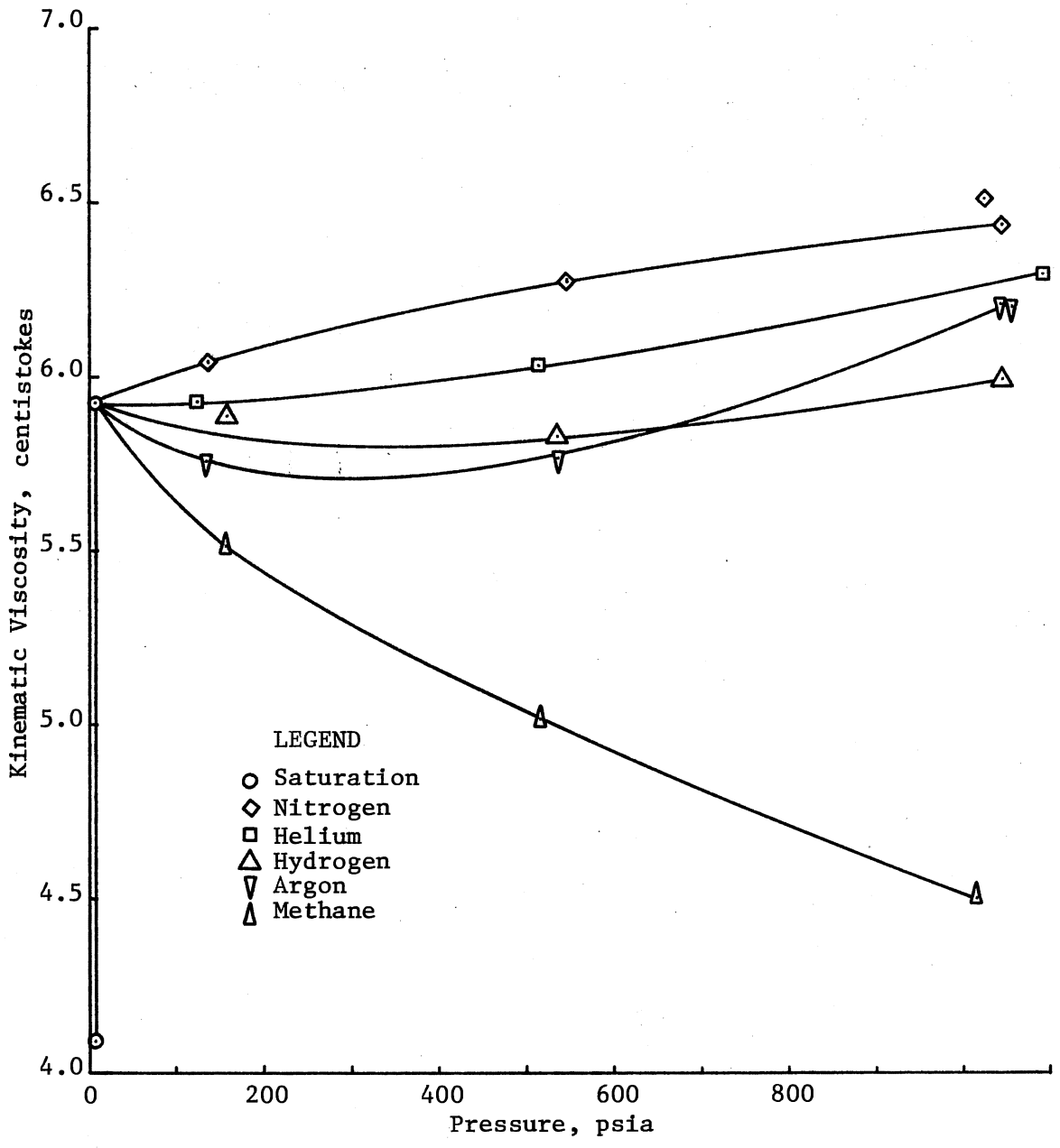

Figure 21. Kinematic Viscosity of n-Octanol Under Various Gas Blankets

CHAPTER V

RECOMMENDATIONS AND CONCLUSIONS

Two types of experimental equipment were used during this study. This section contains recommendations for equipment modification or changes in operational procedures.

Kinematic Viscometer

The kinematic viscometer functioned very well for all systems except the binary system of ethylene and propylene. Recommended equipment modifications are the installation of a liquid trap between the in-line pressure controller and the constant temperature bath and changing the type valves used as valves D and E.

The installation of a liquid trap between the in-line pressure controller and the constant temperature bath would help keep condensate out of the piping system. Currently, no method exists to collect the condensate which can form a liquid plug in the equipment piping. This occurred during measurements of pure components, especially the calibration fluid. The only way to clear the lines is to open the flow system and flow dry filtered air through the lines. The loss of time was not excessive but unnecessary.

Replacing valves D and E with some type quick-opening valve would ease the operation at the beginning of each test run. These valves must be opened to equalize the pressures across the capillary

tube. The valves must be closed to enable the operator to force the test fluid back up the capillary tube. Many valves of the type currently used failed during measurements. The loss of time and fitting costs were substantial. Electrically operated solenoid valves would be the most desirable replacements.

Equipment Malfunction

Measurements of the kinematic viscosity for ethylene - propylene binary mixtures were not done. The experimental apparatus malfunctioned during measurement attempts. Bubbles formed in the viscometer capillary tube causing flow to stop during most of the experimental runs. Runs made with no apparent bubble formation were inconsistent. Flow times varied $\pm$ 100% between consecutive runs. The causes for these experimental difficulties have not been determined. The liquid composition of the mixture under test was found to be 3.2 mole percent ethylene and 96.8 mole percent propylene. The behavior of the mixture should have been very similar to pure liquid propylene.

Future studies should include a definitive investigation to determine the equipment limitations. Some areas for future work are equipment limitations, experimental procedure (technique), test fluid volatility, height of liquid in the viscometer reservoir, differences in the vapor and liquid densities, and consideration of the capillary size as it affects the range of viscosity values that can be measured.

Absolute Viscometer

The absolute viscometer experimental apparatus was easy to operate

and data could be collected much faster than with the kinematic viscometer. Mechanical problems encountered during this study were valves failing to remain operable and cleaning the system between runs on different test samples. The fluidized medium, sand, entered the valve stem packing after a very short period of time causing the valves to become inoperable. The flexibility designed into the apparatus was thus impaired. Measurement precision did not achieve the desired level. Geometric capillary dimensions and differential pressure measurements were the major sources of error. Improvements in the design and instrumentation are discussed in the following sections.

Valve Manifold Blocks

The primary reason for inclusion of the valve manifolds was to provide flexibility in the range of viscosities to be measured. The galling and subsequent failure of the valves during operation resulted in a lack of flexibility and many times caused equipment "down time." Also, the measurements generally were conducted using a single capillary over the temperature and pressure range of interest. Therefore, deletion of the valve manifold will not greatly hamper the operation of the absolute viscometer. The anticipated result is an increase in operation time which will increase the amount of data collected. A block modification deleting the valve arrangement is illustrated in Figure 22. Tables VII and VIII show anticipated pressure losses due to sudden contractions and expansions. The capillary tubes, differential pressure and temperature sensors require

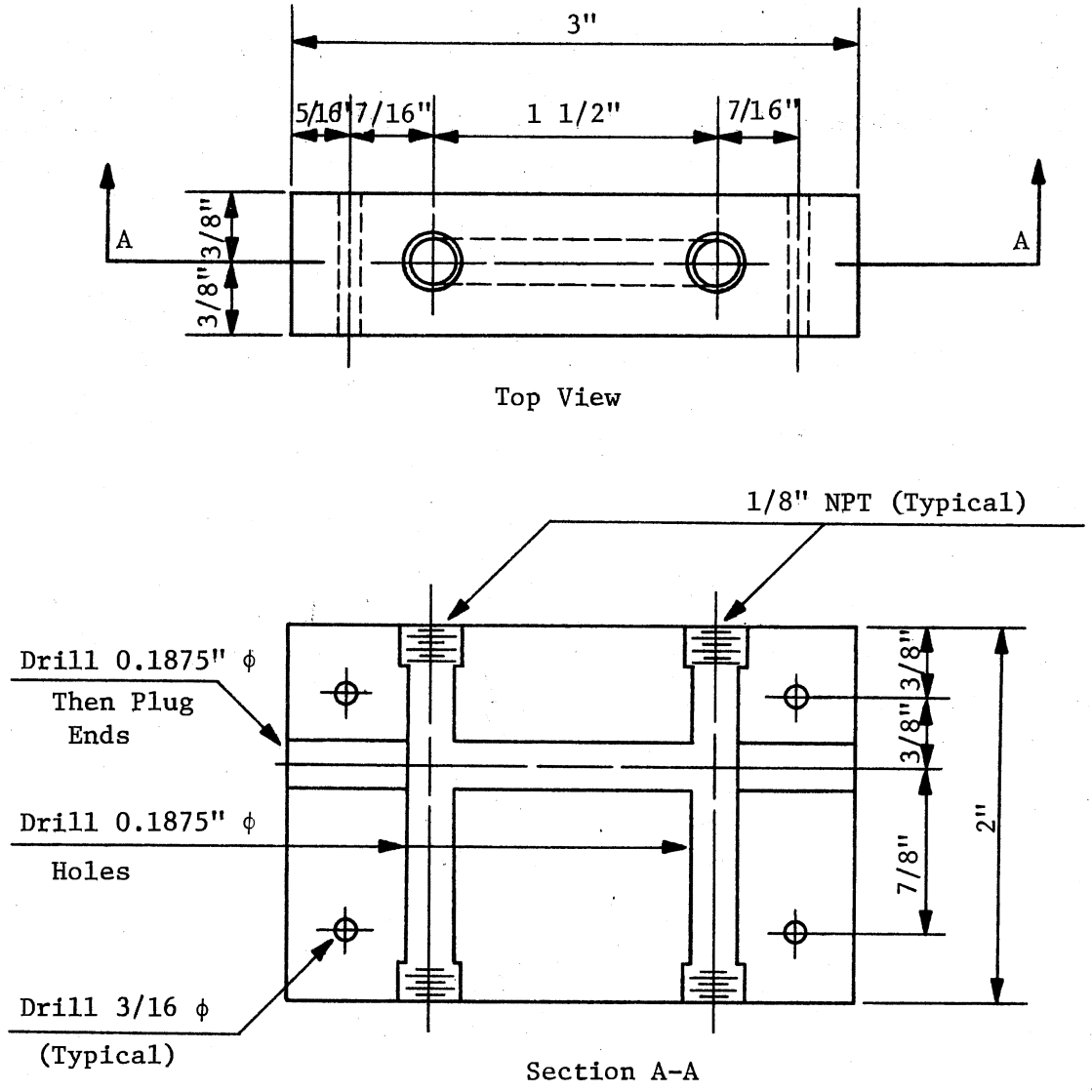

Figure 22. Capillary Support Block

TABLE VII

ANTICIPATED MAXIMUM PRESSURE LOSSES DUE TO SUDDEN PIPING EXPANSIONS

Temperature ^{o}C	Maximum Velocity cm/sec	Maximum Pressure Drop in H_2O	Expansion Pressure Drop in H_2O	Percentage Error
20.0[a]	13.149	300.000	0.0345	0.0115
140.0[a]	67.891	300.000	0.8444	0.2840
260.0[a]	125.738	300.000	2.4570	0.8444
20.0[b]	104.340	293.800	2.1500	0.7293
140.0[b]	104.340	56.913	1.9960	3.5313
260.0[b]	104.340	30.729	1.6889	5.5273
20.0[c]	11.800	3.760	0.0230	0.6218
140.0[c]	11.800	0.729	0.0215	2.9172
260.0[c]	11.800	0.393	0.0184	4.6828

a - small capillary
b - mid-sized capillary
c - large capillary

TABLE VIII

ANTICIPATED MAXIMUM PRESSURE LOSSES DUE TO SUDDEN PIPING CONTRACTIONS

Temperature ^{o}C	Maximum Velocity cm/sec	Maximum Pressure Drop in H_2O	Contraction Pressure Drop in H_2O	Percentage Error
20.0[a]	13.149	300.000	0.0138	0.0046
140.0[a]	67.891	300.000	0.3455	0.1152
260.0[a]	125.738	300.000	0.9980	0.3301
20.0[b]	104.340	293.800	0.8444	0.2840
140.0[b]	104.340	56.913	0.7677	1.3818
260.0[b]	104.340	30.729	0.6756	2.2263
20.0[c]	11.800	3.760	0.0115	0.3071
140.0[c]	11.800	0.729	0.0092	1.2283
260.0[c]	11.800	0.393	0.0077	1.9192

a - small capillary
b - mid-sized capillary
c - large capillary

mechanical support in the temperature bath. This is the only reason to keep a set of blocks in the design.

The flexibility of different capillaries for different ranges of viscosities can be maintained by simply changing the size of capillary between test runs. The redesigned blocks have an added benefit inherent in the design. Fittings throughout the apparatus will be standard, i.e., inventories of multiple type fittings will no longer be necessary.

Cleaning of the flow system will continue to be a problem because no easy modification will alleviate this particular trouble area.

Capillary Dimensions

The length of the capillary used to calculate the viscosity must be the distance between the pressure taps rather than the actual capillary tube length. A standard capillary length of 20 inches should be guaranteed during fabrication of the capillaries. The length would then be the summation of the capillary length and the distances between the capillary connections and the centerline of the pressure taps. The distances between the capillary connections and the centerlines of the pressure taps would be fixed during fabrication and remain constant for all capillary tubes. The preceding assumes that the fittings would not often be replaced.

The capillary radius must be determined experimentally. The difference in weights between the empty capillary and the capillary filled with mercury would be a simple method to determine the average radius of each capillary. Equation 7 illustrates the calculations.

$$r = \left[(m_{Hg} - m_e)/\rho_{Hg}\pi L \right]^{1/2} \qquad (7)$$

The only anticipated experimental difficulties would be ensuring that the capillary tube was completely filled with mercury and that the ends were adequately sealed for weighing. The ends of the capillary could easily be sealed with a tubing fitting.

Differential Pressure Measurement

Currently, differential pressure gauges are used to measure the pressure drop across the capillary tubes. The gauges appear to behave well. However, zero shifts do occur and the slight readjustments could affect the gauge calibrations. The scale divisions of the gauges make differentiation of fractional readings difficult. Installation of a differential pressure transducer should eliminate the problem of fractional readings. The zero shift would not be eliminated, but the shift could easily be determined and allowances made for the associated errors.

Absolute Viscometer Charging with LPG

Materials

Liquefied petroleum gases (LPG) are transported under pressure in cylindrical tanks. The design of the outlet from the cylinders ensures a vapor product. However, the absolute viscometer must be charged with a liquid test sample. Therefore, a scheme to recondense the LPG is required. Two designs were considered - a compression - recondensation scheme and a chilled condensation scheme.

Compression - Recondensation Scheme

The design criteria assumed for the compression - recondensation charging process are as follows:

1. Room temperature = 80°F;
2. Compress the test gas to 700 psia;
3. Compressor efficiency = 60%;
4. Condense the high pressure stream with cooling water;
5. Cooling water outlet temperature = 120°F;
6. Absolute viscometer system volume = 750 cm^3;
7. Charging time = 1 min.

Figure 23 is a schematic flow diagram for this process. The process conditions are noted on the diagram.

A one horsepower compressor is sufficient to charge the system with liquid. The required cooling water flow rate is 25 gal/hr.

Chilled Condensation Scheme

This proposed process simply requires a one liter cylinder immersed in a cold bath to condense the LPG and fill the cylinder. The cylinder is then removed and connected to a device to pump the liquid into the absolute viscometer flow system. The pumping step may be done using either a liquid dip tube in the condensing cylinder connected to a centrifugal pump or a mercury displacement system pressured with compressed air.

The second alternative presented above will be the cheaper process to build. However, difficulty with mercury displacement systems has

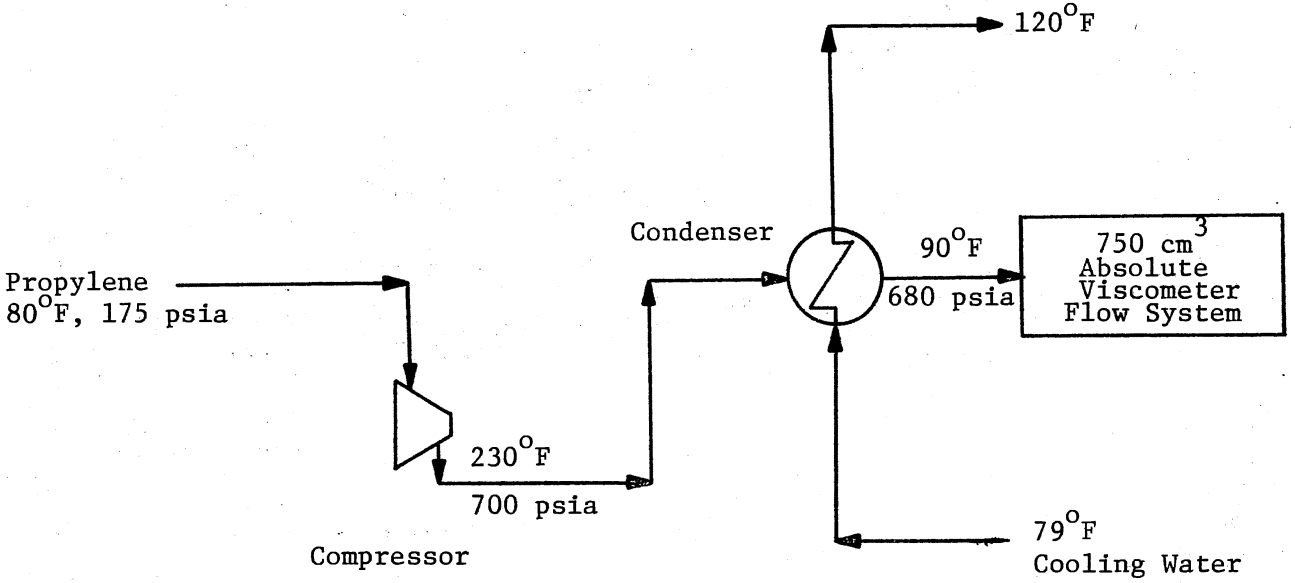

Figure 23. Schematic Flow Diagram for Charging Absolute Viscometer with LPG Type Materials

been encountered in the past. Therefore, the mercury displacement process should be tried first and if no difficulties are encountered continued. The other alternative should be remembered in case operational difficulties arise.

BIBLIOGRAPHY

1. Agaev, N. A. and I. F. Golubev, Gazovaya Prom., 8(5), 45(1963).

2. Agaev, N. A. and I. F. Golubev, Gazovaya Prom., 8(7), 50(1963).

3. Babb, S. E., Jr. and G. J. Scott, J. Chem. Phys., 40(12), 3666(1964).

4. Bagzis, L. D., M. S. Thesis, Oklahoma State University, Stillwater, Oklahoma, May, 1971.

5. Bennett, S. E., M. S. Thesis, Oklahoma State University, Stillwater, Oklahoma, August, 1969.

6. Bicher, L. B., Jr. and D. L. Katz, Ind. Eng. Chem., 35, 754(1943).

7. Bird, R. B., W. E. Stewart, and E. N. Lightfoot, Transport Phenomena, New York: John Wiley and Sons, 1963.

8. Brazier, D. W. and G. R. Freeman, Can. J. Chem., 47(6), 893(1969).

9. Bridgman, P. W., Proc. Natl. Acad. Sci., 11, 603(1925).

10. Bridgman, P. W., Proc. Am. Acad. Arts Sci., 61, 57(1926).

11. Bridgman, P. W., Proc. Am. Acad. Arts Sci., 77, 115(1949).

12. Cannon, M. R., R. E. Manning, and J. D. Bell, Anal. Chem., 32, 355(1960).

13. Carmichael, L. T. and B. H. Sage, J. Chem. Eng. Data, 8(1), 94(1963).

14. Chaudhuri, P. M., R. A. Stager, and G. P. Mathur, J. Chem. Eng. Data, 13(1), 9(1968).

15. Clark, A. L., Trans. Royal Soc., Canada, 9(3), 43(1916).

16. Clark, A. L., Trans. Royal Soc., Canada, 18(3), 329(1924).

17. Dean, W. R., Phil. Mag., Series 7, 4(20), 208(1927).

18. Dean, W. R., Phil. Mag., Series 7, 5(30), 673(1928).

19. Diller, D. E., J. Chem. Phys., 42(6), 2089(1965).

20. Dow, R. B., J. Appl. Phys., 6, 71(1935).

21. Eakin, B. E., K. E. Starling, J. P. Dolan, and R. T. Ellington, J. Chem. Eng. Data, 7(1), 33(1962).

22. Greist, E. M., W. Webb, and R. W. Schiessler, J. Chem. Phys., 29(4), 711(1958).

23. Grevendonk, W., W. Herreman, W. de Pesseroey, and A. de Bock, Rheol. Acta, 8(3), 336(1969).

24. Hawkins, G. A., H. L. Solberg, and A. A. Potter, Trans. A. S. M. E., 57, 395(1935).

25. Heiks, J. R. and E. Orban, J. Phys. Chem., 60, 1025(1956).

26. Hubbard, R. M. and G. G. Brown, Ind. Eng. Chem., 35, 1276(1943).

27. Isakova, N. P. and L. A. Oshueva, Zh. Fiz. Khim., 40(5), 1130(1966).

28. Johnson, J. F., R. L. LeTourneau, and R. Matteson, Anal. Chem., 24, 1505(1952).

29. Kestin, J., J. H. Whitelaw, and T. F. Zein, Physica, 30, 161(1964).

30. Khalilov, Kh. M., Russian J. Phys. Chem., 36(11), 1341(1962).

31. Khalilov, Kh. M., Russian J. Phys. Chem., 37(1), 84(1963).

32. Knudsen, J. G. and D. L. Katz, Fluid Dynamics and Heat Transfer, New York: McGraw-Hill, 1958.

33. Kopylov, N. I., Inzhen.-Fiz. Zh., 97(1960).

34. Lewis, J. R., J. Am. Chem. Soc., 47, 626(1925).

35. Macleod, D. B., Trans. Faraday Soc., 19, 6(1923).

36. Mason, S. G. and O. Maass, Can. J. Research, 18 B, 128(1940).

37. Michels, A., A. Botzen, and W. Schuurman, Physica, 23, 95(1967).

38. McCabe, W. L. and J. C. Smith, Unit Operations of Chemical Engineering, New York: McGraw-Hill, 1967.

39. McCoy, D. D., V. K. Mathur, and R. N. Maddox, Indian J. Chem. Eng., 15(3), 1(1973).

40. Naldrett, S. N. and O. Maass, Can. J. Research, 18 B, 322(1940).

41. Phillips, P., Proc. Royal Soc., London, A 87, 48(1912).

42. Reamer, H. H., G. Cokelet, and B. H. Sage, Anal. Chem., 31 1422(1959).

43. Rein, R. G., Jr., Ph.D. Thesis, University of Oklahoma, Norman, Oklahoma, 1967.

44. Rudolf, H. E., M. S. Thesis, Oklahoma State University, Stillwater, Oklahoma, 1973.

45. Sage, B. H. and W. N. Lacey, Trans. Am. Inst. Mining Met. Eng., 127, 118(1938).

46. Sage, B. H. and W. N. Lacey, Ind. Eng. Chem., 30, 829(1938).

47. Sage, B. H., W. D. Yale, and W. N. Lacey, Ind. Eng. Chem., 31, 223(1939).

48. Schroer, E. and G. Becker, Z. Physik. Chem., A 173, 178(1935).

49. Sigwart, K., Forsch Gebiete Ingen. Wesens., 7 B, 125(1936).

50. Slyusar, V. P., N. S. Rudenko, and V. M. Tret'yakov, Ukr. Fiz. Zh. (Russ. Ed.), 18(2), 190(1973).

51. Smith, A. S. and G. G. Brown, Ind. Eng. Chem., 35(6), 705(1943).

52. Stakelbeck, H., Z. Gesamte Kaehe.-Ind., 40, 33(1933).

53. Starling, K. E., B. E. Eakin, and R. T. Ellington, A.I.Ch.E.J., 6, 438(1960).

54. Starling, K. E., B. E. Eakin, J. P. Dolan, and R. T. Ellington, A. S. M. E. Second Symp. on Thermophysical Properties, Princeton, N. J., 530(1962).

55. Strumpf, H. J., A. F. Collings, and C. J. Pings, J. Chem. Phys., 60(8), 3109(1974).

56. Swift, G. W., J. Lohrenz, and F. Kurata, A.I.Ch.E.J., 6, 415(1960).

57. Trautz, M. and R. Heberling, Ann. Physik., 20, 118(1934).

58. Trautz, M. and I. Husseini, Ann. Physik., 20, 121(1934).

59. Trautz, M. and F. Ruf, Ann. Physik., 20, 127(1934).

60. Trautz, M. and A. Freytag, Ann. Physik., 20, 135(1934).

61. Van Wazer, J. R., J. W. Lyons, K. Y. Kim, and R. E. Colwell, Viscosity and Flow Measurements, New York: Interscience Publishers, 1963.

62. Zollweg, J., G. Hawkins, and G. B. Benedek, Phys. Rev. Lett., 27(18), 1182(1971).

63. Zozulya, V. N. and Yu. P. Blagoi, Zh. Eksp. Teor. Fiz., 66(1), 212(1974).

64. _____, Engineering Sciences Data Unit, Physical Data, Chemical Engineering Sub-Series Volume 1, May, 1975.

65. _____, G.P.A. K&H Computer Program, G.P.A., Tulsa, Okla., 74103.

APPENDIX A

ERROR ANALYSIS

ANALYSIS OF ERROR

Method and Evaluation

Errors associated with experimental measurements are considered to be three types. "Systematic" errors result from improper calibration of measuring devices. "Operator" errors result from experimental blunders. "Random" errors are inherent in all experimental measurements because the experimental equipment has limitations in precision in design. The random errors are the only type of error that are amenable to statistical treatment to estimate the experimental error.

In general, a function W depends upon several independent variables, w_i. Mathematically, for an experiment i,

$$W_i = W(w_1, w_2, w_3, \ldots, w_n) \tag{8}$$

An error in W_i, ΔW_i, is equal to the sum of the errors of the independent variables.

$$\Delta W_i = \sum_{i=1}^{n} \left(\frac{\partial W}{\partial w_i} \right) \delta w_i \tag{9}$$

Squaring both sides of Equation 9 and considering that the experiment was conducted m times

$$\sum_{i=1}^{m} (\Delta W_i)^2 = \sum_{i=1}^{m} \left[\sum_{j=1}^{n} \left(\frac{\partial W}{\partial w_j} \right) \delta w_j \right]^2 \tag{10}$$

Dividing both sides of Equation 10 by m and utilizing the statistical definition of the variance, σ^2, the following equation results

$$\sigma_w^2 = \sum_{j=1}^{n} \left(\frac{\partial W}{\partial w_j}\right)^2 \sigma_{w_j}^2 + 2 \sum_{i=1}^{n} \sum_{j=1}^{n} \tilde{\rho}_{w_i w_j} \left(\frac{\partial W}{\partial w_i}\right)\left(\frac{\partial W}{\partial w_j}\right) \sigma_{w_i} \sigma_{w_j} \quad (11)$$

where $\tilde{\rho}_{w_i w_j}$ is the correlation coefficient of the pair w_i, w_j. This equation can be simplified with the assumption that the independent variables are not correlated, i.e., $\tilde{\rho}_{w_i w_j} = 0$. The resulting expression for the variance of W becomes

$$\sigma_w^2 = \sum_{j=1}^{n} \left(\frac{\partial W}{\partial w_j}\right)^2 \sigma_{w_j}^2 \quad (12)$$

Additional simplification results by dividing Equation 12 by W^2 and taking the square root of the resulting expression. Performing these operations, the following equation results

$$\frac{\sigma_W}{W} = \left[\sum_{j=1}^{n} \left(\frac{\sigma_{w_j}}{w_j}\right)^2\right]^{1/2} \quad (13)$$

The quantity $\frac{\sigma_W}{W}$ is the fractional standard deviation of the dependent variable W. Multiplication of the fractional standard deviation by 100 changes this to the percent deviation. Equation 13 was used as the basis for the error analysis for this study.

Kinematic Viscometer

The relationship between the kinematic viscosity, ν, and time, t, for this study was shown to be

$$\nu = Kt \tag{5}$$

Using Equation 13 the fractional standard deviation in kinematic viscosity is

$$\frac{\sigma_\nu}{\nu} = \left[\left(\frac{\sigma_K}{K} \right)^2 + \left(\frac{\sigma_t}{t} \right)^2 \right]^{1/2} \tag{14}$$

The viscometer constant, K, and the efflux time, t, were evaluated experimentally. The error in K was calculated from the calibration measurements and was found to have a standard deviation of 8.84×10^{-6} for viscometer #U-3501.

To illustrate the errors associated with the kinematic viscosity measurements, two sets of experimental data were selected for calculation of the percent standard deviation of the kinematic viscosity. The experimental measurements of n-octanol and n-octane with a "methane gas blanket" were selected. The n-octanol data required extremely long efflux times. The n-octane with a methane gas blanket required short efflux times. These data illustrate the general range of errors associated with the kinematic viscosity measurements done with viscometer #U-3501. The results are tabulated in Tables IX and X.

The errors in the absolute viscosity, μ, can also be found using Equation 14 with an additional parameter, density. The density was calculated using the G.P.A. K&H program (65). Density is a function of temperature, pressure and the validity of the correlation. To evaluate the errors associated with the density, Equation 13 was used in the following form

TABLE IX

KINEMATIC VISCOSITY PERCENTAGE DEVIATIONS N-OCTANOL

Temperature, ^{o}F	$(\sigma_K/K)^2$	σ_t	Time, sec	$(\sigma_t/t)^2$	$(\sigma_\nu/\nu)(100)$
98.0	5.02×10^{-6}	5.098	1482.7922	1.18×10^{-5}	0.410
114.0	5.02×10^{-6}	5.176	1038.7490	2.48×10^{-5}	0.546
122.0	5.02×10^{-6}	1.108	958.5846	1.34×10^{-6}	0.252
142.0	5.02×10^{-6}	0.818	720.4808	1.29×10^{-6}	0.251
155.0	5.02×10^{-6}	1.358	589.9044	5.30×10^{-6}	0.321

TABLE X

KINEMATIC VISCOSITY PERCENTAGE DEVIATIONS
N-OCTANE WITH METHANE GAS BLANKET

Temperature, ^{o}F	$(\sigma_K/K)^2$	σ_t	Time, sec	$(\sigma_t/t)^2$	$(\sigma_\nu/\nu)(100)$
104.5	5.02×10^{-6}	1.186	178.795	4.40×10^{-5}	0.700
104.2	5.02×10^{-6}	0.629	165.243	1.45×10^{-5}	0.442
140.8	5.02×10^{-6}	0.289	152.095	3.61×10^{-6}	0.294
101.0	5.02×10^{-6}	2.515	152.212	2.73×10^{-4}	1.667

$$\sigma_\rho^2 = \left(\frac{\partial \rho}{\partial T}\right)^2 \sigma_T^2 + \left(\frac{\partial \rho}{\partial P}\right)^2 \sigma_P^2 + C \qquad (15)$$

where C is the estimated correlation error, T is the temperature, and P is the pressure of the system. The partial derivatives were evaluated by numerical techniques using the computer program. Table XI shows the examples selected for the analysis of errors in the liquid density. Table XII shows the deviations found for the density from Equation 15.

TABLE XI

SELECTED EXAMPLES FOR ERROR ESTIMATE

Mixture	Temperature ^{o}F	Pressure psia	Kinematic Viscosity centistokes
n-Octane - Hydrogen	103.0	156.34	0.69347
n-Octane - Methane	104.5	116.38	0.70544
n-Octane - Nitrogen	105.0	484.41	0.71751

The form of Equation 14 used to evaluate the errors in the absolute viscosity was

$$\frac{\sigma_\mu}{\mu} = \left[\left(\frac{\sigma_\nu}{\nu} \right)^2 + \left(\frac{\sigma_\rho}{\rho} \right)^2 \right]^{1/2} \qquad (16)$$

The results of the calculations are shown in Table XIII.

TABLE XII

DENSITY STANDARD DEVIATIONS

Temperature ^oF	$\frac{\partial \rho}{\partial T}$	σ_T ^oF	$\frac{\partial \rho}{\partial P}$	σ_P psi	σ_ρ gm/cm^3
103.0	0.00047	2	0.00001	1	0.00024
104.5	0.00045	2	0.00005	1	0.00023
105.0	0.00047	2	0.00001	1	0.00024

TABLE XIII

ABSOLUTE VISCOSITY PERCENT DEVIATIONS

Temperature ^oF	σ_ρ	ρ	$\frac{\sigma_\rho}{\rho}$	$\frac{\sigma_\nu}{\nu}$	$\frac{\sigma_\mu}{\mu}(100)$
103.0	0.00024	0.69119	0.00035	0.0032	0.322
104.5	0.00023	0.68574	0.00034	0.0070	0.701
105.0	0.00024	0.68798	0.00035	0.0080	0.801

From the preceding error analysis, the sources of error are very close to the same magnitude. The measurement technique should not be altered to attain more precision because the errors are essentially minimized.

Absolute Viscometer

The relationship between the absolute viscosity, μ, and the geometric and experimentally measured quantities; r, L, (ΔP) and Q, was shown to be

$$\mu = \frac{\pi r^4}{8 L} \frac{(\Delta P)}{Q} \tag{6}$$

Using Equation 12, the fractional standard deviation in the absolute viscosity is

$$\frac{\sigma_\mu}{\mu} = \left[\left(\frac{4\sigma_r}{r} \right)^2 + \left(\frac{\sigma_L}{L} \right)^2 + \left(\frac{\sigma_{\Delta P}}{\Delta P} \right)^2 + \left(\frac{\sigma_Q}{Q} \right)^2 \right] 1/2 \tag{17}$$

Equation 17 was used to estimate the minimum experimental fractional standard deviation associated with measurements made with the absolute viscometer during this study. Reasonable estimates of the standard deviations in r, L, (ΔP) and Q are 0.0001 in., 0.05 in., 0.01 (ΔP) and 0.001 ml/sec, respectively. These estimates were based on the scale divisions of the instruments involved and the measurements made to determine the geometric quantities. Table XIV illustrates the fractional standard deviation in the absolute viscosity expected for each capillary size based upon the assumed standard deviations.

TABLE XIV

ANTICIPATED FRACTIONAL STANDARD DEVIATIONS
IN ABSOLUTE VISCOSITY

Capillary Radius in	$\frac{\sigma_r}{r}$	$\frac{\sigma_L}{L}$	$\frac{\sigma_{\Delta P}}{\Delta P}$	$\frac{\sigma_Q}{Q}$	$\frac{\sigma_\mu}{\mu}$
0.00325	0.03077	0.00261	0.01	0.037	0.1289
0.00925	0.01081	0.00274	0.01	0.037	0.0578
0.02750	0.00364	0.00271	0.01	0.037	0.0411

To determine which variable has the greatest effect on the fractional standard deviation of the absolute viscosity, selected values of the standard deviation for each variable were chosen and applied in Equation 17. In each case, the standard deviations of all other variables were held constant. Tables XV through XVIII show the results of the calculations. Figures 24 through 27 graphically illustrate the functional behavior of σ_μ/μ as a function of each variable.

Effect of Capillary Curvature on Liquid Viscosity Measurements

The effect of curved pipes on the motion of fluids has been analized in great mathematical detail by Dean (17,18). The first article cites only qualitative results from his analysis. In the second paper, Dean attempts to quantify the results of the first paper. However, his results (by his own admission) are only order of magnitude estimates. No attempt was made during this study to present

TABLE XV

σ_{μ}/μ AS A FUNCTION OF RADIUS STANDARD DEVIATION

σ_r	$\frac{\sigma_\mu}{\mu}$		
	r=0.00325	r=0.00925	r=0.0275
1.0×10^{-5}	0.0404	0.0387	0.0385
2.0×10^{-5}	0.0457	0.0394	0.0386
3.0×10^{-5}	0.0533	0.0406	0.0387
4.0×10^{-5}	0.0625	0.0422	0.0389
5.0×10^{-5}	0.0726	0.0441	0.0391
6.0×10^{-5}	0.0833	0.0464	0.0394
7.0×10^{-5}	0.0943	0.0489	0.0398
8.0×10^{-5}	0.1057	0.0517	0.0402
9.0×10^{-5}	0.1173	0.0547	0.0406
1.0×10^{-4}	0.1289	0.0578	0.0411

TABLE XVI

σ_{μ}/μ AS A FUNCTION OF LENGTH STANDARD DEVIATION

σ_L	$\frac{\sigma_\mu}{\mu}$		
	r=0.00325	r=0.00925	r=0.0275
0.01	0.12892	0.05781	0.04103
0.03	0.12893	0.05783	0.04106
0.05	0.12894	0.05787	0.04112
0.07	0.12897	0.05794	0.04120
0.09	0.12900	0.05802	0.04132
0.10	0.12902	0.05807	0.04139

TABLE XVII

$\sigma_{\mu/\mu}$ AS A FUNCTION OF DIFFERENTIAL PRESSURE STANDARD DEVIATION

$\sigma_{\Delta P}$	$\frac{\sigma_\mu}{\mu}$		
	r=0.00325	r=0.00925	r=0.0275
0.005	0.12865	0.05722	0.04020
0.007	0.12875	0.05743	0.04049
0.009	0.12887	0.05771	0.04089
0.010	0.12890	0.05787	0.04112
0.011	0.12900	0.05805	0.04137
0.013	0.12920	0.05847	0.04195
0.015	0.12943	0.05894	0.04261

TABLE XVIII

$\sigma_{\mu/\mu}$ AS A FUNCTION OF FLOW RATE STANDARD DEVIATION

σ_Q	$\frac{\sigma_\mu}{\mu}$		
	r=0.00325	r=0.00925	r=0.0275
0.0005	0.12489	0.04817	0.025730
0.0007	0.12620	0.05147	0.031480
0.0009	0.12793	0.05558	0.037820
0.0010	0.12890	0.05787	0.041120
0.0012	0.13126	0.06287	0.047898
0.0016	0.13699	0.07409	0.061890
0.0020	0.14402	0.08640	0.076196

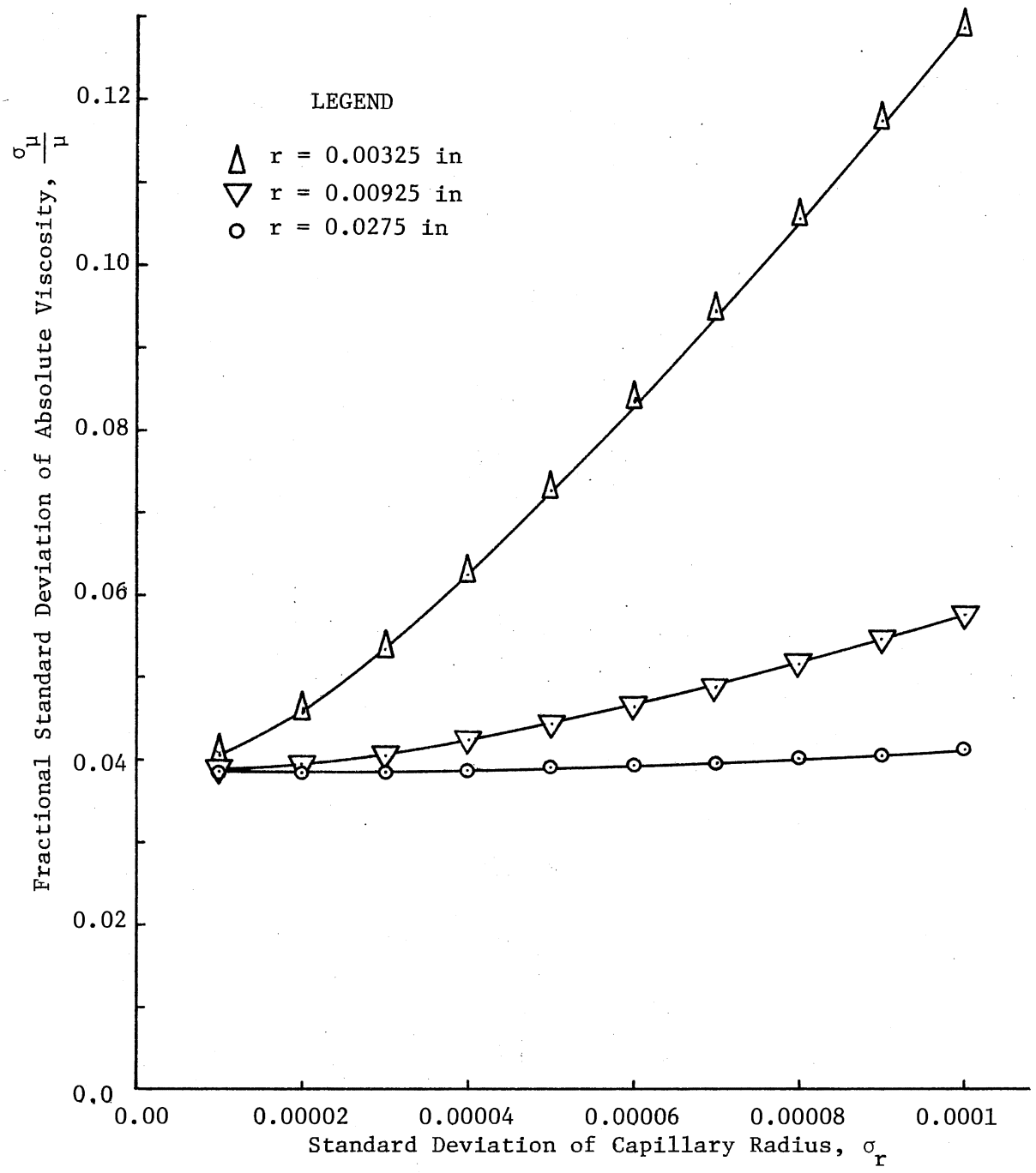

Figure 24. Fractional Standard Deviation of Absolute Viscosity as a Function of the Standard Deviation of the Capillary Radius

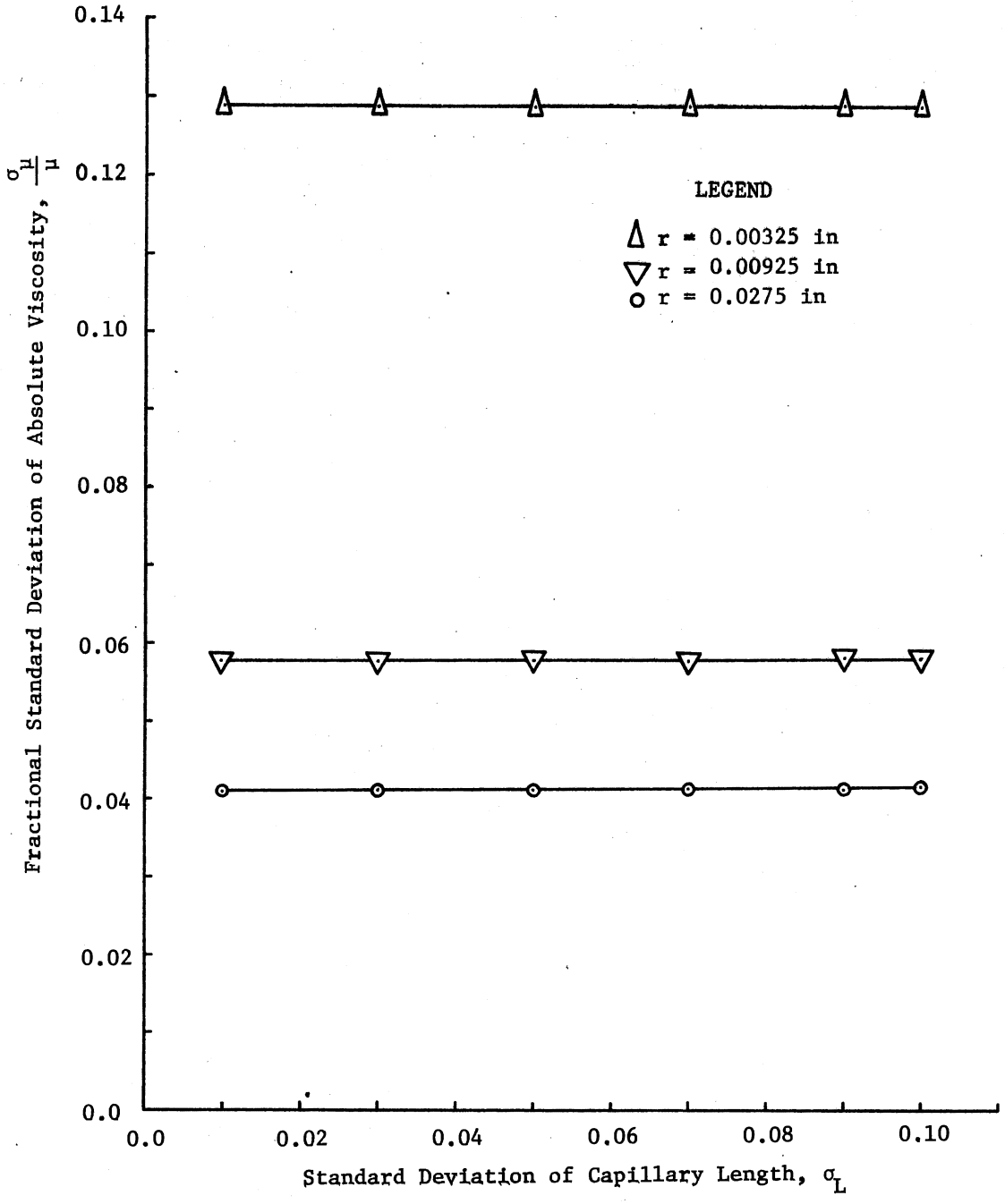

Figure 25. Fractional Standard Deviation of Absolute Viscosity as a Function of the Standard Deviation of the Capillary Radius

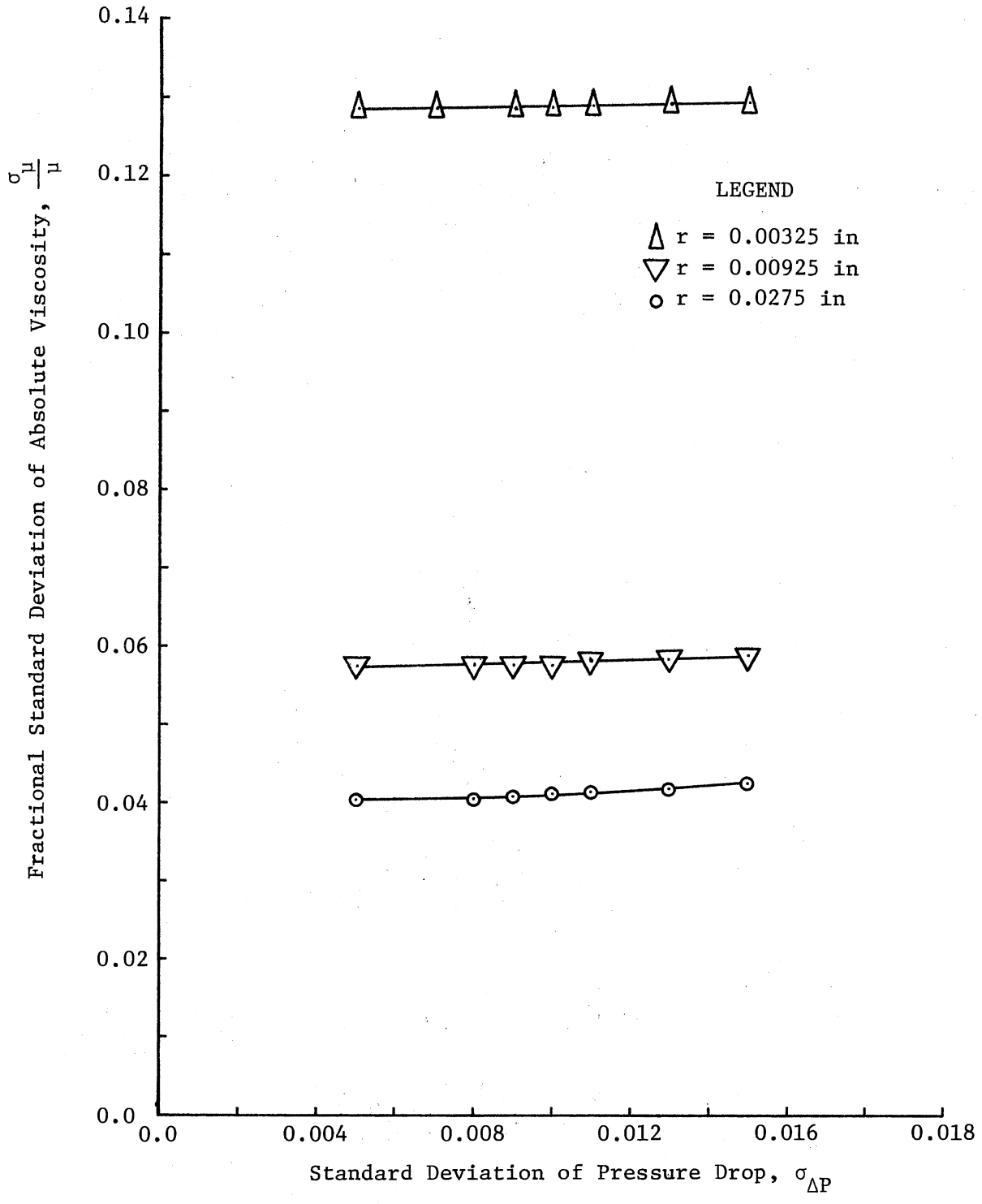

Figure 26. Fractional Standard Deviation of Absolute Viscosity as a Function of the Standard Deviation of the Pressure Drop

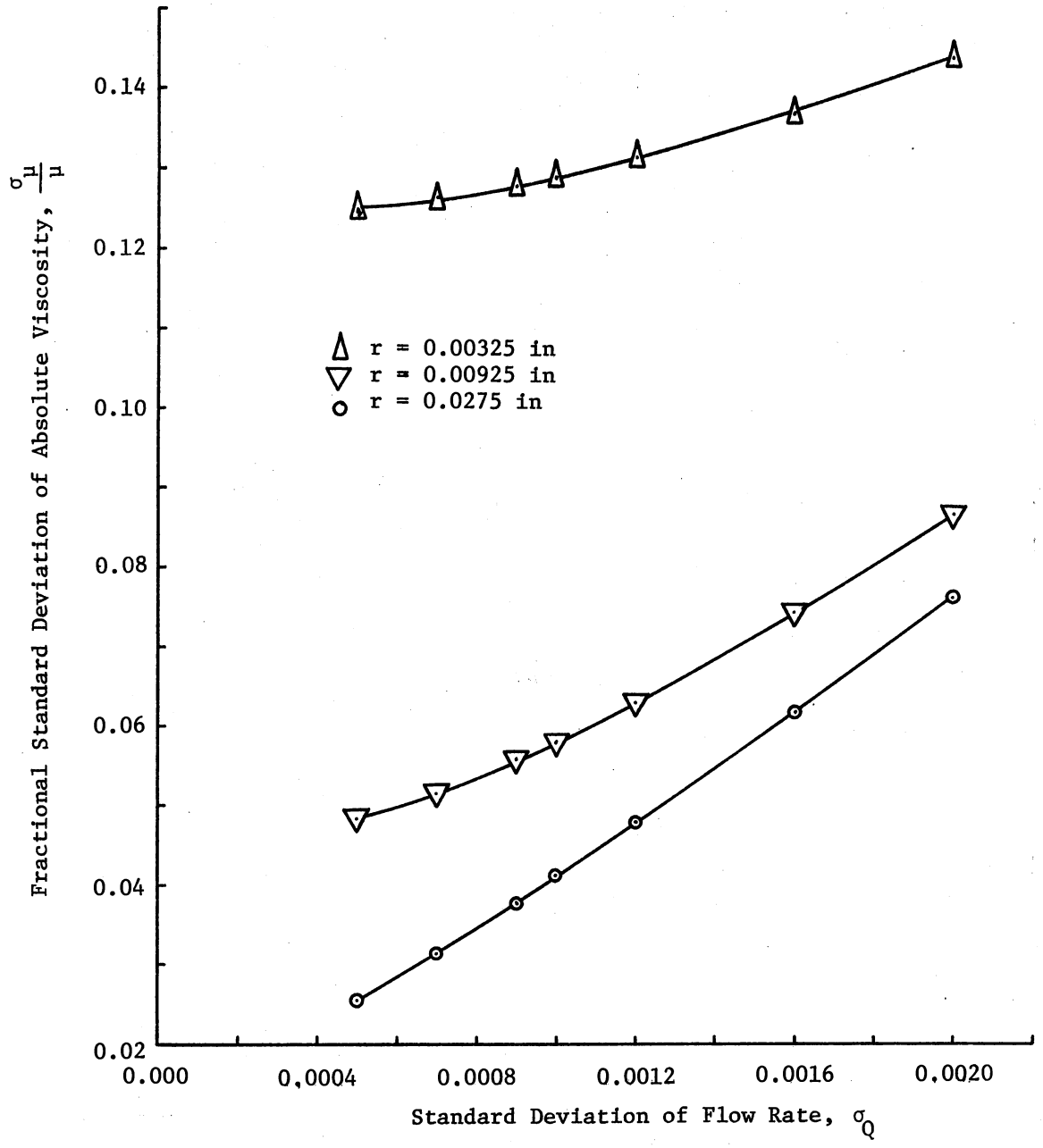

Figure 27. Fractional Standard Deviation of Absolute Viscosity as a Function of the Standard Deviation of the Flow Rate

the mathematical model development done by Dean. The reader is referred to the original works for more detailed information. The pertinent results of Dean's work follow.

For slow fluid motion, Dean derived the following expression

$$K' = 2\, R_e^{\,2}\, r/R \tag{18}$$

where

K' = single flow variable

R_e = Reynolds' number

r = radius of curved tube

R = radius of curvature (180^{o} bend)

An expression was derived for the flow flux through a curved tube, F_c, as a function of the flow flux through a straight tube, F_s, and K', defined in Equation 18.

$$\frac{F_c}{F_s} = 1 - (K'/576)^2(0.03058) \tag{19}$$

Equation 19 can be easily converted into a percentage error expression

$$\frac{(F_s - F_c)}{F_s}\,(100) = 3.058\,(K'/576)^2 \tag{20}$$

Using the transport properties tabulated by the Engineering Science Data Unit (64), the results in Table XIX were calculated for three temperatures. To insure that the calculated percentage errors were maximized the maximum possible flow rate was used in each case, i.e., the ratio of $\Delta P/Q$ was at the maximum value. All capillaries had approximately two inch radii of curvature.

TABLE XIX

ERRORS RESULTING FROM CAPILLARY CURVATURE

Temperature °C	Velocity cm/sec	Density gm/cm^3	Viscosity centipoise	Reynolds' Number	Percentage Error
20.0[a]	13.149	0.99820	1.0020	0.2163	3.3×10^{-14}
140.0[a]	67.891	0.92587	0.1941	5.3470	1.2×10^{-8}
260.0[a]	125.738	0.78407	0.1048	15.5310	8.8×10^{-7}
20.0[b]	104.340	0.99820	1.0020	0.9962	1.2×10^{-10}
140.0[b]	104.340	0.92587	0.1941	23.3870	3.7×10^{-5}
260.0[b]	104.340	0.78407	0.1048	36.6820	2.2×10^{-4}
20.0[c]	11.802	0.99820	1.0020	1.6430	7.9×10^{-9}
140.0[c]	11.802	0.92587	0.1941	7.8650	4.1×10^{-6}
260.0[c]	11.802	0.78407	0.1048	12.3350	2.5×10^{-5}

a - small capillary
b - mid-sized capillary
c - large capillary

The results tabulated in Table XIX show that the curvature effects on the measurement of the absolute viscosity are negligible.

Analysis of Errors Due to Entrance and Exit Piping Configurations

The effect of piping configuration on the measurement of the absolute viscosity are generally considered to result from sudden contractions and/or sudden expansions in the piping. The worst possible case for each configuration is sharp-edged geometry. McCabe and Smith (38) show the relationship between pressure drop and

configuration changes is a function of flow velocity and the cross-sectional areas of the respective pipes. These authors presented Equation 21 for sudden contractions and Equation 22 for sudden expansions.

$$h_{f_c} = 0.4 \left(1 - \frac{S_a}{S_b}\right) \frac{\bar{V}_b^2}{2 g_c} \tag{21}$$

$$h_{f_e} = \left(1 - \frac{S_a}{S_b}\right)^2 \frac{\bar{V}_a^2}{2 g_c} \tag{22}$$

In Equations 21 and 22, the subscripts a and b refer to upstream and downstream, respectively. To express the results in pressure drop units of measurement, these equations must be multiplied by the fluid density. Water was selected to calculate the configuration effects because the physical properties are readily available. Tables XX and XXI illustrate the maximum percentage errors predicted for the entrance and exit configuration effects, respectively. The maximum possible flow rates were used in the calculations. Three temperatures were considered.

As shown in Tables XX and XXI, the maximum percentage error anticipated for entrance and exit piping configurations reached 5.513 percent of the pressure drop. The absolute viscosity is directly proportional to the pressure drop so that the same percentage error would be associated with the measured absolute viscosity.

The recommended redesign of the absolute viscometer should take this source of error into account. The capillary entrance and exit should be carefully machined to provide a smooth path for the fluid to

flow. The smooth condition of the entrance and exit would eliminate the pressure loss due to "sudden" contractions and expansions.

TABLE XX

MAXIMUM PERCENTAGE ERRORS PREDICTED FOR PIPING CONTRACTIONS

Temperature ^{o}C	Maximum Velocity cm/sec	Maximum Pressure Drop in. H_2O	Contraction Pressure Drop in. H_2O	Percentage Error
20.0[a]	13.149	300.000	0.0138	0.0046
140.0[a]	67.891	300.000	0.3423	0.1140
260.0[a]	125.738	300.000	0.9944	0.3310
20.0[b]	104.340	293.800	0.8675	0.2950
140.0[b]	104.340	56.913	0.8047	1.4100
260.0[b]	104.340	30.729	0.6814	2.2200
20.0[c]	11.802	3.760	0.0106	0.2820
140.0[c]	11.802	0.729	0.0099	1.3500
260.0[c]	11.802	0.393	0.0083	2.1200

a - small capillary
b - mid-sized capillary
c - large capillary

Entrance Length Required for Flow Profile to be 99% of Fully Developed

The velocity distribution for fully developed laminar flow is parabolic in shape. The preceding section on entrance and exit configuration effects illustrated that the flow profile is disturbed when the piping changes direction or contains sudden contractions

and/or expansions. Knudsen and Katz (32) present an expression for calculation of the length required to develop 99 percent of the fully developed laminar flow profile.

$$L_e = 0.115\ r\ R_e \qquad (23)$$

Table XXII presents the entrance length requirement for each test capillary in the absolute viscometer.

TABLE XXI

MAXIMUM PERCENTAGE ERRORS PREDICTED FOR PIPING EXPANSIONS

Temperature ^{o}C	Maximum Velocity cm/sec	Maximum Pressure Drop in. H_2O	Expansion Pressure Drop in. H_2O	Percentage Error
20.0[a]	13.149	300.000	0.0346	0.0115
140.0[a]	67.891	300.000	0.8550	0.0285
260.0[a]	125.738	300.000	2.4840	0.0828
20.0[b]	104.340	293.800	2.1570	0.0734
140.0[b]	104.340	56.913	2.0010	3.5160
260.0[b]	104.340	30.729	1.6940	5.5130
20.0[c]	11.802	3.760	0.0253	0.6720
140.0[c]	11.802	0.729	0.0234	3.2180
260.0[c]	11.802	0.393	0.0199	5.0460

a - small capillary
b - mid-sized capillary
c - large capillary

The results tabulated in Table XXII illustrate that the length of capillary required to develop fully developed laminar flow is a small

percentage of the capillary length. When compared to other sources of error studied, the entrance length effect is nearly negligible.

TABLE XXII

ENTRANCE LENGTH REQUIREMENT

Capillary Radius in	Capillary Length in	Reynolds' Number	Entrance Length in	Percentage of Length Required for Flow Profile Development
0.00325	19.1250	15.531	0.00581	0.0334
0.00925	18.2500	36.682	0.03900	0.0214
0.02750	18.4375	12.335	0.03900	0.0212

APPENDIX B

EXPERIMENTAL DATA SUMMARY

TABLE XXIII

ABSOLUTE VISCOSITY OF ETHANOL IN THE CRITICAL REGION

Temperature °F	Pressure psia	Pressure Drop in H_2O	Flow Rate ml/sec	Viscosity centipoise
346.4	304.25	21.800	0.0885	0.18741
394.9	394.37	18.357	0.0880	0.15871
394.3	555.80	19.143	0.0880	0.16550
437.1	579.64	17.288	0.0880	0.14946
456.6	837.95	16.871	0.0795	0.16145

TABLE XXIV

ABSOLUTE VISCOSITY OF N-PROPANOL IN THE CRITICAL REGION

Temperature °F	Pressure psia	Pressure Drop in H_2O	Flow Rate ml/sec	Viscosity centipoise
343.8	151.99	26.600	0.0890	0.22739
391.2	226.10	28.720	0.1070	0.20421
401.1	290.31	27.540	0.1060	0.19767
401.1	571.14	27.743	0.1050	0.20102
442.9	383.52	23.629	0.1060	0.16960

TABLE XXV

ABSOLUTE VISCOSITY OF N-OCTANE IN THE CRITICAL REGION

Temperature ^{o}F	Pressure psia	Pressure Drop in H_2O	Flow Rate ml/sec	Viscosity centipoise
95.0	14.33	16.7690	0.03012	0.42357
183.0	14.30	11.9875	0.03046	0.29941
183.0	14.34	11.1250	0.03022	0.28008
292.0	40.89	7.7000	0.02924	0.20035
292.0	42.22	7.6880	0.02961	0.19754
393.0	132.64	15.0880	0.06000	0.19132
510.0	250.20	16.7130	0.08850	0.14368
558.0	534.90	14.3630	0.08800	0.12418
560.0	395.36	11.2950	0.08800	0.09765

TABLE XXVI

ABSOLUTE VISCOSITY OF N-OCTANE UNDER PRESSURE

Temperature °F	Pressure psia	Pressure Drop in H_2O	Flow Rate ml/sec	Viscosity centipoise
95.0	14.33	16.7690	0.03012	0.42357
93.0	127.20	17.8000	0.03053	0.44358
94.0	554.47	18.3560	0.03022	0.46212
94.0	1028.71	19.0440	0.02965	0.48866
183.4	14.33	11.1250	0.03022	0.28010
183.0	135.08	11.2375	0.03123	0.27380
183.2	533.30	11.8500	0.03121	0.28890
183.4	1041.30	12.3560	0.03043	0.30890

TABLE XXVII

ABSOLUTE VISCOSITY OF N-OCTANOL UNDER PRESSURE

Temperature ^{o}F	Pressure psia	Pressure Drop in H_2O	Flow Rate ml/sec	Viscosity centipoise
245.9	16.33	89.5000	0.0905	0.7524
246.6	125.70	91.0000	0.0895	0.7736
246.9	527.95	93.0625	0.0880	0.8046
246.8	1019.21	95.7500	0.0875	0.8325
346.4	19.22	48.8130	0.0905	0.4104
348.1	148.86	49.5000	0.0892	0.4222
349.3	535.49	49.9400	0.0880	0.4318
348.8	1059.61	52.3750	0.0875	0.4554

TABLE XXVIII

KINEMATIC VISCOSITY OF N-OCTANE UNDER COMPRESSED GAS BLANKETS

Compressed Gas	Temperature °F	Pressure psia	Kinematic Viscosity centistokes
Argon	105.0	163.33	0.73661
Argon	105.0	519.49	0.76362
Argon	106.0	1003.57	0.78618
Helium	104.0	216.44	0.75740
Helium	104.0	486.42	0.74091
Helium	105.0	1030.44	0.77553
Helium	101.8	1030.49	0.75790
Hydrogen	103.0	156.34	0.69347
Hydrogen	100.8	151.28	0.65519
Hydrogen	102.0	515.28	0.71351
Hydrogen	101.8	1055.29	0.73261
Nitrogen	105.0	96.52	0.70860
Nitrogen	105.0	484.41	0.71751
Nitrogen	104.0	992.49	0.77539
Nitrogen	103.9	1046.32	0.78641
Methane	104.5	116.38	0.70544
Methane	104.2	506.39	0.65197
Methane	104.8	1024.33	0.60009
Methane	101.0	1064.38	0.60055

TABLE XXIX

ABSOLUTE VISCOSITY OF N-OCTANE UNDER COMPRESSED GAS BLANKETS

Compressed Gas	Temperature ^{o}F	Pressure psia	Kinematic Viscosity centistokes	Mole Fraction n-Octane	Density gm/cm^3	Absolute Viscosity centipoise
Hydrogen	103.0	156.34	0.69347	0.9916	0.69119	0.4793
Hydrogen	100.8	151.28	0.65519	0.9919	0.69231	0.4536
Hydrogen	102.0	515.28	0.71351	0.9729	0.68750	0.4905
Hydrogen	101.8	1055.29	0.73261	0.9467	0.68141	0.4992
Methane	104.5	116.38	0.70544	0.9599	0.68574	0.4837
Methane	104.2	506.39	0.65197	0.8359	0.66362	0.4327
Methane	104.8	1024.33	0.60009	0.6955	0.63462	0.3868
Methane	101.0	1064.38	0.60055	0.6830	0.63365	0.3805
Nitrogen	105.0	96.52	0.70860	0.9893	0.69135	0.4899
Nitrogen	105.0	484.41	0.71751	0.9479	0.68798	0.4936
Nitrogen	104.0	992.49	0.77539	0.8984	0.68429	0.5306
Nitrogen	103.9	1046.32	0.78641	0.8935	0.68397	0.5379

TABLE XXX

N-OCTANOL KINEMATIC VISCOSITY MEASUREMENTS

Temperature ^{o}F	Pressure psia	Flow Time sec	Kinematic Viscosity centistokes
98.0	5.90	1482.7922	5.8504
102.9	8.70	1038.7490	4.0984
104.4	9.98	958.5846	3.7821
141.0	12.36	720.4808	2.8427
155.0	13.23	589.9044	2.3275

TABLE XXXI

KINEMATIC VISCOSITY OF N-OCTANOL UNDER COMPRESSED GAS BLANKETS

Compressed Gas	Temperature °F	Pressure psia	Kinematic Viscosity centistokes
Argon	99.0	132.29	5.7690
Argon	99.0	535.24	5.7705
Argon	102.0	1057.42	6.2037
Argon	97.0	1043.50	6.2179
Helium	99.0	123.25	5.9382
Helium	98.0	512.33	6.0758
Helium	97.0	1094.34	6.2971
Hydrogen	97.0	159.52	5.8965
Hydrogen	97.0	535.58	5.8300
Hydrogen	98.0	1049.40	5.9514
Nitrogen	98.0	136.46	6.0410
Nitrogen	101.0	545.40	6.2751
Nitrogen	96.0	1043.57	6.4355
Nitrogen	97.0	1033.58	6.5012
Methane	96.0	153.66	5.5389
Methane	97.0	514.54	5.0255
Methane	97.0	1011.49	4.5307

APPENDIX C

INSTRUMENT CALIBRATIONS

INSTRUMENT CALIBRATIONS

Calibration of Pressure Sensors

The calibration of the system pressure sensors for both viscometers used during this study was done using a Ruska Model 2400HL dead weight pressure system. The accuracy of this equipment (manufacturer specification) was a minimum of 0.01 percent of reading up to a pressure of 12140 psi.

The sensors calibrated were a Consolidated Electrodynamics Corporation Model 4-317 pressure transducer (Serial Number 8642) and a Martin-Dicker bourdon tube pressure gauge, Model Number WA30-0600-1 (Serial Number 6540). The calibration data for these sensors are tabulated in Tables XXXII and XXXIII. The results are illustrated in Figures 28 and 29.

An Ashcroft compound gauge was also used during this study. The compound gauge was calibrated against a 30 inch mercury-in-glass-manometer. The results for the Ashcroft gauge are tabulated in Table XXXIV and illustrated in Figure 30. The pressure range of the calibrations was more than adequate for purposes of this study.

Two ITT Barton differential pressure indicators were used to measure the differential pressure across the capillary tubes of the absolute viscometer. A 30 inch mercury-in-glass-manometer was used to calibrate these gauges. The calibration data are tabulated in Tables XXXV and XXXVI. Figures 31 and 32 illustrate the results of the calibrations.

TABLE XXXII

CALIBRATION OF CEC MODEL 4-317 PRESSURE TRANSDUCER
SERIAL NUMBER 8642

Dead Weight Tester psig	Null Indicator	Actual Pressure psig	Pressure Transducer mV
-	-	-	3.86020
26.1 + 3 gm	0	26.612	4.01195
121.7	-20	121.338	4.82184
222.9 + 2 gm	-6	223.154	5.61653
325.5 + 4 gm	-6	326.096	6.42214
430.3	13	430.588	7.24474
528.7	4	528.809	8.01830
629.0	19	629.406	8.80666
730.4	22	730.864	9.60572
833.1	-21	832.716	10.41627
929.3	10	929.529	11.17404
1023.4	-20	1023.038	11.91285
962.5	15	962.828	11.40666
864.4	-4	864.332	10.62285
758.7	4	758.809	9.78004
651.7	-6	651.613	8.94036
553.7	-14	553.454	8.16733
451.4 + 3 gm	-10	451.741	7.36495
355.0 + 3 gm	-1	355.614	6.61412
249.7 + 2 gm	-7	249.934	5.79159
147.1 + 2 gm	-9	147.293	4.98890
47.9	4	48.009	4.21608
-	-	-	3.83925

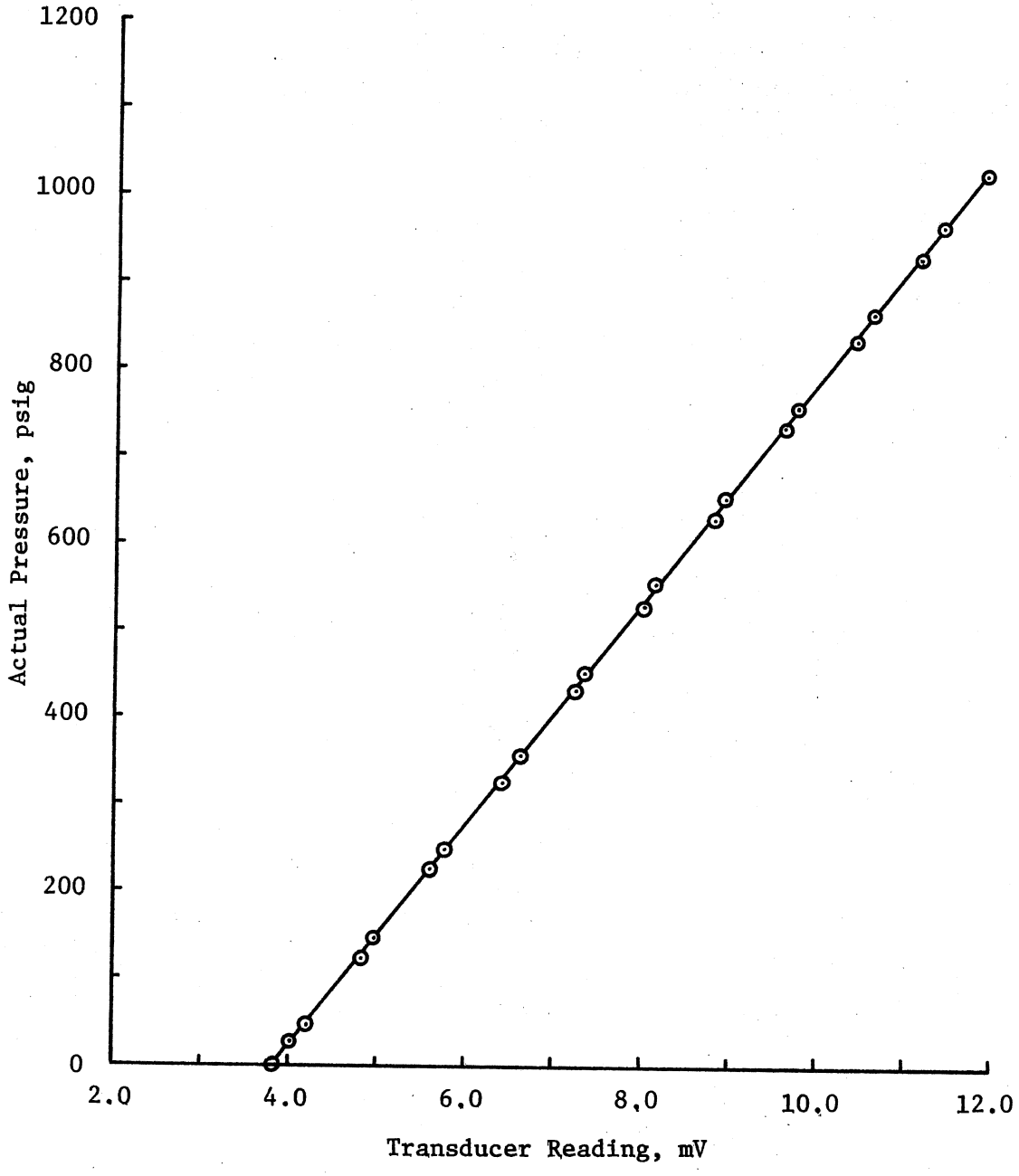

Figure 28. Calibration Curve for CEC Pressure Transducer (Serial Number 8642) for System Pressure Measurements on the Kinematic Viscometer

TABLE XXXIII

CALIBRATION OF MARTIN-DECKER PRESSURE GAUGE
SERIAL NUMBER 6540

Dead Weight Tester psig	Actual Pressure psig	Pressure Gauge psig
-	0.0	0.0
26.1 + 3 gm	26.6	23.0
121.7	121.3	119.0
222.9 + 2 gm	223.2	220.0
325.5 + 4 gm	326.1	320.0
430.3	430.6	421.0
528.7	528.8	522.0
629.0	629.4	621.0
730.4	730.9	721.0
833.1	832.7	821.0
929.3	929.5	920.0
1023.4	1023.0	1016.0
962.5	962.8	957.0
864.4	864.3	856.0
758.7	758.8	750.0
651.7	651.6	648.0
553.7	553.5	550.0
451.4 + 3 gm	451.7	445.0
355.0 + 3 gm	355.6	350.0
249.7 + 2 gm	249.9	249.0
147.1 + 2 gm	147.3	148.0
47.9	48.0	49.0
-	-	0.0

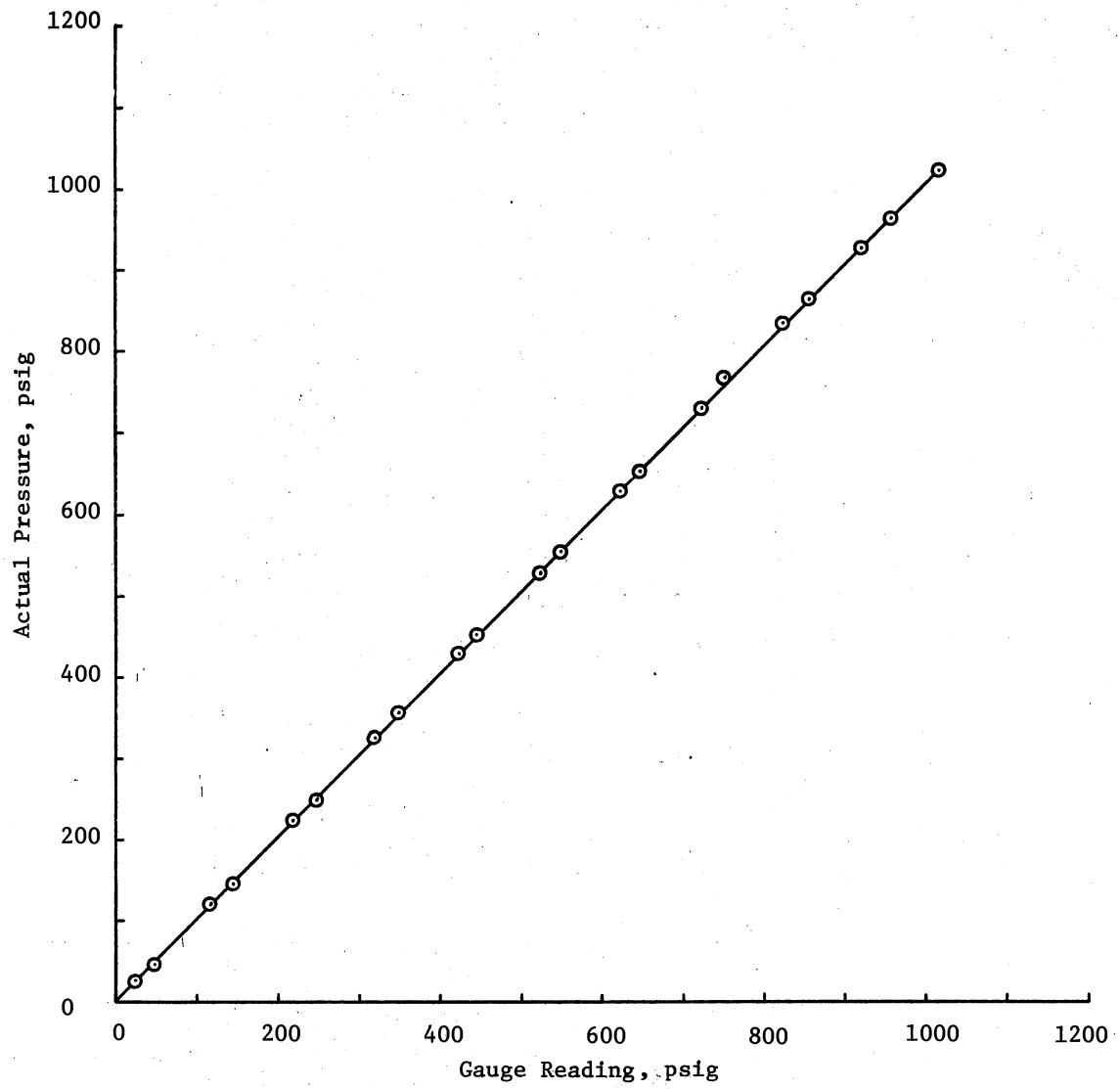

Figure 29. Calibration Curve for Martin-Decker Pressure Gauge (Serial Number 6540) for System Pressure Measurements on the Absolute Viscometer

TABLE XXXIV

CALIBRATION OF ASHCROFT COMPOUND GAUGE

Upper Meniscus cm	Lower Meniscus cm	Difference cm Hg	Difference in Hg	Difference psig	Gauge Reading in Hg Vac
89.735	15.7950	73.9400	29.110		28.70
86.615	18.8600	67.7550	26.680		26.20
84.365	21.1200	63.2450	24.900		24.50
82.035	23.4000	58.6350	23.080		22.95
76.875	28.4775	48.3975	19.050		18.90
72.025	33.3450	38.6800	15.230		15.00
66.310	38.9825	27.3275	10.760		10.80
61.830	43.4725	18.3575	7.230		7.30
58.575	46.7200	11.8550	4.670		4.60
55.045	50.2300	4.8150	1.900		2.00
0.000	0.0000	0.0000	0.000		Set
					Pressure psig
91.945	14.1725	77.7725		15.040	15.00
87.620	18.4525	69.1625		13.370	13.30
82.500	23.4000	59.1000		11.430	11.35
78.240	27.5000	50.7400		9.810	9.90
74.270	31.330	42.9400		8.300	8.20
69.330	36.1925	33.1375		6.410	6.35
64.240	41.1600	23.0800		4.460	4.30
58.8625	46.4100	12.4525		2.410	2.30

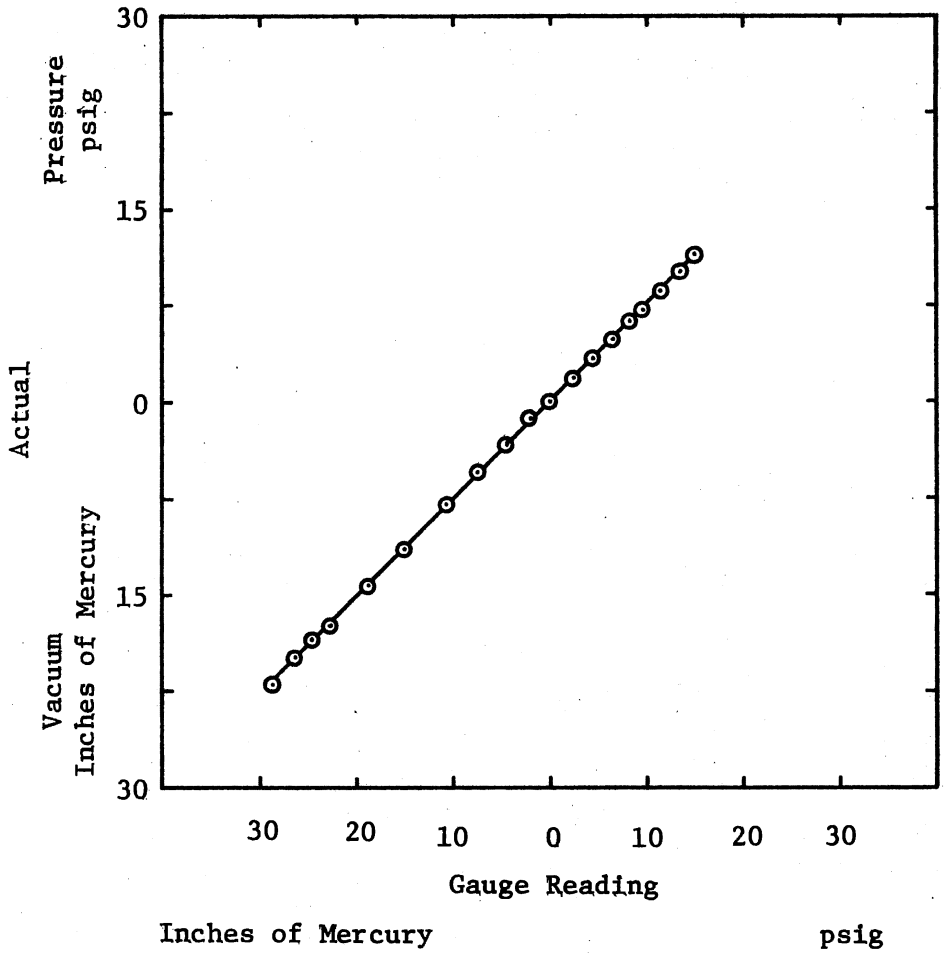

Figure 30. Calibration Curve for Ashcroft Compound Gauge for Vacuum and Low System Pressure Measurements on the Kinematic Viscometer

TABLE XXXV

CALIBRATION OF ITT BARTON DIFFERENTIAL PRESSURE GAUGE (SERIAL NUMBER 62566)

Lower Meniscus cm Hg	Upper Meniscus cm Hg	Difference cm Hg	Actual Pressure Difference in H_2O	Gauge Reading in H_2O
-	-	-	0.0	0.00
46.3300	50.2425	3.9125	20.95	22.00
44.4425	52.0500	7.6075	40.73	41.50
42.5850	53.8700	11.2850	60.42	61.50
40.6800	55.7275	15.0475	80.57	81.00
38.8400	57.5225	18.6825	100.03	100.50
36.9575	59.3800	22.4225	120.06	120.50
35.0800	61.1850	26.1050	139.77	140.00
33.2150	62.9800	29.7650	159.37	160.50
31.2600	64.8900	33.6300	180.07	180.50
29.3600	66.7650	37.4050	200.28	200.25
27.4300	68.6600	41.2300	220.76	220.25
25.4525	70.5900	45.1375	241.68	240.25
23.6050	72.4000	48.7950	261.26	260.50
21.7050	74.2650	52.5600	281.42	280.25
19.9475	75.9925	56.0450	300.08	300.00
20.8975	75.0400	54.1425	289.90	290.00
22.8850	73.1075	50.2225	268.91	269.75
24.6550	71.3675	46.7125	250.11	250.25
26.6100	69.4650	42.8550	229.46	229.75
28.5150	67.5850	39.0700	209.19	210.00
30.4925	65.6825	35.1900	188.42	189.75
32.3700	63.8100	31.4400	168.34	169.75
34.2050	62.0350	27.8300	149.01	150.00
36.0250	60.2625	24.2375	129.78	130.50
37.9600	58.3725	20.4125	109.30	110.25
39.8500	56.4675	16.6175	88.98	90.50
41.7900	54.6075	12.8175	68.63	70.25
43.6625	52.7700	9.1075	48.76	50.50
45.5250	50.9700	5.4450	29.15	30.25
47.4275	49.1050	1.6775	8.98	10.00
-	-	-	0.00	0.50

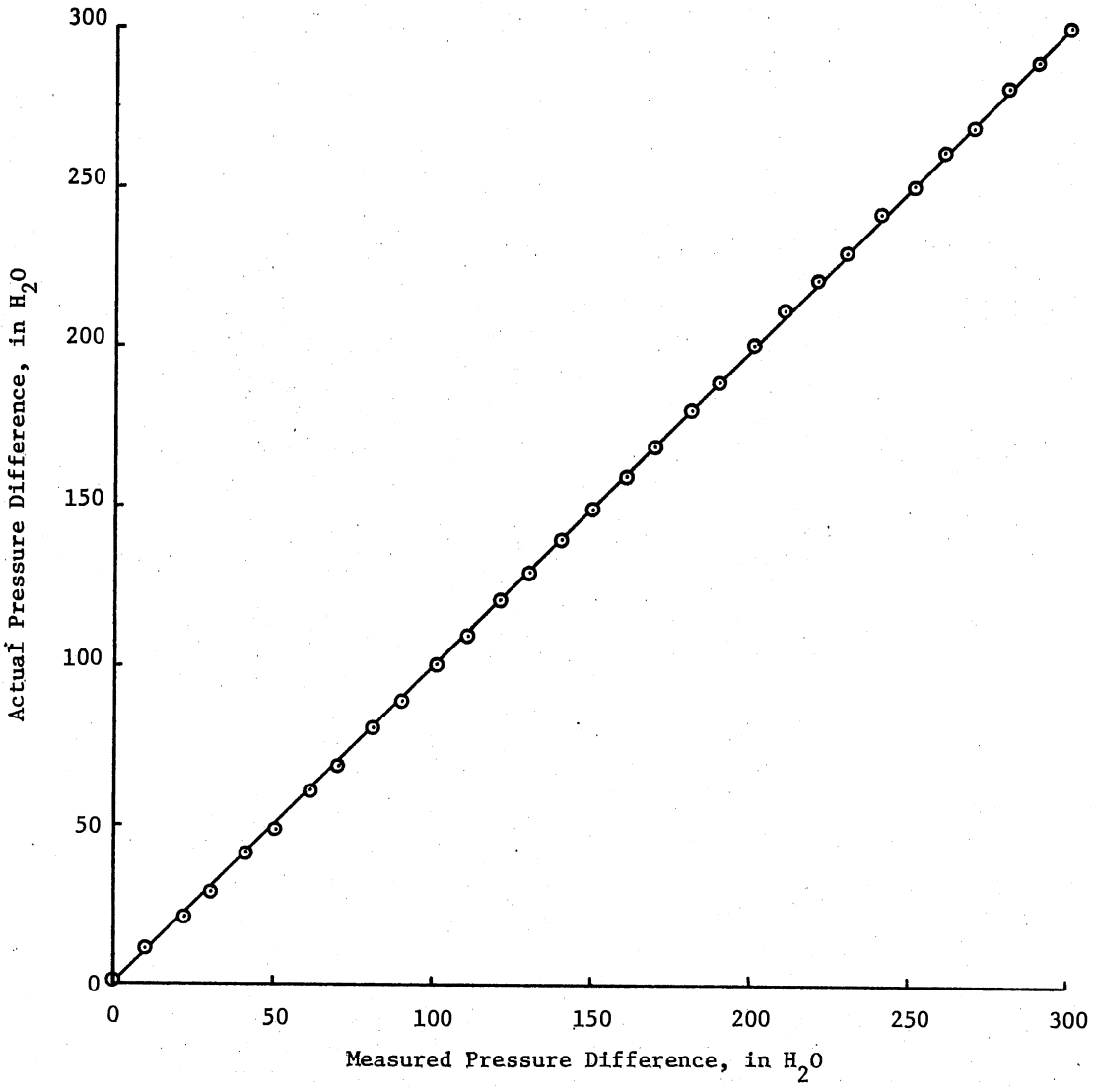

Figure 31. Calibration Curve for Differential Pressure Gauge DP-2 (Serial Number 62566) for the Absolute Viscometer

TABLE XXXVI

CALIBRATION OF ITT BARTON DIFFERENTIAL PRESSURE GAUGE (SERIAL NUMBER 67612)

Lower Meniscus cm Hg	Upper Meniscus cm Hg	Difference cm Hg	Actual Pressure Difference in H_2O	Gauge Reading in H_2O
-	-	-	0.000	0.00
47.2500	49.2825	2.0325	10.883	10.50
46.2850	50.2475	3.9625	21.217	20.30
45.2800	51.2350	5.9550	31.885	30.70
44.3600	52.1300	7.7700	41.603	40.10
43.3300	53.1375	9.8075	52.513	50.20
42.2950	54.1450	11.8500	63.449	60.70
41.3675	55.0300	13.6625	73.154	69.80
41.8500	54.5550	12.7050	68.027	65.00
42.9200	53.5250	10.6050	56.783	54.25
43.8300	52.6475	8.8175	47.212	45.00
44.8150	51.6650	6.8500	36.677	35.00
45.7950	50.7050	4.9100	26.290	25.00
46.7800	49.7525	2.9725	15.916	15.00
47.8000	48.7550	0.9550	5.113	4.80
-	-	-	0.000	0.10

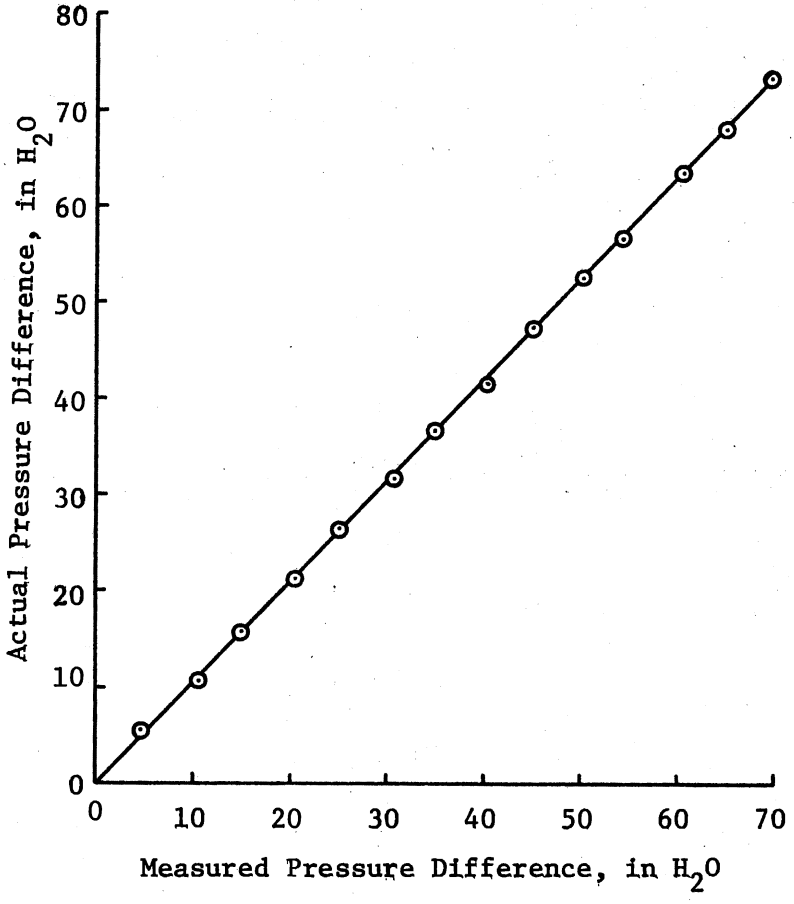

Figure 32. Calibration Curve for Differential Pressure Gauge DP-1 (Serial Number 62566) for the Absolute Viscometer

Thermocouple Calibrations

The two copper-constantan thermocouples used during the operation of the kinematic viscometer were calibrated against a N. B. S. calibrated Leeds and Northrup Corporation platinum resistance thermometer serial number 1761202. The range of temperatures covered by the calibration was from -78.153^{o} to 402.024^{o}F. Two readings were made at each temperature with the thermocouple referenced to an ice bath. Tables XXXVII and XXXVIII present the tabulated data. Figures 33 and 34 are graphical presentations of the arithmetic average thermocouple readings for each temperature and thermocouple.

The thermocouple used to measure the temperature during operation of the absolute viscometer was calibrated by using the melting and boiling points of water and the boiling points of n-octane and n-octanol. The resulting straight line (Figure 35) was extrapolated slightly to evaluate temperatures outside the range of the calibrations. The calibration fluids, boiling points and measured thermocouple readings are tabulated in Table XXXIX.

TABLE XXXVII

CALIBRATION DATA FOR PRESSURE CELL THERMOCOUPLE

Actual Temperature Degree Centigrade	Actual Temperature Degree Fahrenheit	Thermocouple Reading mV
-61.196	-78.153	-2.191050
-61.274	-78.293	-2.192530
-56.195	-69.151	-2.026220
-56.230	-69.214	-2.027070
-52.281	-62.106	-1.896130
-52.339	-62.210	-1.898485
-46.804	-52.247	-1.711395
-46.781	-52.206	-1.710930
-39.575	-39.235	-1.462425
-39.564	-39.215	-1.462255
-34.226	-29.607	-1.275170
-34.225	-29.605	-1.275275
-29.250	-20.650	-1.098025
-29.263	-20.674	-1.098415
-24.586	-12.255	-0.929630
-24.495	-12.091	-0.926170
-20.389	- 4.520	-0.775395
-20.309	- 4.556	-0.775760
-14.678	5.579	-0.567800
-14.612	5.698	-0.564960
- 9.177	15.481	-0.361540
- 9.131	15.564	-0.359875
8.102	46.583	0.309460
8.128	46.630	0.310510
18.960	66.128	0.741905
18.976	66.156	0.742995
24.826	76.687	1.101905
24.825	76.685	1.102650
31.580	88.844	1.347980
31.589	88.860	1.355500
40.551	104.991	1.721890
40.541	104.973	1.725005
51.613	124.903	2.199425
51.623	124.921	2.206530
61.511	142.720	2.641720
61.511	142.720	2.646190
71.601	160.881	3.095790
71.601	160.881	3.100875
80.765	177.377	3.509560
80.750	177.350	3.509580
90.313	194.563	3.987390
90.313	194.563	3.995120

TABLE XXXVII (Continued)

Actual Temperature Degree Centigrade	Actual Temperature Degree Fahrenheit	Thermocouple Reading mV
98.910	210.038	4.228380
98.907	210.032	4.227090
97.401	207.322	4.163100
97.485	207.473	4.167150
102.559	216.606	4.402815
102.427	216.368	4.397090
112.230	234.014	4.861490
112.246	234.042	4.861985
131.748	269.146	5.801875
131.763	269.173	5.803035
149.315	300.767	6.671280
149.331	300.795	6.673310
169.350	336.830	7.687485
169.333	336.799	7.686275
185.908	366.634	8.545095
185.880	366.584	8.543290
186.533	367.759	8.582440
186.566	367.819	8.585095
205.563	402.013	9.598080
205.569	402.024	9.598910

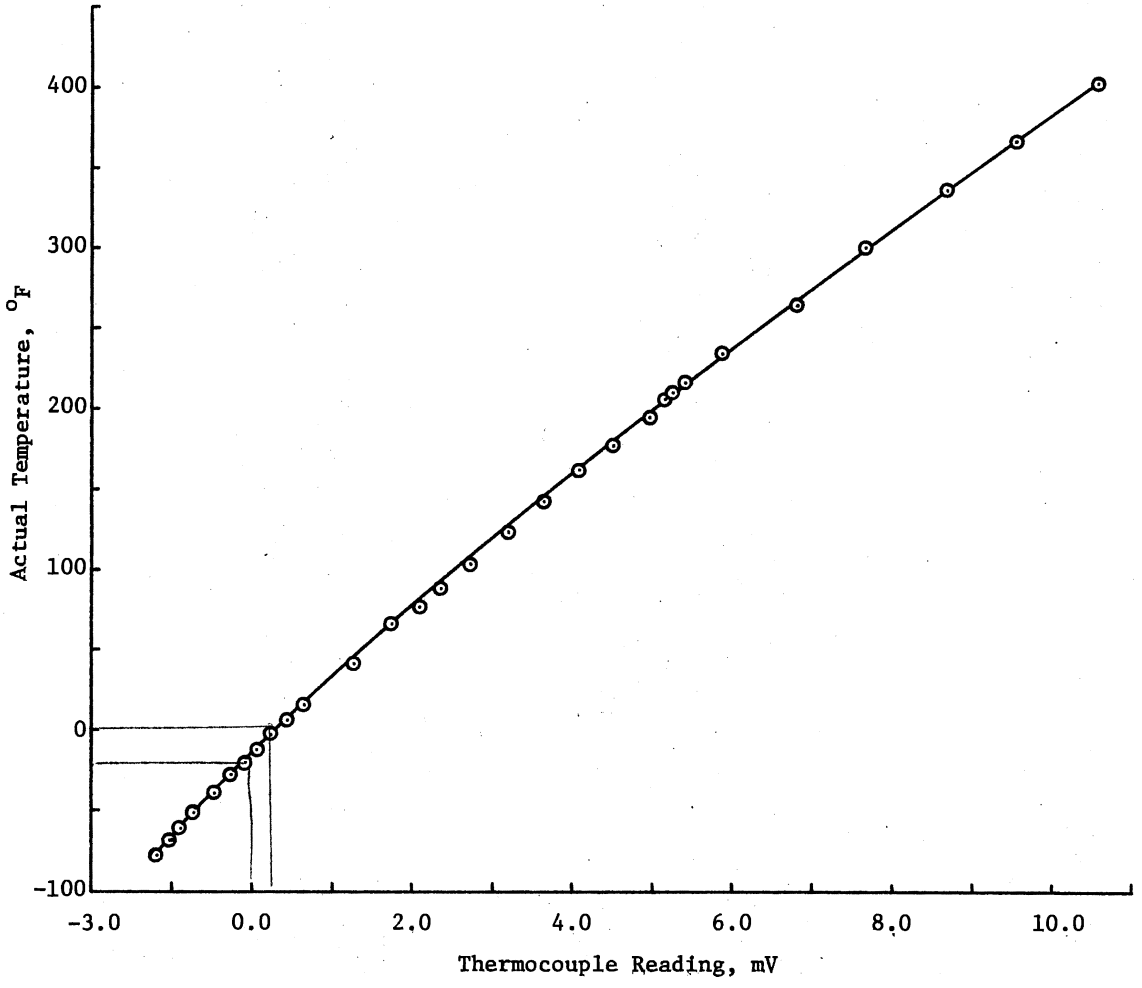

Figure 33. Calibration Curve for the Pressure Cell Thermocouple for the Kinematic Viscometer

TABLE XXXVIII

CALIBRATION DATA FOR CONSTANT TEMPERATURE BATH THERMOCOUPLE

Actual Temperature Degree Centigrade	Actual Temperature Degree Fahrenheit	Thermocouple Reading mV
-61.219	-78.194	-2.189435
-61.289	-78.320	-2.191905
-56.207	-69.173	-2.025780
-56.230	-69.214	-2.025975
-52.300	-62.140	-1.895820
-52.339	-62.210	-1.896860
-46.801	-52.242	-1.710615
-46.758	-52.165	-1.710315
-39.559	-39.206	-1.461345
-39.567	-39.221	-1.461360
-34.227	-29.609	-1.275880
-34.245	-29.641	-1.274535
-29.258	-20.665	-1.097730
-29.247	-20.645	-1.096655
-24.588	-12.259	-0.929175
-24.498	-12.097	-0.926655
-20.292	- 4.526	-0.775190
-20.304	- 4.547	-0.775425
-14.679	5.577	-0.566700
-14.623	5.678	-0.565350
- 9.184	15.469	-0.361345
- 9.163	15.506	-0.360965
8.362	47.051	0.309915
8.121	46.617	0.310555
18.964	66.135	0.742550
18.981	66.166	0.743500
24.825	76.685	1.105030
24.832	76.697	1.104300
31.584	88.851	1.352300
31.584	88.851	1.351255
40.546	104.982	1.722340
40.539	104.970	1.714430
51.616	124.909	2.201405
51.619	124.914	2.201275
61.511	142.720	2.636710
61.516	142.729	2.635850
71.603	160.885	3.096455
71.603	160.885	3.096035
80.750	177.350	3.501520
80.750	177.350	3.496225
90.313	194.563	3.986930
90.313	194.563	3.994160

TABLE XXXVIII (Continued)

Actual Temperature Degree Centigrade	Actual Temperature Degree Fahrenheit	Thermocouple Reading mV
98.909	210.036	4.225385
98.904	210.027	4.217290
97.428	207.370	4.162000
97.478	207.460	4.159510
102.483	216.469	4.387515
102.473	216.451	4.387410
112.240	234.032	4.846630
112.230	234.014	4.847235
131.769	269.184	5.785175
131.784	269.211	5.786025
149.310	300.758	6.649155
149.310	300.758	6.650255
169.360	336.848	7.659910
169.354	336.837	7.660270
185.882	366.587	8.509825
185.877	366.578	8.509455
186.514	367.725	8.551510
186.530	367.753	8.553450
205.553	401.995	9.562920
205.563	402.013	9.563525

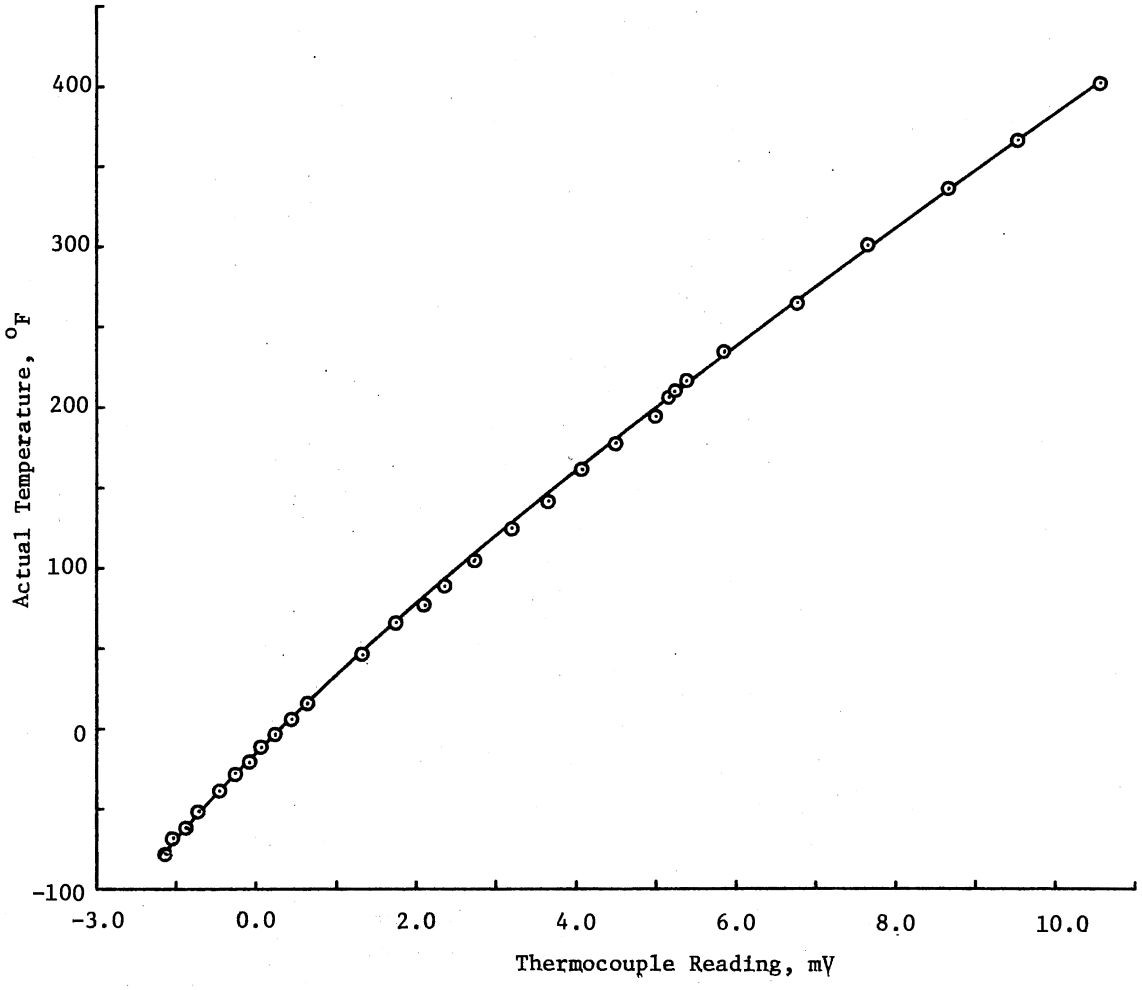

Figure 34. Calibration Curve for the Constant Temperature Bath Thermocouple for the Kinematic Viscometer

TABLE XXXIX

ABSOLUTE VISCOMETER THERMOCOUPLE CALIBRATION

Fluid (state)	Actual Temperature °F	Thermocouple Reading mV
Water (melting)	32.0	-0.015
Water (boiling)	212.0	6.332
n-Octane (boiling)	258.4	8.103
n-Octanol (boiling)	383.0	12.849

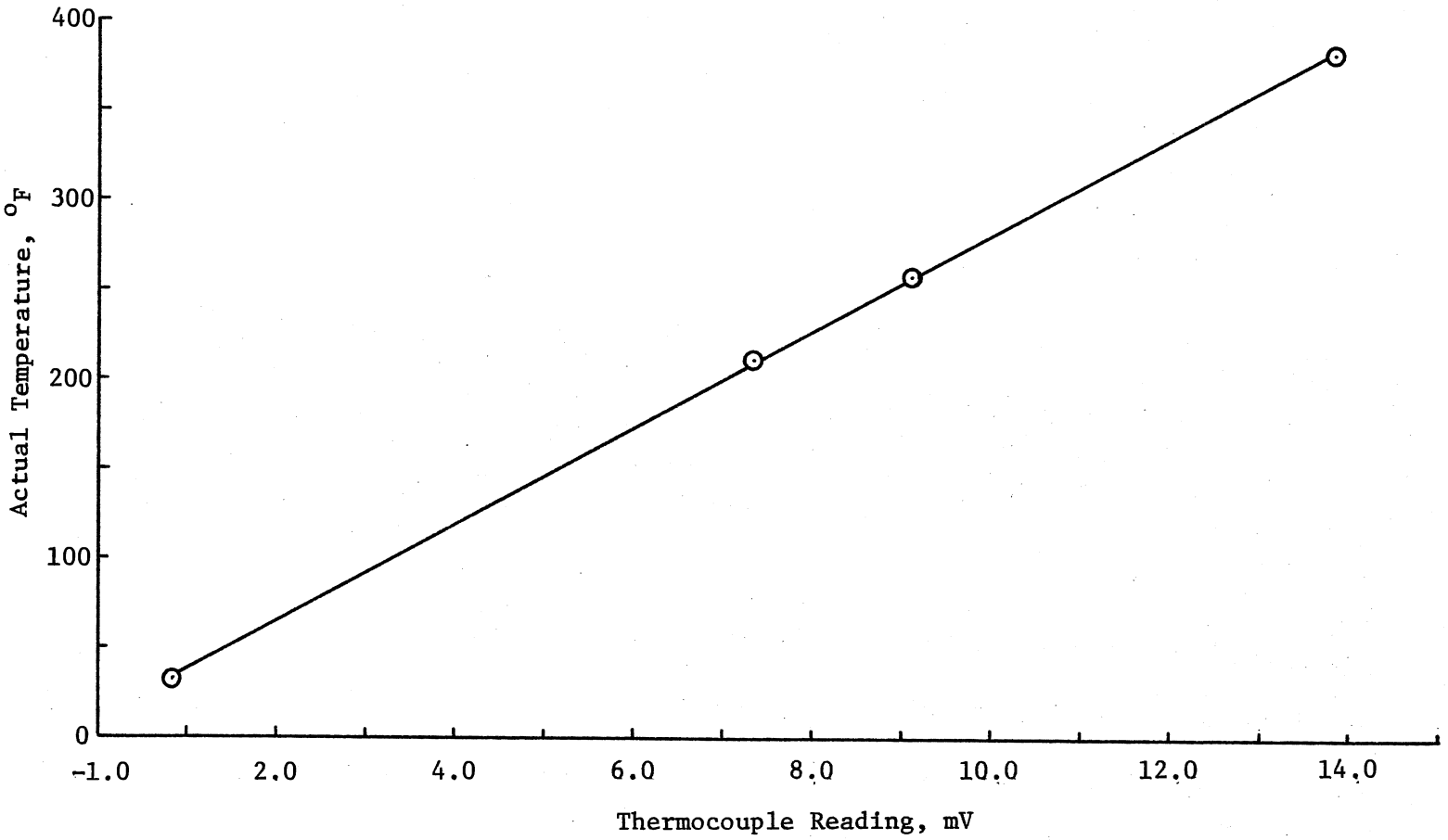

Figure 35. Calibration Curve for the Absolute Viscometer Thermocouple

Pump Calibration

The constant volume Ruska pump serial number 17753 was calibrated by measuring the efflux time required for a volume of water to be discharged from the flow system of the absolute viscometer. Three pressures were considered to determine the effect of back pressure on the constant volume discharge of the pump. Tables X through XLII are the tabulated results of the calibration measurements. The effect of back pressure was significant and measurements made at pressures above atmospheric were corrected by means of the calibration curves. Figure 36 presents the low range flow rate as a function of the pump controller set point. Figure 40 graphically presents the high range flow rate of the pump as a function of the pump controller set point and the system back pressure. The back pressure effect was not examined for the low gear box range because all measurements were made with the gear box range set to the high range. This was justified by the high percentage errors anticipated by using the small capillary (see the error analysis).

TABLE XL

CALIBRATION DATA FOR RUSKA CONSTANT VOLUME PUMP AT ATMOSPHERIC PRESSURE (SERIAL NUMBER 17753)

Pump Speed set	Gear Box set	Liquid Volume ml	Flow Time sec	Flow Rate ml/sec
1.0	low	10.0	2406.569	0.004155
2.0	low	10.0	1149.815	0.008697
3.0	low	10.0	754.333	0.013257
4.0	low	20.0	1112.990	0.017970
5.0	low	20.0	899.568	0.022233
5.0	low	20.0	897.203	0.022291
5.0	low	20.0	888.193	0.022518
5.0	low	20.0	874.584	0.022868
6.0	low	20.0	735.448	0.027194
6.0	low	20.0	725.245	0.027577
6.0	low	20.0	735.287	0.027200
6.0	low	20.0	721.712	0.027712
7.0	low	20.0	632.509	0.031620
7.0	low	20.0	631.320	0.031680
7.0	low	20.0	630.229	0.031734
7.0	low	20.0	630.429	0.031724
8.0	low	20.0	580.068	0.034479
8.0	low	20.0	570.142	0.035079
8.0	low	20.0	566.967	0.035275
8.0	low	20.0	563.111	0.035517
9.0	low	20.0	498.990	0.040081
9.0	low	20.0	494.381	0.040455
9.0	low	20.0	496.046	0.040319
9.0	low	20.0	495.601	0.040355
9.9	low	20.0	445.003	0.044944
9.9	low	20.0	447.770	0.044666
9.9	low	20.0	445.852	0.044858
9.9	low	20.0	444.132	0.045032
1.0	high	20.0	1268.468	0.015767
1.0	high	20.0	1238.773	0.016145
1.0	high	20.0	1232.561	0.016226
1.0	high	20.0	1231.151	0.016245
2.0	high	20.0	584.129	0.034239
2.0	high	20.0	580.473	0.034455
2.0	high	20.0	580.194	0.034471
2.0	high	20.0	579.768	0.034497
3.0	high	30.0	567.635	0.052851
3.0	high	30.0	569.650	0.052664
3.0	high	30.0	567.795	0.052836
3.0	high	30.0	568.441	0.052776

TABLE XL (Continued)

Pump Speed set	Gear Box set	Liquid Volume ml	Flow Time sec	Flow Rate ml/sec
4.0	high	40.0	560.830	0.071323
4.0	high	40.0	562.911	0.071059
4.0	high	40.0	564.163	0.070901
4.0	high	40.0	563.082	0.071038
5.0	high	50.0	551.782	0.090615
5.0	high	50.0	554.583	0.090158
5.0	high	50.0	552.071	0.090568
5.0	high	50.0	552.852	0.090440
6.0	high	60.0	548.898	0.109310
6.0	high	60.0	550.735	0.108945
6.0	high	60.0	551.380	0.108818
6.0	high	60.0	547.850	0.109519
7.0	high	70.0	546.669	0.128048
7.0	high	70.0	550.857	0.127075
7.0	high	70.0	545.109	0.128415
7.0	high	70.0	548.017	0.127733
8.0	high	80.0	562.038	0.142339
8.0	high	80.0	563.137	0.142061
8.0	high	80.0	561.170	0.142559
8.0	high	80.0	558.291	0.143294
9.0	high	90.0	555.910	0.161897
9.0	high	90.0	551.291	0.163253
9.0	high	90.0	552.227	0.162976
9.0	high	90.0	552.512	0.162892
9.9	high	90.0	499.300	0.180252
9.9	high	90.0	498.254	0.180631
9.9	high	90.0	496.130	0.181404
9.9	high	90.0	496.092	0.181418

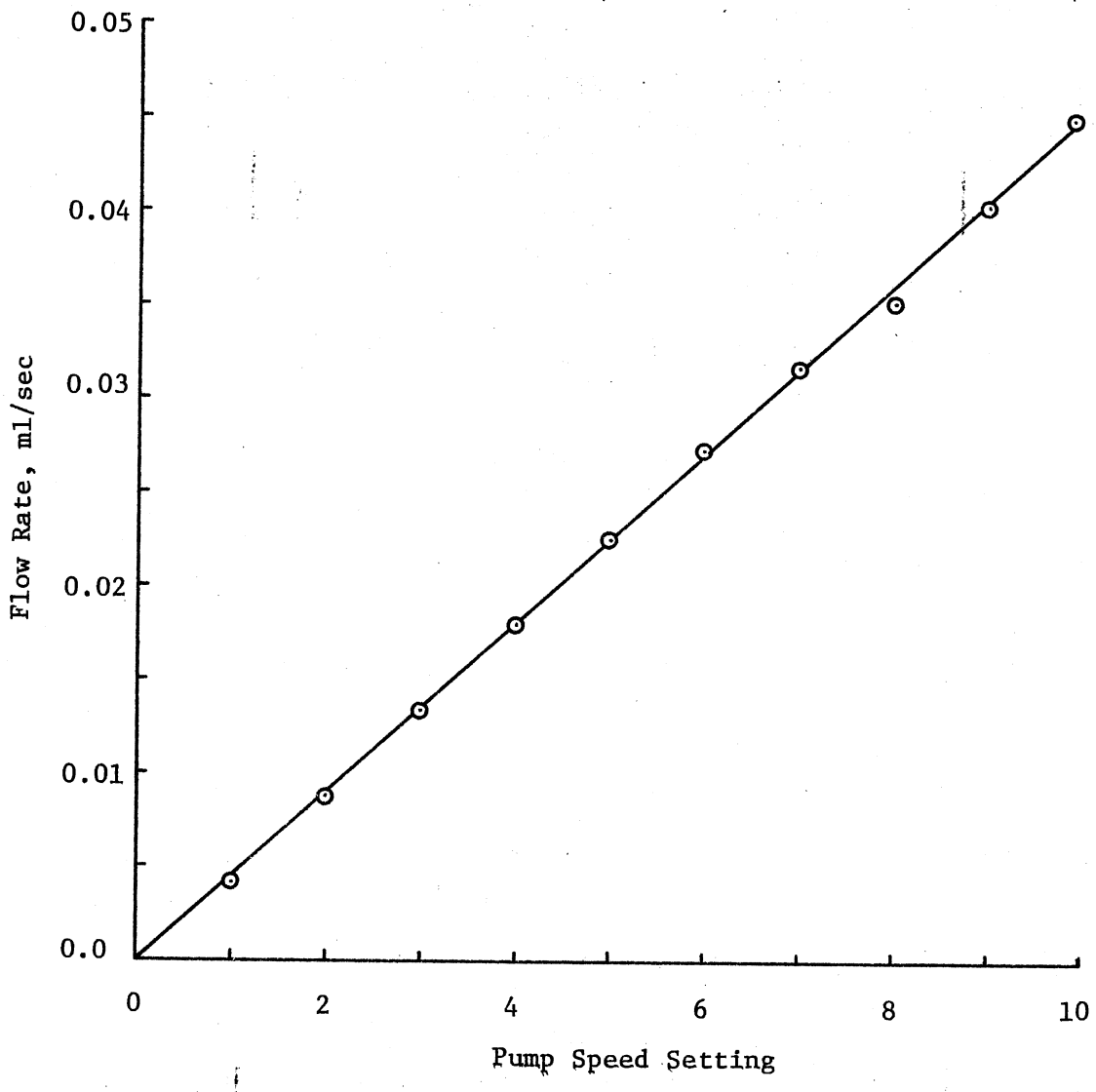

Figure 36. Calibration Curve for the Absolute Viscometer Ruska Constant Volume Pump (Serial Number 17753) at Atmospheric Pressure with the Gear Box in the Low Range Setting

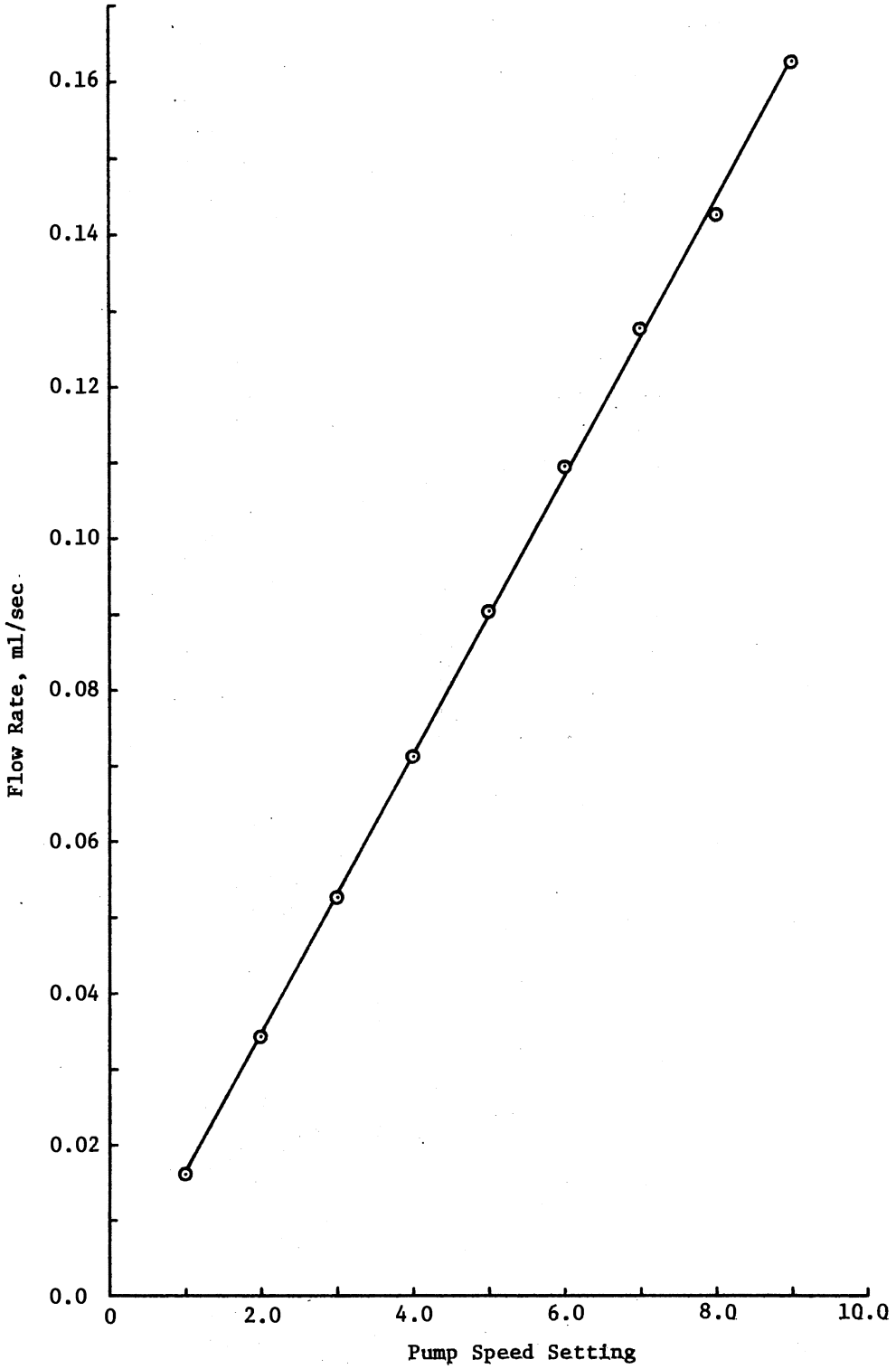

Figure 37. Calibration Curve for the Absolute Viscometer Ruska Constant Volume Pump (Serial Number 17753) at Atmospheric Pressure with the Gear Box in the High Range Setting

TABLE XLI

CALIBRATION DATA FOR RUSKA CONSTANT VOLUME PUMP AT 500 PSIG PRESSURE (SERIAL NUMBER 17753)

Pump Speed set	Gear Box set	Liquid Volume ml	Flow Time sec	Flow Rate ml/sec
3.0	high	10.0	196.	0.051020
3.0	high	10.0	197.	0.050760
3.0	high	10.0	195.	0.051280
3.0	high	10.0	193.	0.051813
4.0	high	10.0	143.	0.069930
4.0	high	10.0	142.	0.070420
4.0	high	10.0	140.	0.071428
4.0	high	10.0	141.	0.070920
5.0	high	10.0	112.	0.089280
5.0	high	10.0	114.	0.087720
5.0	high	10.0	111.	0.090009
5.0	high	10.0	114.	0.087720
6.0	high	20.0	190.	0.105260
6.0	high	20.0	192.	0.104166
6.0	high	20.0	192.	0.104166
6.0	high	20.0	192.	0.104166
7.0	high	20.0	161.	0.124220
7.0	high	20.0	163.	0.122699
7.0	high	20.0	160.	0.125000
7.0	high	20.0	162.	0.123450
8.0	high	20.0	141.	0.141840
8.0	high	20.0	141.	0.141840
8.0	high	20.0	143.	0.139860
8.0	high	20.0	140.	0.142860
9.0	high	20.0	125.	0.160000
9.0	high	20.0	126.	0.158730
9.0	high	20.0	127.	0.157400
9.0	high	20.0	125.	0.160000

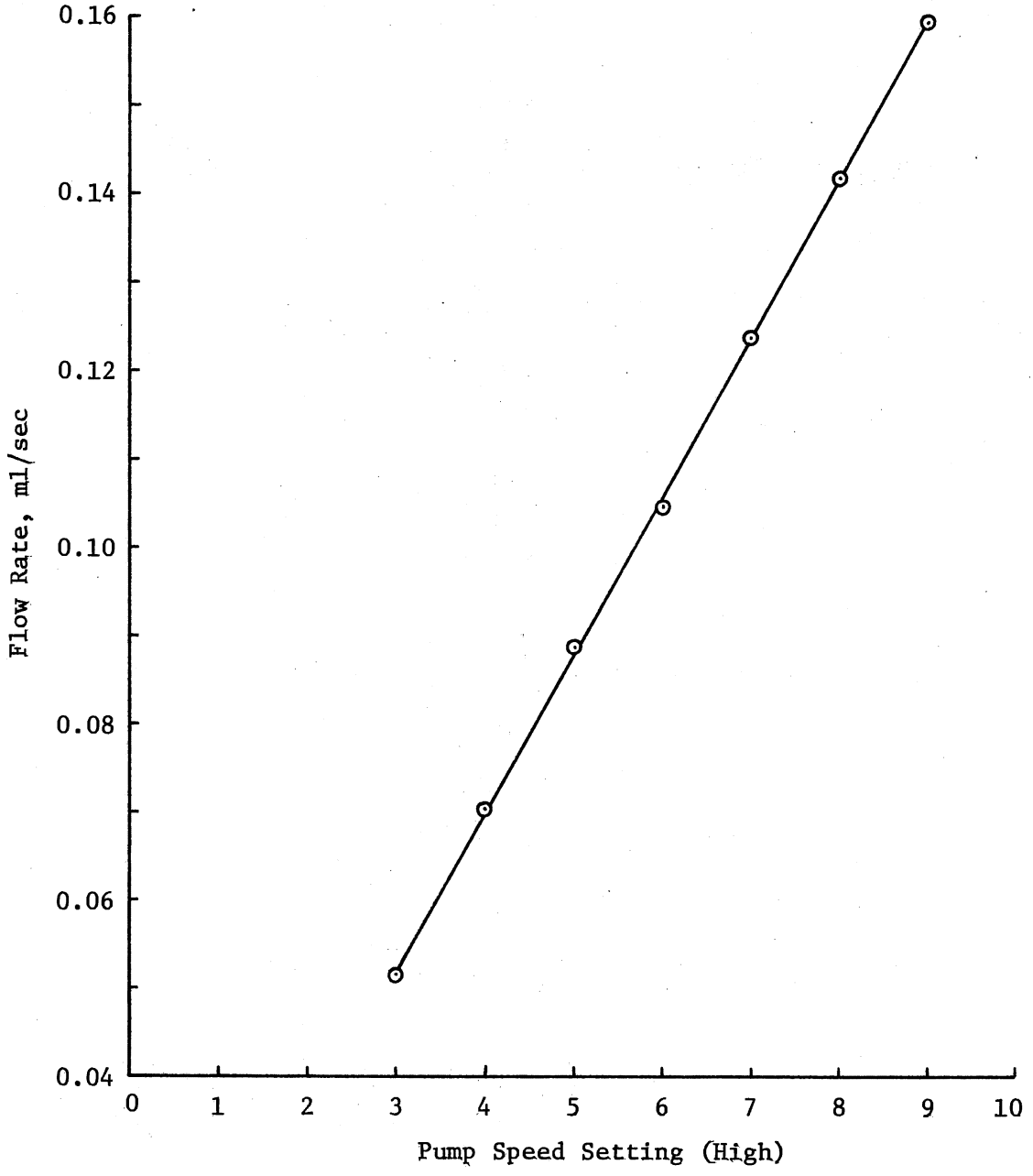

Figure 38. Calibration Curve for the Absolute Viscometer Ruska Constant Volume Pump (Serial Number 17753) at 500 psig Back Pressure with the Gear Box in the High Range Setting

TABLE XLII

CALIBRATION DATA FOR RUSKA CONSTANT VOLUME PUMP AT 1000 PSIG PRESSURE (SERIAL NUMBER 17753)

Pump Speed set	Gear Box set	Liquid Volume ml	Flow Time sec	Flow Rate ml/sec
3.0	high	10.0	200.5	0.04988
3.0	high	10.0	206.5	0.04845
3.0	high	10.0	201.2	0.04970
3.0	high	10.0	193.4	0.05170
3.0	high	10.0	197.4	0.05136
4.0	high	10.0	152.2	0.06570
4.0	high	10.0	143.3	0.06978
4.0	high	10.0	156.5	0.06390
4.0	high	10.0	149.8	0.06676
4.0	high	10.0	145.9	0.06854
5.0	high	10.0	120.0	0.08333
5.0	high	10.0	120.0	0.08333
5.0	high	10.0	121.3	0.08242
5.0	high	10.0	119.6	0.08361
5.0	high	20.0	235.9	0.08478
6.0	high	10.0	94.1	0.10627
6.0	high	10.0	94.1	0.10627
6.0	high	10.0	96.3	0.10384
6.0	high	10.0	97.2	0.10288
6.0	high	10.0	94.0	0.10638
7.0	high	10.0	86.2	0.11600
7.0	high	20.0	166.3	0.12026
7.0	high	20.0	166.5	0.12017
7.0	high	20.0	167.1	0.11970
8.0	high	20.0	139.4	0.14397
8.0	high	20.0	141.6	0.14120
8.0	high	10.0	72.6	0.13774
8.0	high	20.0	141.9	0.14090
8.0	high	10.0	72.6	0.13774
9.0	high	20.0	126.7	0.15790
9.0	high	20.0	125.5	0.15940
9.0	high	10.0	64.5	0.15500
9.0	high	10.0	62.5	0.16000
9.0	high	20.0	123.4	0.16200

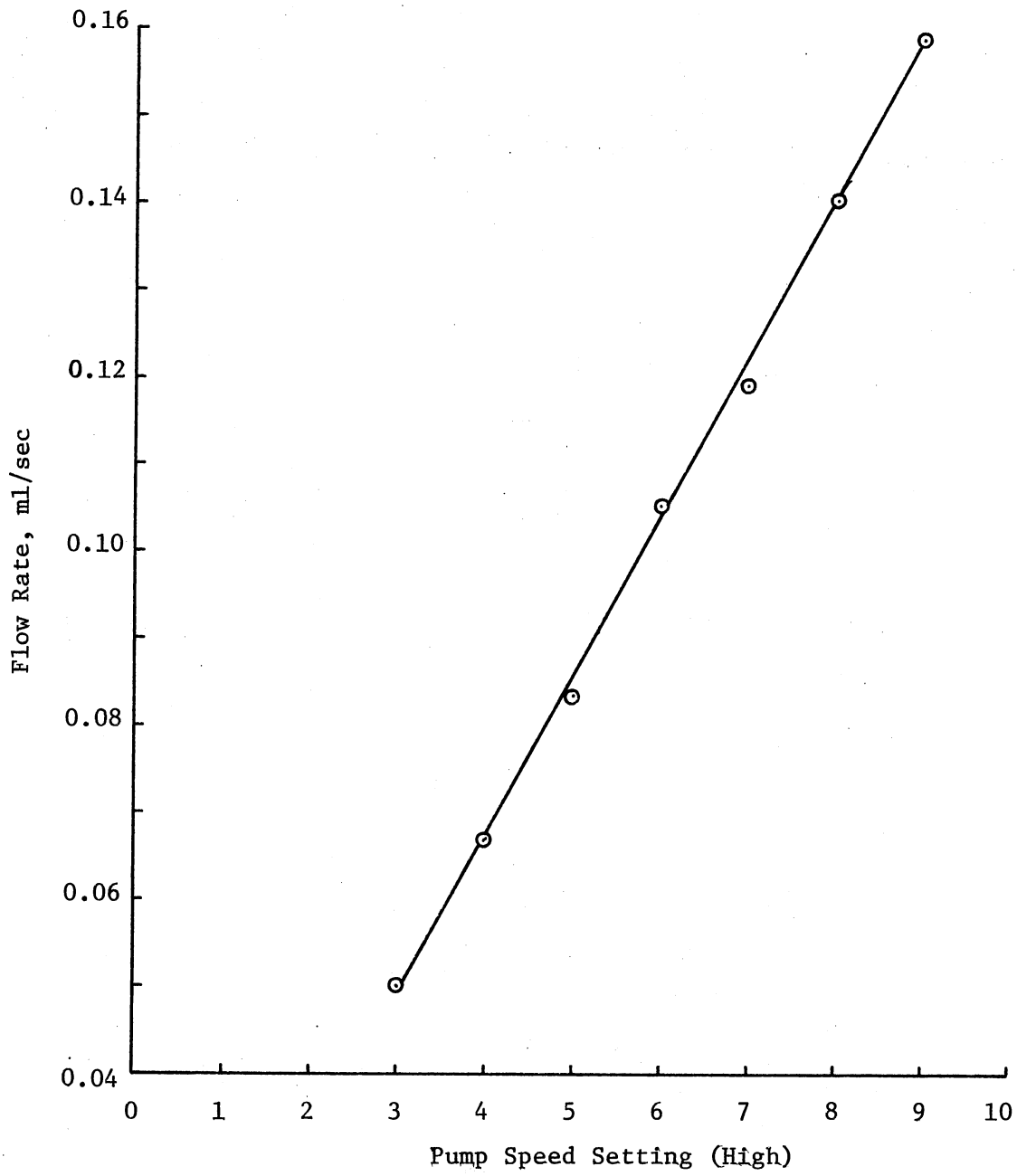

Figure 39. Calibration Curve for the Absolute Viscometer Ruska Constant Volume Pump (Serial Number 17753 at 1000 psig Back Pressure with the Gear Box in the High Range Setting

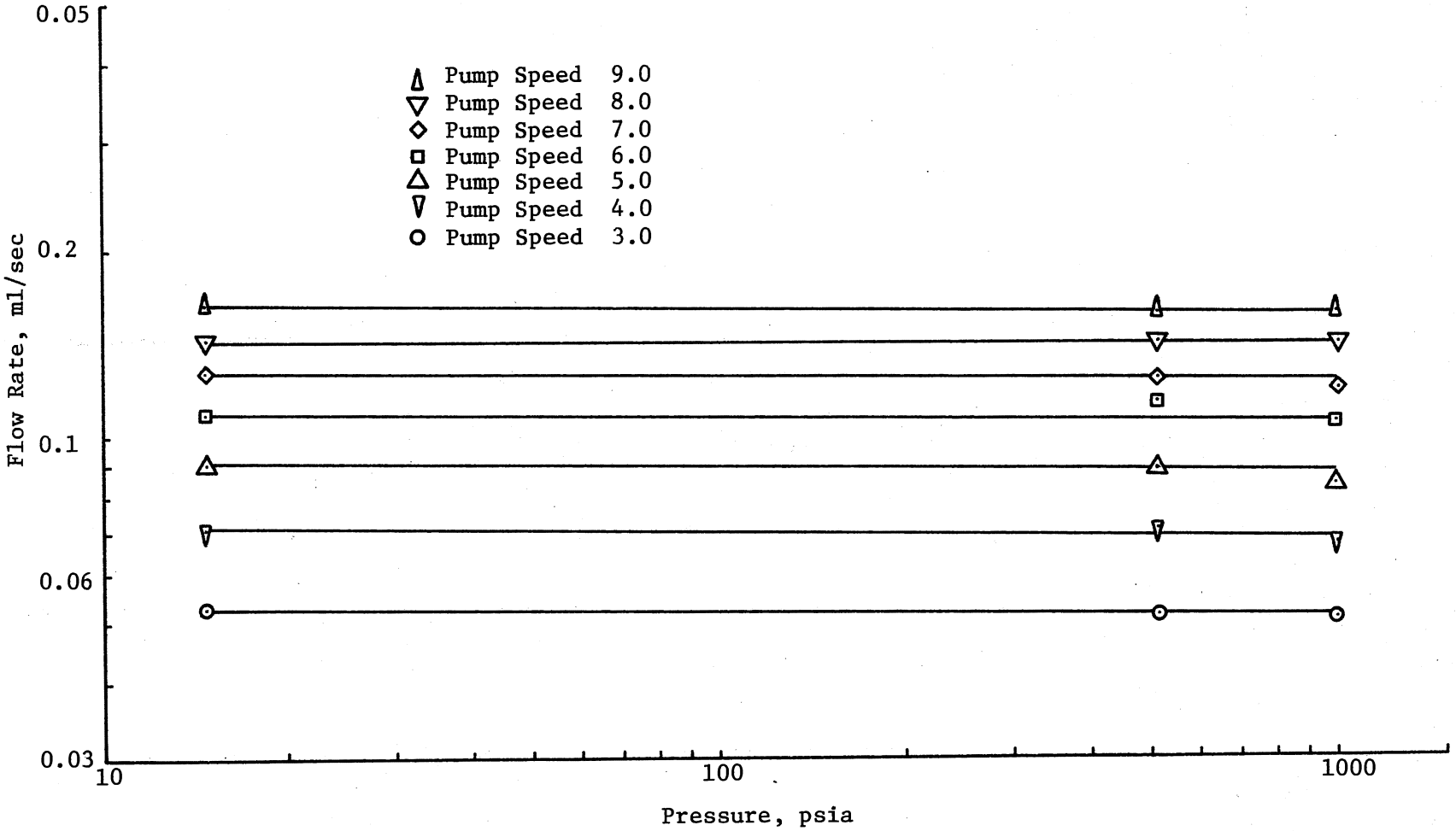

Figure 40. Calibration Curves for the Absolute Viscometer Ruska Constant Volume Pump (Serial Number 17753) as a Function of Back Pressure

TABLE XLIII

CHROMATOGRAPH CALIBRATION - STANDARD SAMPLE 1

Run	Ethylene Area	Propylene Area	Total Area	Ethylene Fraction	Propylene Fraction	Ethylene % Deviation
1	2684	2051	4735	0.5668	0.4332	-0.1057
2	2555	1944	4499	0.5679	0.4321	0.0881
3	2332	1779	4111	0.5673	0.4327	-0.0176
4	2638	2002	4640	0.5685	0.4315	0.1939
5	2754	2106	4860	0.5667	0.4333	-0.1234
6	2554	1889	4443	0.5748	0.4252	1.3042
7	2860	2176	5036	0.5679	0.4321	0.0881
8	2591	1911	4502	0.5755	0.4245	1.4276
9	2796	2113	4909	0.5696	0.4304	0.3877
10	2461	1849	4310	0.5710	0.4290	0.6345
11	2331	1718	4049	0.5757	0.4243	1.4628
12	2630	1983	4613	0.5701	0.4299	0.4759
13	2589	1971	4560	0.5678	0.4322	0.0705
14	2774	2129	4903	0.5658	0.4342	-0.2820
15	2671	2024	4695	0.5689	0.4311	0.2644
16	2651	1986	4637	0.5717	0.4283	0.7578
17	2460	1871	4331	0.5680	0.4320	0.1057
18	2187	1615	3802	0.5752	0.4248	1.3747
19	2654	2063	4717	0.5626	0.4374	-0.8460
20	2892	2208	5100	0.5671	0.4329	-0.0529
21	2869	2254	5123	0.5600	0.4400	-1.3042
22	2958	2309	5267	0.5616	0.4384	-1.0222
23	3087	2431	5518	0.5594	0.4406	-1.4099
24	2929	2330	5259	0.5569	0.4431	-1.8505
25	2459	1917	4376	0.5619	0.4381	-0.9693
26	2499	1931	4430	0.5641	0.4359	-0.5816
Avg				0.5674	0.4326	

TABLE XLIV

CHROMATOGRAPH CALIBRATION - STANDARD SAMPLE 2

Run	Ethylene Area	Propylene Area	Total Area	Ethylene Fraction	Propylene Fraction	Propylene % Deviation
1	2066	2962	5028	0.4109	0.5891	-1.8003
2	1687	2463	4150	0.4065	0.5935	-1.0668
3	1865	2775	4640	0.4019	0.5981	-0.3001
4	2268	3366	5634	0.4026	0.5974	-0.4167
5	2270	3398	5668	0.4005	0.5995	-0.0667
6	1658	2435	4093	0.4051	0.5949	-0.8335
7	1944	2870	4814	0.4038	0.5962	-0.6168
8	2096	3131	5227	0.4010	0.5990	-0.1500
9	1815	2691	4506	0.4028	0.5972	-0.4501
10	2026	2997	5023	0.4033	0.5967	-0.5334
11	1837	2738	4575	0.4015	0.5985	-0.2334
12	2070	3115	5185	0.3992	0.6008	0.1500
13	2207	3359	5566	0.3965	0.6035	0.6001
14	2221	3344	5565	0.3991	0.6009	0.1667
15	2201	3298	5499	0.4003	0.5997	-0.0333
16	1886	2824	4710	0.4004	0.5996	-0.0500
17	1869	2813	4682	0.3992	0.6008	0.1500
18	1635	2399	4034	0.4053	0.5947	-0.8668
19	1918	2896	4814	0.3984	0.6016	0.2834
20	2233	3363	5596	0.3990	0.6010	0.1834
21	2097	3162	5259	0.3987	0.6013	0.2334
22	2395	3618	6013	0.3983	0.6017	0.3001
23	1915	2872	4787	0.4000	0.6000	0.0166
24	2365	3590	5955	0.3971	0.6029	0.5001
25	2280	3432	5712	0.3992	0.6008	0.1500
26	2241	3408	5649	0.3967	0.6033	0.5668
27	2242	3446	5688	0.3942	0.6058	0.9835
28	1934	2925	4859	0.3980	0.6020	0.3501
29	2360	3613	5973	0.3951	0.6049	0.8335
30	2313	3519	5832	0.3966	0.6034	0.5834
31	3878	5982	9860	0.3933	0.6067	1.1335
Avg				0.4001	0.5999	

TABLE XLV

CHROMATOGRAPH CALIBRATION - STANDARD SAMPLE 3

Run	Ethylene Area	Propylene Area	Total Area	Ethylene Fraction	Propylene Fraction	Ethylene % Deviation
1	2079	10535	12614	0.1648	0.8352	1.1664
2	1992	10317	12309	0.1618	0.8382	-0.6753
3	2133	10822	12955	0.1646	0.8354	1.0436
4	1998	10384	12382	0.1614	0.8386	-0.9208
5	2030	10539	12569	0.1615	0.8385	-0.8594
6	2126	10812	12938	0.1643	0.8357	0.8594
7	2017	10518	12535	0.1609	0.8391	-1.2277
8	1972	10286	12258	0.1609	0.8391	-1.2277
9	1959	10291	12250	0.1599	0.8401	-1.8416
10	2050	10512	12562	0.1632	0.8368	0.1842
11	1642	8431	10073	0.1630	0.8370	0.0614
12	2071	10643	12714	0.1629	0.8371	0.0000
13	2054	10409	12463	0.1648	0.8352	1.1664
14	1888	9927	11815	0.1598	0.8402	-1.9030
15	1961	10283	12244	0.1602	0.8398	-1.6575
16	1697	8694	10391	0.1633	0.8367	0.2455
17	1978	9993	11971	0.1652	0.8348	1.4119
18	1869	9525	11394	0.1640	0.8360	0.6753
19	1974	10082	12056	0.1637	0.8363	0.4911
20	1993	10316	12309	0.1619	0.8381	-0.6139
21	1899	9836	11735	0.1618	0.8382	-0.6753
22	1826	9436	11262	0.1621	0.8379	-0.4911
23	1855	9713	11568	0.1604	0.8396	-1.5347
24	1953	10025	11978	0.1630	0.8370	0.0614
25	1793	9151	10944	0.1638	0.8362	0.5525
26	1867	9495	11362	0.1643	0.8357	0.8594
27	1812	9242	11054	0.1639	0.8361	0.6139
28	1998	9889	11887	0.1681	0.8319	3.1921
29	1544	7844	9388	0.1645	0.8355	0.9822
30	1447	7385	8832	0.1638	0.8362	0.5525
Avg				0.1629	0.8371	

TABLE XLVI

CHROMATOGRAPH CALIBRATION - STANDARD SAMPLE 4

Run	Ethylene Area	Propylene Area	Total Area	Ethylene Fraction	Propylene Fraction	Ethylene % Deviation
1	3078	630	3708	0.8301	0.1699	-0.4318
2	2380	462	2842	0.8374	0.1626	0.4438
3	2843	570	3413	0.8330	0.1670	-0.0840
4	2968	593	3561	0.8335	0.1665	-0.0240
5	3612	737	4349	0.8305	0.1695	-0.3838
6	3567	728	4295	0.8305	0.1695	-0.3838
7	2840	549	3389	0.8380	0.1620	0.5158
8	3167	621	3788	0.8361	0.1639	0.2879
9	3733	763	4496	0.8303	0.1697	-0.4078
10	3510	687	4197	0.8363	0.1637	0.3119
11	3773	745	4518	0.8351	0.1649	0.1679
12	4114	830	4944	0.8321	0.1679	-0.1919
13	3871	764	4635	0.8352	0.1648	0.1799
14	4028	803	4831	0.8338	0.1662	0.0120
15	3453	688	4141	0.8339	0.1661	0.0240
16	4239	864	5103	0.8307	0.1693	-0.3598
17	3853	782	4635	0.8313	0.1687	-0.2879
18	3821	766	4587	0.8330	0.1670	-0.0840
19	3048	593	3641	0.8371	0.1629	0.4078
20	3220	620	3840	0.8385	0.1615	0.5757
21	3774	762	4536	0.8320	0.1680	-0.2039
22	3408	680	4088	0.8337	0.1663	0.0000
23	3886	792	4678	0.8307	0.1693	-0.3598
24	3330	664	3994	0.8338	0.1662	0.0120
25	3744	743	4487	0.8344	0.1656	0.0840
26	3314	652	3966	0.8356	0.1644	0.2279
Avg				0.8337	0.1663	

TABLE XLVII

CHROMATOGRAPH CALIBRATION - STANDARD SAMPLE 5

Run	Ethylene Area	Propylene Area	Total Area	Ethylene Fraction	Propylene Fraction	Ethylene % Deviation
1	34984	3280	38264	0.9143	0.0857	0.5609
2	2730	215	2945	0.9270	0.0730	1.9578
3	10076	978	11054	0.9115	0.0885	0.2530
4	9667	951	10618	0.9104	0.0896	0.1320
5	9493	865	10358	0.9165	0.0835	0.8029
6	9403	883	10286	0.9142	0.0858	0.5499
7	9366	852	10218	0.9166	0.0834	0.8139
8	9486	969	10455	0.9073	0.0927	-0.2090
9	9501	896	10397	0.9138	0.0862	0.5059
10	9641	1031	10672	0.9034	0.0966	-0.6379
11	9623	951	10574	0.9101	0.0899	0.0990
12	9404	948	10352	0.9084	0.0916	-0.0880
13	9414	969	10383	0.9067	0.0933	-0.2750
14	9414	953	10367	0.9081	0.0919	-0.1210
15	9591	974	10565	0.9078	0.0922	-0.1540
16	9490	993	10483	0.9053	0.0947	-0.4289
17	9180	952	10132	0.9060	0.9040	-0.3520
18	9545	1024	10569	0.9031	0.0969	-0.6709
19	9746	1011	10757	0.9060	0.0940	-0.3520
20	9636	1002	10638	0.9058	0.0942	-0.3740
21	9701	985	10686	0.9078	0.0922	-0.1540
22	9400	987	10387	0.9050	0.0950	-0.4619
23	9474	953	10427	0.9086	0.0914	-0.0660
24	9528	993	10521	0.9056	0.0944	-0.3960
25	9558	996	10554	0.9056	0.0944	-0.3960
26	9421	999	10420	0.9041	0.0959	-0.5609
Avg				0.9092	0.0908	

TABLE XLVIII

CHROMATOGRAPH CALIBRATION - STANDARD SAMPLE 6

Run	Ethylene Area	Propylene Area	Total Area	Ethylene Fraction	Propylene Fraction	Ethylene % Deviation
1	3732	5985	9717	0.3841	0.6159	-0.2078
2	3917	6260	10177	0.3849	0.6151	0.0000
3	4214	6829	11043	0.3816	0.6184	-0.8574
4	4184	6731	10915	0.3833	0.6167	-0.4157
5	4120	6611	10731	0.3839	0.6161	-0.2598
6	4182	6669	10851	0.3854	0.6146	0.1299
7	4375	6935	11310	0.3868	0.6132	0.4936
8	4334	6958	11292	0.3838	0.6162	-0.2858
9	4418	7017	11435	0.3864	0.6136	0.3897
10	4279	6833	11112	0.3851	0.6149	0.0520
11	4350	6892	11242	0.3869	0.6131	0.5196
12	4243	6686	10929	0.3882	0.6118	0.8574
13	4113	6559	10672	0.3854	0.6146	0.1299
14	4228	6767	10995	0.3845	0.6155	-0.1039
15	4005	6414	10419	0.3844	0.6156	-0.1299
16	4006	6339	10345	0.3872	0.6128	0.5976
17	4264	6832	11096	0.3843	0.6157	-0.1559
18	4325	6855	11180	0.3869	0.6131	0.5196
19	4376	7038	11414	0.3834	0.6166	-0.3897
20	4078	6444	10522	0.3876	0.6124	0.7015
21	4114	6629	10743	0.3829	0.6171	-0.5196
22	4311	6973	11284	0.3820	0.6180	-0.7534
23	4089	6553	10642	0.3842	0.6158	-0.1819
Avg				0.3849	0.6151	

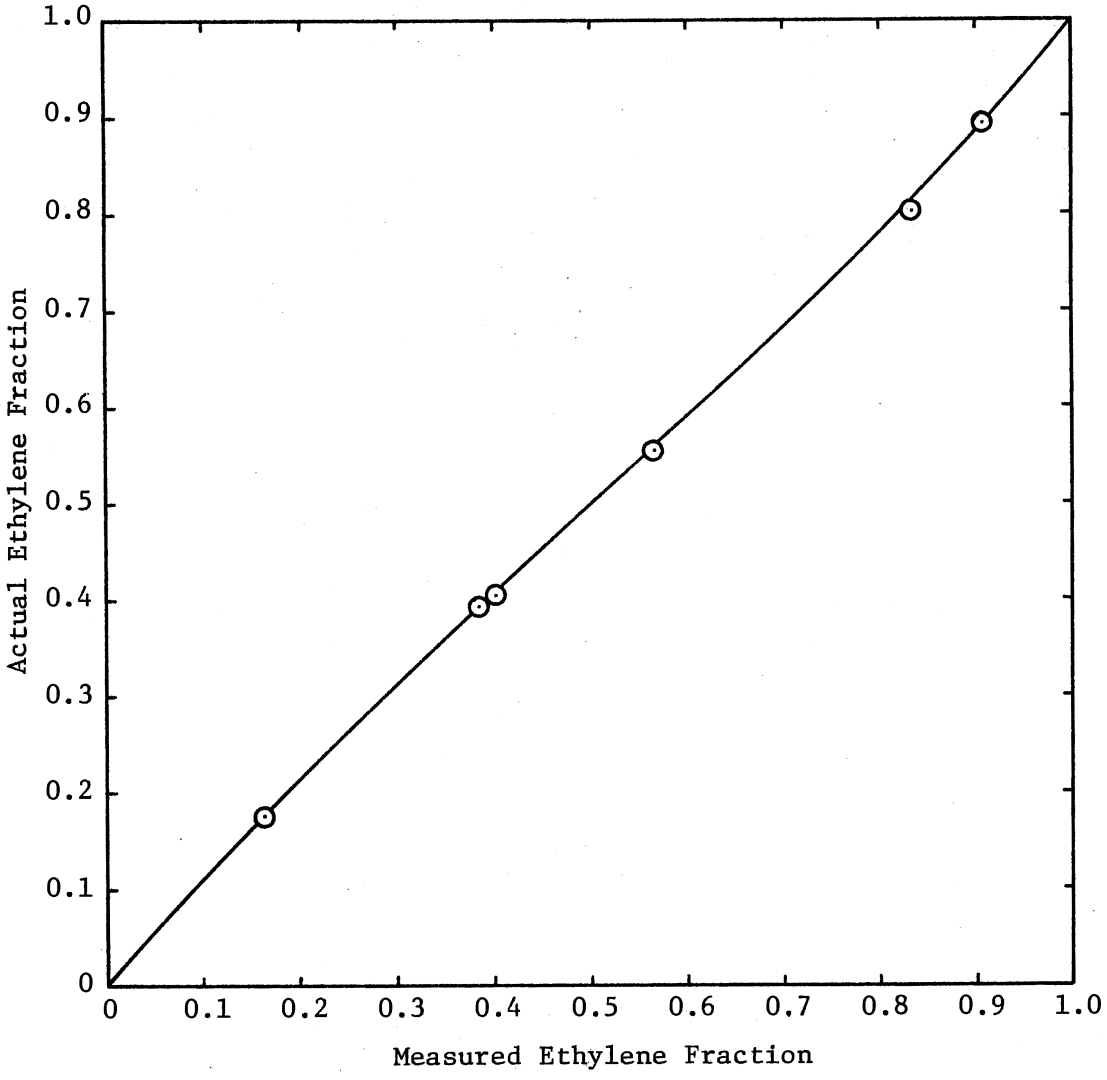

Figure 41. Calibration Curve for F & M Scientific Company Gas Chromatograph for Ethylene - Propylene Binary Mixtures

Viscometer Calibrations

The kinematic viscometer required a capillary constant to calculate the test fluid kinematic viscosity from the experimental measurements. Water, a fluid of known density and absolute viscosity, was used as the calibration fluid during this study.

Two samples were run in viscometer #U-3501. The samples were distilled water with one significant difference. Sample 2 was also degassed. The degassing step required rapid boiling of the sample in an apparatus consisting of a boiling flask with a vented condenser for approximately one hour. After boiling, the sample temperature was maintained above 180°F for an additional hour to ensure that all dissolved gases were removed.

The effect of fluid degassing on the calibration constant, K, was significant as shown in Table XLIX.

TABLE XLIX

KINEMATIC VISCOMETER #U-3501 CALIBRATIONS

Sample	Temperature °F	Time sec	Viscosity cp	Density gm ml	Kinematic Viscosity cs	Calibration Constant cs/sec
1	104.0	177.0447	0.65390	0.99225	0.65901	3.7223×10^{-3}
1	106.5	176.5975	0.63916	0.99166	0.64454	3.6497×10^{-3}
2	96.0	183.3976	0.71807	0.99375	0.72259	3.9400×10^{-3}
2	115.0	150.5979	0.58906	0.98967	0.59521	3.9523×10^{-3}
2	123.0	139.4569	0.54332	0.98776	0.55005	3.9442×10^{-3}

The value of K used during this study for viscometer #U-3501 was 3.9455×10^{-3}, the average of the calibrations run on sample 2. Table L illustrates experimental viscometer calibration measurements for sample 1. Table LI illustrates the corresponding measurements for sample 2.

TABLE L

CALIBRATION MEASUREMENTS - SAMPLE 1

Run	Cell Temperature, mV	Atmospheric Pressure, mm Hg	Flow Time, seconds	Percent Deviation
		T = 1.607 mV		
1	1.628	743.3	176.523	-0.295
2	1.628		176.713	-0.187
3	1.632		176.670	-0.212
4	1.619		176.650	-0.223
5	1.596		176.643	-0.227
6	1.595		176.751	-0.166
7	1.576		177.070	0.014
8	1.590		177.071	0.015
9	1.582		177.220	0.099
10	1.588		177.236	0.108
11	1.599		177.141	0.054
12	1.615		177.293	0.140
13	1.619		177.438	0.222
14	1.626		177.358	0.177
15	1.616		177.656	0.345
16	1.610	743.4	177.282	0.134
Avg	1.607	743.35	177.0447	
		T = 1.668 mV		
1	1.656	748.1	177.262	0.376
2	1.655		176.435	-0.092
3	1.669		176.943	0.196
4	1.660		176.829	0.131
5	1.664		176.602	0.003
6	1.656		177.039	0.250
7	1.669		176.901	0.172
8	1.663		176.779	0.103
9	1.676		176.710	0.064
10	1.675		176.650	0.030
11	1.680		176.556	-0.023
12	1.680		176.211	-0.219
13	1.680		176.215	-0.217
14	1.676		176.270	-0.185
15	1.665		176.138	-0.260
16	1.662	748.5	176.020	-0.327
Avg	1.668	748.3	176.5975	

TABLE LI

CALIBRATION MEASUREMENTS - SAMPLE 2

Run	Cell Temperature, mV	Gauge Pressure, in Hg Vac	Atmospheric Pressure, mm Hg	Flow Time, seconds	Percent Deviation
		T = 1.405 mV			
1	1.395	17.9	733.2	183.622	0.122
2	1.395	17.9		183.203	-0.106
3	1.399	17.9		183.239	-0.086
4	1.399	17.9		183.406	0.005
5	1.399	17.9		183.273	-0.068
6	1.404	17.8	733.3	183.518	0.066
7	1.405	17.9		183.270	-0.070
8	1.405	17.8		183.413	0.008
9	1.405	17.7		183.405	0.004
10	1.410	17.7		183.399	0.001
11	1.410	17.8	733.3	183.470	0.039
12	1.413	17.8		183.480	0.045
13	1.406	17.8		183.507	0.060
14	1.411	17.8		183.407	0.005
15	1.411	17.7		183.468	0.038
16	1.417	17.7	733.3	183.281	-0.064
Avg	1.405	17.813	733.275	183.3976	
		T = 1.860 mV			
1	1.844	15.4	732.9	150.712	0.076
2	1.848	15.2		151.142	0.361
3	1.854	15.1		151.001	0.268
4	1.854	15.0		151.066	0.311
5	1.853	15.0		150.768	0.113
6	1.858	14.9	732.9	150.539	-0.039
7	1.858	14.9		150.324	-0.182
8	1.861	14.8		150.402	-0.130
9	1.861	14.3		150.472	-0.084
10	1.861	14.2		150.415	-0.121
11	1.861	14.1	733.3	150.320	-0.185
12	1.861	14.0		150.291	-0.204
13	1.870	14.0		151.550	0.632
14	1.870	14.0		150.122	-0.316
15	1.870	14.0		150.141	-0.303
16	1.870	14.0	733.5	150.302	-0.196
Avg	1.860	14.556	733.15	150.5979	

TABLE LI (Continued)

Run	Cell Temperature, mV	Gauge Pressure, in Hg Vac	Atmospheric Pressure, mm Hg	Flow Time, seconds	Percent Deviation
		T = 2.055 mV			
1	2.050	13.2	735.4	139.727	0.194
2	2.055	13.2		139.688	0.166
3	2.055	13.2		139.690	0.167
4	2.055	13.2		139.547	0.065
5	2.054	13.2		138.931	-0.377
6	2.054	13.2	735.6	139.581	0.089
7	2.052	13.2		139.632	0.126
8	2.052	13.2		139.540	0.060
9	2.055	13.2		139.561	0.075
10	2.055	13.2		139.509	0.037
11	2.055	13.2	735.6	139.606	0.107
12	2.055	12.9		139.354	-0.074
13	2.055	12.8		139.338	-0.085
14	2.055	13.0		139.010	-0.320
15	2.060	13.3		139.574	0.084
16	2.060	13.2	736.4	139.022	-0.312
Avg	2.055	13.15	735.75	139.4569	

APPENDIX D

RAW DATA

TABLE LII

EXPERIMENTAL MEASUREMENTS OF ETHANOL ABSOLUTE VISCOSITY

Run	Temperature, mV	Gauge Pressure, psig	Atmospheric Pressure, mm Hg	Pressure Drop, in H_2O	Flow Rate, ml/sec
		T = 11.431 mV			
1	11.461	280.	749.8	22.0	0.0885
2	11.438	288.	749.8	22.1	0.0885
3	11.443	290.	749.7	21.6	0.0885
4	11.435	292.	749.7	21.7	0.0885
5	11.426	292.	749.5	21.7	0.0885
6	11.425	292.	749.5	21.7	0.0885
7	11.425	292.	749.5	21.8	0.0885
8	11.397	292.	749.5	21.8	0.0885
Avg	11.431	289.75	749.625	21.8	0.0885
		T = 13.237 mV			
1	13.270	372.	742.9	18.2	0.0880
2	13.222	370.	742.9	18.2	0.0880
3	13.229	380.	742.8	18.3	0.0880
4	13.241	385.	742.8	18.4	0.0880
5	13.232	384.	743.0	18.5	0.0880
6	13.230	384.	743.0	18.4	0.0880
7	13.236	385.	743.0	18.5	0.0880
Avg	13.237	380.	742.91	18.357	0.0880
		T = 13.215 mV			
1	13.231	510.	742.8	19.1	0.0880
2	13.235	532.	742.8	19.0	0.0880
3	13.229	548.	742.5	19.1	0.0880
4	13.227	550.	742.5	19.2	0.0880
5	13.215	550.	742.8	19.2	0.0880
6	13.218	550.	742.8	19.2	0.0880
7	13.152	550.	742.8	19.2	0.0880
Avg	13.215	541.43	742.71	19.143	0.0880

TABLE LII (Continued)

Run	Temperature, mV	Gauge Pressure, psig	Atmospheric Pressure, mm Hg	Pressure Drop, in H_2O	Flow Rate, ml/sec
			T = 14.805 mV		
1	14.807	600.	744.3	17.8	0.0880
2	14.796	560.	744.3	17.2	0.0880
3	14.805	562.	744.0	17.3	0.0880
4	14.805	560.	744.0	17.2	0.0880
5	14.804	560.	744.2	17.2	0.0880
6	14.804	560.	744.2	17.2	0.0880
7	14.814	560.	744.2	17.2	0.0880
8	14.805	560.	744.2	17.2	0.0880
Avg	14.805	565.25	744.175	17.288	0.0880
			T = 15.529 mV		
1	15.635	840.	743.9	16.4	0.0795
2	15.582	835.	743.9	16.9	0.0795
3	15.552	820.	743.7	16.9	0.0795
4	15.516	815.	743.7	16.9	0.0795
5	15.500	815.	743.5	16.9	0.0795
6	15.470	820.	743.5	17.0	0.0795
7	15.445	820.	743.5	17.1	0.0795
Avg	15.529	823.57	743.67	16.871	0.0795

TABLE LIII

EXPERIMENTAL MEASUREMENTS OF N-PROPANOL ABSOLUTE VISCOSITY

Run	Temperature, mV	Gauge Pressure, psig	Atmospheric Pressure, mm Hg	Pressure Drop, in H_2O	Flow Rate ml/sec
		T = 11.337 mV			
1	11.392	138.	736.1	26.6	0.0890
2	11.379	138.	736.1	26.6	0.0890
3	11.380	135.	736.1	26.6	0.0890
4	11.385	138.	736.1	26.6	0.0890
5	11.376	138.	736.1	26.6	0.0890
6	11.372	138.	736.1	26.6	0.0890
7	11.379	138.	736.1	26.6	0.0890
8	11.375	139.	736.1	26.6	0.0890
Avg	11.337	137.75	736.1	26.6	0.0890
		T = 13.099 mV			
1	13.056	215.	745.8	29.0	0.1070
2	13.106	211.	745.8	28.9	0.1070
3	13.119	211.	745.9	28.8	0.1070
4	13.126	211.	745.9	28.7	0.1070
5	13.138	211.	745.9	28.7	0.1070
6	13.146	211.	745.9	28.2	0.1070
Avg	13.099	211.67	745.867	28.72	0.1070
		T = 13.467 mV			
1	13.486	270.	746.3	27.5	0.1060
2	13.479	271.	746.3	27.5	0.1060
3	13.467	273.	746.2	27.5	0.1060
4	13.464	276.	746.2	27.5	0.1060
5	13.464	278.	746.0	27.5	0.1060
6	13.460	280.	746.0	27.6	0.1060
7	13.456	280.	745.8	27.6	0.1060
8	13.456	280.	745.8	27.6	0.1060
Avg	13.467	275.875	746.075	27.54	0.1060

TABLE LIII (Continued)

Run	Temperature, mV	Gauge Pressure, psig	Atmospheric Pressure, mm Hg	Pressure Drop, in H_2O	Flow Rate, ml/sec
		T = 13.465 mV			
1	13.475	550.	746.2	27.9	0.1050
2	13.469	552.	746.2	27.6	0.1050
3	13.464	555.	746.1	27.6	0.1050
4	13.460	560.	746.1	27.7	0.1050
5	13.470	560.	746.0	27.8	0.1050
6	13.456	560.	746.0	27.8	0.1050
7	13.459	560.	746.0	27.8	0.1050
Avg	13.465	556.71	746.09	27.743	0.1050
		T = 15.020 mV			
1	14.994	362.	736.3	23.6	0.1060
2	14.961	370.	736.3	23.7	0.1060
3	14.953	369.	736.1	23.7	0.1060
4	14.942	370.	736.1	23.7	0.1060
5	15.065	370.	736.1	23.6	0.1060
6	15.102	372.	736.1	23.5	0.1060
7	15.122	372.	736.1	23.6	0.1060
Avg	15.020	369.286	736.157	23.629	0.1060

TABLE LIV

EXPERIMENTAL MEASUREMENTS OF N-OCTANE ABSOLUTE VISCOSITY

Run	Temperature, mV	Gauge Pressure, psig	Atmospheric Pressure, mm Hg	Pressure Drop, in H_2O	Flow Rate, ml/sec
		T = 2.117 mV, P = 0.0 psig			
1	2.184	0.	740.8	16.30	0.02946
2	2.170	0.	740.7	16.55	0.02922
3	2.154	0.	740.7	16.70	0.02980
4	2.134	0.	740.6	16.80	0.03065
5	2.113	0.	740.7	16.90	0.03067
6	2.079	0.	740.7	16.90	0.03030
7	2.062	0.	740.5	16.90	0.03000
8	2.040	0.	740.4	17.10	0.03099
Avg	2.117	0.	740.64	16.769	0.03012
		T = 2.048 mV, P = 112.875 psig			
1	2.046	112.	740.4	17.70	0.03065
2	2.080	112.	740.4	17.75	0.03057
3	2.066	112.	740.4	17.75	0.03101
4	2.051	112.	740.5	17.80	0.03058
5	2.038	113.	740.5	17.80	0.03040
6	2.025	114.	740.6	17.80	0.03048
7	2.020	113.	740.8	17.90	0.03008
8	2.057	115.	740.8	17.90	0.03049
Avg	2.048	112.875	740.55	17.80	0.03053
		T = 2.058 mV, P = 540.13 psig			
1	2.100	540.	741.1	18.25	0.02985
2	2.079	541.	741.2	18.30	0.03060
3	2.061	539.	741.2	18.30	0.03045
4	2.027	541.	741.4	18.10	0.02960
5	2.021	540.	741.5	18.60	0.03037
6	2.020	540.	741.6	18.50	0.03023
7	2.055	540.	741.8	18.40	0.03051
8	2.097	540.	741.9	18.40	0.03016
Avg	2.058	540.13	741.46	18.356	0.03022

TABLE LIV (Continued)

Run	Temperature, mV	Gauge Pressure, psig	Atmospheric Pressure, mm Hg	Pressure Drop, in H_2O	Flow Rate, ml/sec
		T = 2.069 mV, P = 1014.25 psig			
1	2.046	1022.	747.4	18.60	0.02957
2	2.033	1019.	747.5	19.00	0.03002
3	2.030	1010.	747.5	19.25	0.02973
4	2.067	1020.	747.3	19.10	0.02991
5	2.123	1020.	747.3	18.80	0.02954
6	2.101	1008.	747.4	19.30	0.02979
7	2.086	1016.	747.4	18.90	0.02919
8	2.068	999.	747.2	19.20	0.02950
Avg	2.069	1014.25	747.375	19.044	0.02965
		T = 5.372 mV, P = 0.0 psig			
1	5.358	0.0	739.1	11.9	0.02929
2	5.369	0.0	739.3	12.0	0.03074
3	5.371	0.0	739.0	12.0	0.02995
4	5.372	0.0	739.0	12.0	0.03001
5	5.375	0.0	739.0	12.0	0.02991
6	5.375	0.0	739.0	12.0	0.03046
7	5.376	0.0	739.0	12.0	0.03157
8	5.377	0.0	739.2	12.0	0.03177
Avg	5.372	0.0	739.075	11.9875	0.03046
		T = 5.371 mV, P = 0.0 psig			
1	5.359	0.0	741.2	10.9	0.02891
2	5.364	0.0	741.2	11.1	0.02957
3	5.370	0.0	741.3	11.1	0.03049
4	5.371	0.0	741.5	11.1	0.02915
5	5.375	0.0	741.6	11.2	0.02967
6	5.377	0.0	741.6	11.2	0.03083
7	5.375	0.0	741.4	11.2	0.03160
8	5.376	0.0	741.5	11.2	0.03150
Avg	5.371	0.0	741.41	11.125	0.03022

TABLE LIV (Continued)

Run	Temperature, mV	Gauge Pressure, psig	Atmospheric Pressure, mm Hg	Pressure Drop, in H_2O	Flow Rate, ml/sec
		T = 5.357 mV, P = 120.75 psig			
1	5.347	120.0	740.7	10.9	0.02825
2	5.355	121.0	740.6	11.1	0.03062
3	5.360	121.0	740.5	11.2	0.03228
4	5.360	120.0	740.7	11.3	0.03191
5	5.356	121.0	740.8	11.3	0.03137
6	5.360	121.0	740.8	11.3	0.03199
7	5.360	121.0	740.8	11.4	0.03131
8	5.356	121.0	740.8	11.4	0.03210
Avg	5.557	120.75	740.71	11.2375	0.03123
		T = 5.361 mV, P = 519.0 psig			
1	5.354	517.0	739.4	11.6	0.02911
2	5.359	519.0	739.3	11.8	0.02990
3	5.362	520.0	739.3	11.9	0.02952
4	5.361	518.0	739.2	11.9	0.03311
5	5.365	519.0	739.2	11.9	0.03210
6	5.363	519.0	739.1	11.9	0.03164
7	5.360	520.0	739.1	11.9	0.03237
8	5.361	520.0	739.0	11.9	0.03191
Avg	5.361	519.0	739.2	11.85	0.03121
		T = 5.372 mV, P = 1027.0 psig			
1	5.369	1031.0	739.2	12.20	0.02988
2	5.376	1030.0	739.2	12.25	0.03138
3	5.376	1030.0	739.2	12.30	0.03059
4	5.376	1029.0	739.3	12.40	0.02985
5	5.375	1020.0	739.4	12.50	0.03123
6	5.372	1020.0	739.6	12.40	0.03184
7	5.363	1029.0	739.4	12.40	0.02931
8	5.365	1027.0	739.5	12.40	0.02939
Avg	5.372	1027.0	739.35	12.356	0.03043

TABLE LIV (Continued)

Run	Temperature, mV	Gauge Pressure, psig	Atmospheric Pressure, mm Hg	Pressure Drop, in H_2O	Flow Rate, ml/sec
		T = 9.413 mV, P = 26.5 psig			
1	9.420	27.	743.8	7.60	0.02885
2	9.415	27.	743.8	7.70	0.03065
3	9.415	26.	743.9	7.70	0.02849
4	9.410	26.	744.0	7.70	0.02906
5	9.414	27.	744.0	7.70	0.02889
6	9.410	26.	743.9	7.75	0.02974
7	9.416	27.	743.9	7.75	0.02894
8	9.401	26.	743.8	7.70	0.02932
Avg	9.413	26.5	743.89	7.70	0.02924
		T = 9.402 mV, P = 27.875 psig			
1	9.403	21.	741.5	7.6	0.02830
2	9.405	28.	741.7	7.7	0.02954
3	9.400	29.	741.8	7.7	0.02845
4	9.409	29.	741.6	7.7	0.03158
5	9.394	29.	741.6	7.7	0.02947
6	9.395	29.	741.5	7.7	0.02979
7	9.404	29.	741.5	7.7	0.03104
8	9.406	29.	741.4	7.7	0.02873
Avg	9.402	27.875	741.575	7.688	0.02961
		T = 13.110 mV, P = 118.5 psig			
1	13.064	119.	730.8	15.0	0.0600
2	13.098	119.	730.9	15.1	0.0600
3	13.104	119.	731.2	15.1	0.0600
4	13.112	118.	731.2	15.1	0.0600
5	13.128	118.	731.3	15.1	0.0600
6	13.125	118.	731.4	15.1	0.0600
7	13.120	119.	731.5	15.1	0.0600
8	13.130	118.	731.4	15.1	0.0600
Avg	13.110	118.5	731.21	15.088	0.0600

TABLE LIV (Continued)

Run	Temperature, mV	Gauge Pressure, psig	Atmospheric Pressure, mm Hg	Pressure Drop, in H_2O	Flow Rate, ml/sec
		T = 17.504 mV, P = 235.875 psig			
1	17.541	238.	740.8	16.50	0.0885
2	17.525	237.	740.7	16.80	0.0885
3	17.520	237.	740.8	16.70	0.0885
4	17.513	237.	740.8	16.70	0.0885
5	17.491	233.	740.8	16.80	0.0885
6	17.491	236.	740.8	16.75	0.0885
7	17.480	235.	740.9	16.75	0.0885
8	17.467	234.	741.0	16.70	0.0885
Avg	17.504	235.875	740.83	16.713	0.0885
		T = 19.673 mV, P = 520.63 psig			
1	19.546	520.	737.8	14.5	0.0880
2	19.621	521.	737.8	14.3	0.0880
3	19.671	520.	737.8	14.3	0.0880
4	19.670	521.	737.8	14.1	0.0880
5	19.698	521.	737.9	14.1	0.0880
6	19.715	521.	738.0	14.1	0.0880
7	19.728	522.	738.0	14.2	0.0880
8	19.735	519.	738.0	14.1	0.0880
Avg	19.673	520.63	737.89	14.363	0.0880
		T = 19.749 mV, P = 381.0 psig			
1	19.760	381.	742.5	11.20	0.0880
2	19.768	381.	742.5	11.30	0.0880
3	19.758	380.	742.5	11.50	0.0880
4	19.754	382.	742.5	11.30	0.0880
5	19.750	381.	742.5	11.25	0.0880
6	19.742	381.	742.5	11.25	0.0880
7	19.731	381.	742.5	11.20	0.0880
8	19.735	381.	742.5	11.20	0.0880
Avg	19.749	381.	742.5	11.275	0.0880

TABLE LV

EXPERIMENTAL MEASUREMENTS OF N-OCTANE VISCOSITY WITH AN ARGON ATMOSPHERE

Run	Cell Temperature, mV	Gauge Pressure, mV	Atmospheric Pressure, mm Hg	Flow Time, seconds	Percent Deviation
		P = 4.987 mV			
1	1.713	5.084	741.0	186.467	-0.123
2	1.708	5.084		186.468	-0.122
3	1.699	5.096		186.619	-0.041
4	1.701	4.999		186.500	-0.105
5	1.713	4.918		186.501	-0.104
6	1.709	4.955	740.9	186.863	0.089
7	1.709	4.981		186.914	0.117
8	1.710	4.922		186.788	0.049
9	1.702	4.970		187.058	0.194
10	1.716	4.865	740.9	186.780	0.045
Avg	1.708	4.987	740.933	186.696	
		P = 7.838 mV			
1	1.711	7.735		193.407	-0.070
2	1.715	7.890		194.283	0.383
3	1.715	7.537	749.0	193.340	-0.104
4	1.713	7.774		193.322	-0.114
5	1.715	7.870		193.384	-0.082
6	1.715	7.739		193.609	0.035
7	1.714	7.993		193.638	0.050
8	1.718	7.986		193.424	-0.061
9	1.723	7.917		193.441	-0.052
10	1.724	7.941	749.2	193.569	0.014
Avg	1.716	7.838	749.1	193.542	
		P = 11.620 mV			
1	1.744	11.871		199.790	0.266
2	1.749	11.831		199.065	-0.097
3	1.749	11.860		199.193	-0.033
4	1.751	11.840	753.2	199.630	0.186
5	1.753	11.807		199.110	-0.075
6	1.749	11.727		198.865	-0.198
7	1.749	11.751		198.969	-0.146
8	1.749	11.434		199.434	0.088
9	1.747	11.299	753.2	199.297	0.019
10	1.751	10.778		199.241	-0.009
Avg	1.749	11.620	753.2	199.259	

TABLE LVI

EXPERIMENTAL MEASUREMENTS OF N-OCTANE VISCOSITY WITH A HELIUM ATMOSPHERE

Run	Cell Temperature, mV	Gauge Pressure, mV	Atmospheric Pressure, mm Hg	Flow Time, seconds	Percent Deviation
		P = 5.468 mV			
1	1.694	5.595	746.7	192.311	0.180
2	1.686	5.582		191.671	-0.153
3	1.682	5.630		192.852	0.462
4	1.687	5.467		191.381	-0.304
5	1.684	5.413		191.908	-0.030
6	1.695	5.335		191.460	-0.263
7	1.687	5.323		191.369	-0.310
8	1.690	5.412		192.491	0.274
9	1.711	5.475		192.577	0.319
10	1.706	5.449	746.3	191.630	-0.175
Avg.	1.692	5.468	746.5	191.965	
		P = 7.581 mV			
1	1.679	7.296	745.6	187.981	0.103
2	1.680	7.330		187.661	-0.067
3	1.680	7.874		186.491	-0.690
4	1.680	7.149		186.781	-0.536
5	1.680	7.249		188.390	0.321
6	1.695	7.863		188.649	0.459
7	1.697	7.890		187.504	-0.151
8	1.711	7.820		187.250	-0.286
9	1.707	7.563		188.523	0.392
10	1.703	7.779	745.6	188.638	0.453
Avg.	1.692	7.581	745.6	187.787	
		P = 11.866 mV			
1	1.628	11.892	748.8	201.633	2.581
2	1.629	11.892		200.555	2.032
3	1.640	11.890	748.9	197.739	0.600
4	1.639	11.890		197.217	0.334
5	1.645	11.877		196.229	-0.168
6	1.646	11.875		196.057	-0.256
7	1.646	11.866		198.757	1.118
8	1.646	11.864	749.1	197.341	0.397
9	1.649	11.839		192.918	-1.853
10	1.650	11.824		192.927	-1.848
11	1.656	11.820	748.8	191.224	-2.715
Avg	1.643	11.866	748.9	196.560	

TABLE LVI (Continued)

Run	Cell Temperature, mV	Gauge Pressure, mV	Atmospheric Pressure, mm Hg	Flow Time, seconds	Percent Deviation
		P = 11.863 mV			
1	1.701	11.275	746.4	192.171	0.041
2	1.711	11.985		192.119	0.014
3	1.714	12.015		192.699	0.315
4	1.720	12.008		191.862	-0.120
5	1.720	11.975		191.820	-0.142
6	1.730	11.238		192.150	0.030
7	1.734	11.965		192.220	0.066
8	1.735	12.040		191.960	-0.069
9	1.734	12.084		191.977	-0.060
10	1.734	12.042	746.4	191.953	-0.073
Avg	1.723	11.863	746.4	192.093	

TABLE LVII

EXPERIMENTAL MEASUREMENTS OF N-OCTANE VISCOSITY WITH A HYDROGEN ATMOSPHERE

Run	Cell Temperature, mV	Gauge Pressure, mV	Atmospheric Pressure, mm Hg	Flow Time, seconds	Percent Deviation
		P = 4.919 mV			
1	1.609	4.916	738.4	175.303	-0.261
2	1.609	4.918		175.409	-0.201
3	1.605	4.918	738.4	175.529	-0.133
4	1.605	4.919		175.766	0.002
5	1.606	4.919		176.207	0.253
6	1.606	4.920		175.560	-0.115
7	1.609	4.920		176.101	0.193
8	1.609	4.919	738.5	175.341	-0.240
9	1.610	4.919		176.565	0.457
10	1.609	4.920	738.5	175.840	0.044
Avg	1.609	4.919	738.45	175.762	
		P = 4.976 mV			
1	1.670	4.983	741.1	166.048	-0.008
2	1.677	4.981		166.078	0.010
3	1.674	4.978		165.860	-0.121
4	1.665	4.978		166.130	0.042
5	1.672	4.974	741.2	165.966	-0.057
6	1.670	4.974		166.081	0.012
7	1.670	4.974		166.188	0.076
8	1.680	4.974		166.176	0.069
9	1.682	4.971		166.079	0.011
10	1.681	4.970	741.3	165.999	-0.037
Avg	1.674	4.976	741.2	166.061	
		P = 7.808 mV			
1	1.647	7.811	738.8	178.439	-1.402
2	1.640	7.810		178.151	-1.488
3	1.640	7.813		178.150	-1.489
4	1.634	7.810		179.934	-0.502
5	1.639	7.809	738.3	180.481	-0.200
6	1.643	7.809		181.660	0.452
7	1.644	7.811		182.993	1.189

TABLE LVII (Continued)

Run	Cell Temperature, mV	Gauge Pressure, mV	Atmospheric Pressure, mm Hg	Flow Time, seconds	Percent Deviation
		P = 7.808 mV (Continued)			
8	1.640	7.811		181.422	0.321
9	1.640	7.809		180.028	-0.450
10	1.646	7.802	738.3	184.043	1.770
11	1.646	7.808		184.382	1.958
12	1.639	7.805		184.484	2.014
13	1.657	7.805		177.683	-1.751
14	1.665	7.805		182.669	1.010
15	1.661	7.808	738.1	176.974	-2.127
16	1.660	7.808		181.974	0.626
Avg	1.646	7.808	738.375	180.842	
		P = 12.041 mV			
1	1.639	12.077	738.2	186.953	0.684
2	1.639	12.069		183.841	-0.992
3	1.641	12.063		188.057	1.279
4	1.641	12.055		187.990	1.242
5	1.644	12.055	738.4	188.547	1.542
6	1.644	12.051		183.503	-1.174
7	1.639	12.045		188.262	1.389
8	1.639	12.040		183.764	-1.033
9	1.632	12.040		183.995	-0.881
10	1.626	12.036	739.8	186.494	0.437
11	1.632	12.030		186.426	0.400
12	1.626	12.027		185.691	0.004
13	1.627	12.027		184.228	-0.784
14	1.642	12.015	739.4	184.132	-0.835
15	1.642	12.013		184.779	-0.487
16	1.648	12.013	739.4	184.270	-0.761
Avg	1.638	12.041	739.04	185.683	

TABLE LVIII

EXPERIMENTAL MEASUREMENTS OF N-OCTANE VISCOSITY WITH A NITROGEN ATMOSPHERE

Run	Cell Temperature, mV	Gauge Pressure, mV	Atmospheric Pressure, mm Hg	Flow Time, seconds	Percent Deviation
		P = 4.503 mV			
1	1.722	4.744	750.7	179.186	-0.229
2	1.715	4.726		179.588	-0.006
3	1.710	4.671		179.756	0.088
4	1.719	4.725		180.190	0.330
5	1.713	4.731	750.5	178.970	-0.350
6	1.720	4.740		179.150	-0.249
7	1.723	4.710		179.649	0.028
8	1.729	4.446		179.703	0.058
9	1.731	4.055		179.886	0.160
10	1.730	3.480	750.7	179.905	0.171
Avg	1.721	4.503	750.633	179.598	
		P = 7.556 mV			
1	1.706	7.640	745.0	181.655	-0.110
2	1.710	7.610		182.997	0.628
3	1.712	7.575		183.065	0.665
4	1.710	7.484		179.311	-1.399
5	1.711	7.569	745.0	180.981	-0.481
6	1.716	7.581		181.650	-0.113
7	1.711	7.581		182.229	0.206
8	1.718	7.320		179.868	-1.093
9	1.716	7.591		182.928	0.590
10	1.720	7.605	745.0	183.861	1.103
Avg	1.713	7.556	745.0	181.855	
		P = 11.567 mV			
1	1.671	11.593	749.1	196.750	0.114
2	1.674	11.645		195.384	-0.581
3	1.678	11.691		196.964	0.223
4	1.675	11.518		196.569	0.022
5	1.674	11.560		196.061	-0.236
6	1.675	11.656		196.270	-0.130

TABLE LVIII (Continued)

Run	Cell Temperature, mV	Gauge Pressure, mV	Atmospheric Pressure, mm Hg	Flow Time, seconds	Percent Deviation
		P = 11.567 mV (Continued)			
7	1.679	11.740		198.108	0.805
8	1.693	11.796		197.177	0.332
9	1.705	11.431		196.335	-0.097
10	1.726	11.526		195.336	-0.605
11	1.726	11.182		195.711	-0.414
12	1.740	11.225	749.1	197.635	0.565
Avg	1.693	11.567	749.1	196.525	
		P = 11.989 mV			
1	1.692	12.015	740.7	198.658	-0.331
2	1.681	11.619		199.885	0.284
3	1.685	11.982		200.259	0.472
4	1.686	12.052		198.192	-0.565
5	1.685	12.051	740.4	199.261	-0.029
6	1.690	12.050		199.688	0.186
7	1.688	12.036		199.179	-0.070
8	1.693	12.035		199.615	0.149
9	1.696	12.030		199.444	0.063
10	1.696	12.025	740.0	199.000	-0.160
Avg	1.689	11.989	740.367	199.318	

TABLE LIX

EXPERIMENTAL MEASUREMENTS OF N-OCTANE VISCOSITY WITH A METHANE ATMOSPHERE

Run	Cell Temperature, mV	Gauge Pressure, mV	Atmospheric Pressure, mm Hg	Flow Time, seconds	Percent Deviation
		P = 4.673 mV			
1	1.705	4.675	743.2	179.433	0.357
2	1.715	4.679		179.599	0.450
3	1.707	4.676		178.859	0.036
4	1.712	4.677		176.130	-1.491
5	1.710	4.677	743.4	177.693	-0.616
6	1.708	4.676		178.901	0.059
7	1.719	4.672		179.829	0.578
8	1.708	4.676		177.597	-0.670
9	1.707	4.676		179.257	0.258
10	1.709	4.675	743.5	179.543	0.418
11	1.706	4.676		178.895	0.056
12	1.705	4.663		179.694	0.503
13	1.701	4.668		180.650	1.038
14	1.705	4.665		177.761	-0.578
15	1.702	4.672		179.630	0.467
16	1.705	4.672	743.3	177.247	-0.866
Avg	1.708	4.673	743.35	178.795	
		P = 7.722 mV			
1	1.680	7.731	744.0	164.808	-0.263
2	1.684	7.731		165.101	-0.086
3	1.677	7.754		165.347	0.063
4	1.684	7.749	744.0	166.096	0.516
5	1.689	7.747		164.347	-0.542
6	1.690	7.745		164.239	-0.608
7	1.694	7.739		165.205	-0.023
8	1.695	7.736		165.144	-0.060
9	1.701	7.734		165.757	0.311
10	1.713	7.713	744.0	165.071	-0.104
11	1.710	7.713		165.321	0.047
12	1.714	7.698		165.050	-0.117
13	1.719	7.693		165.412	0.102
14	1.720	7.690		166.890	0.997
15	1.719	7.690		165.118	-0.076
16	1.719	7.684	743.9	164.982	-0.158
Avg	1.701	7.722	743.975	165.243	

TABLE LIX (Continued)

Run	Cell Temperature, mV	Gauge Pressure, mV	Atmospheric Pressure, mm Hg	Flow Time, seconds	Percent Deviation
		P = 11.802 mV			
1	1.710	11.830	741.0	152.058	-0.024
2	1.719	11.823		152.070	-0.016
3	1.715	11.814		151.927	-0.110
4	1.713	11.805		152.192	0.064
5	1.719	11.801		151.861	-0.154
6	1.711	11.794	741.0	152.050	-0.030
7	1.711	11.789		152.330	0.155
8	1.724	11.786		152.379	0.187
9	1.714	11.790		151.534	-0.369
10	1.711	11.785	741.0	152.550	0.299
Avg	1.715	11.802	741.0	152.095	
		P = 12.118 mV			
1	1.608	12.110	743.2	155.292	2.023
2	1.612	12.110		154.439	1.463
3	1.612	12.129		154.940	1.792
4	1.621	12.129		152.900	0.452
5	1.621	12.125	743.3	154.670	1.615
6	1.619	12.125		153.121	0.597
7	1.621	12.121		152.980	0.505
8	1.620	12.111		148.150	-2.669
9	1.623	12.116		149.779	-1.598
10	1.621	12.110	743.3	149.009	-2.104
11	1.621	12.115		149.608	-1.711
12	1.632	12.110		151.651	-0.369
Avg	1.619	12.118	743.27	152.212	

TABLE LX

EXPERIMENTAL MEASUREMENTS OF N-OCTANOL ABSOLUTE VISCOSITY

Run	Cell Temperature, mV	Gauge Pressure, psig	Atmospheric Pressure, mm Hg	Pressure Drop, in H_2O	Flow Rate, ml/sec
		T = 7.696 mV, P = 2.0 psig			
1	7.696	2.0	741.4	89.5	0.0905
2	7.698	2.0	741.4	89.5	0.0905
3	7.695	2.0	740.4	89.5	0.0905
4	7.698	2.0	740.4	89.5	0.0905
5	7.696	2.0	740.5	89.5	0.0905
6	7.695	2.0	740.5	89.5	0.0905
7	7.697	2.0	740.5	89.5	0.0905
8	7.695	2.0	740.5	89.5	0.0905
Avg	7.696	2.0	740.7	89.5	0.0905
		T = 7.721 mV, P = 111.37 psig			
1	7.722	100.0	740.9	91.0	0.0895
2	7.721	108.0	740.9	91.0	0.0895
3	7.723	109.0	740.6	91.0	0.0895
4	7.717	111.0	740.6	91.0	0.0895
5	7.722	111.0	740.8	91.0	0.0895
6	7.720	115.0	740.8	91.0	0.0895
7	7.721	117.0	740.8	91.0	0.0895
8	7.724	120.0	740.8	91.0	0.0895
Avg	7.721	111.37	740.775	91.0	0.0895
		T = 7.733 mV, P = 513.625 psig			
1	7.732	492.0	740.5	93.0	0.0880
2	7.735	498.0	740.5	93.0	0.0880
3	7.731	511.0	740.5	93.0	0.0880
4	7.732	517.0	740.5	93.0	0.0880
5	7.734	520.0	740.8	93.0	0.0880
6	7.731	520.0	740.8	93.5	0.0880
7	7.733	523.0	740.8	93.0	0.0880
8	7.734	528.0	740.8	93.0	0.0880
Avg	7.733	513.625	740.65	93.063	0.0880

TABLE LX (Continued)

Run	Cell Temperature, mV	Gauge Pressure, mV	Atmospheric Pressure, mm Hg	Pressure Drop, in H_2O	Flow Rate, ml/sec
		T = 7.728 mV, P = 1004.875 psig			
1	7.728	950.0	740.8	98.0	0.0875
2	7.721	979.0	740.8	95.0	0.0875
3	7.725	982.0	740.8	95.0	0.0875
4	7.728	1000.0	740.8	95.5	0.0875
5	7.732	1020.0	741.0	95.0	0.0875
6	7.733	1055.0	741.0	95.0	0.0875
7	7.730	1040.0	741.0	96.5	0.0875
8	7.725	1013.0	741.0	96.0	0.0875
Avg	7.728	1004.875	740.9	95.75	0.0875
		T = 11.432 mV, P = 5.0 psig			
1	11.444	5.0	735.4	49.0	0.0905
2	11.432	5.0	735.4	49.0	0.0905
3	11.427	5.0	735.3	49.0	0.0905
4	11.425	5.0	735.3	49.0	0.0905
5	11.428	5.0	735.3	48.5	0.0905
6	11.430	5.0	735.3	48.5	0.0905
7	11.433	5.0	735.2	49.0	0.0905
8	11.435	5.0	735.2	48.5	0.0905
Avg	11.432	5.0	735.3	48.813	0.0905
		T = 11.495 mV, P = 134.625 psig			
1	11.489	129.0	735.8	49.5	0.0892
2	11.483	130.0	735.8	49.5	0.0892
3	11.489	132.0	735.8	49.5	0.0892
4	11.492	135.0	735.8	49.5	0.0892
5	11.498	135.0	735.7	49.5	0.0892
6	11.504	138.0	735.7	49.5	0.0892
7	11.507	139.0	735.7	49.5	0.0892
8	11.500	139.0	735.7	49.5	0.0892
Avg	11.495	134.625	735.75	49.5	0.0892

TABLE LX (Continued)

Run	Cell Temperature, mV	Gauge Pressure, mV	Atmospheric Pressure, mm Hg	Pressure Drop, in H_2O	Flow Rate, ml/sec
		T = 11.540 mV, P = 521.25 psig			
1	11.540	509.0	736.6	49.5	0.0880
2	11.536	515.0	736.6	50.0	0.0880
3	11.540	520.0	736.6	50.0	0.0880
4	11.539	520.0	736.6	50.0	0.0880
5	11.544	525.0	736.2	50.0	0.0880
6	11.541	525.0	736.2	50.0	0.0880
7	11.540	528.0	736.2	50.0	0.0880
8	11.536	528.0	736.2	50.0	0.0880
Avg	11.540	521.25	736.4	49.94	0.0880
		T = 11.521 mV, P = 1045.375 psig			
1	11.532	970.0	736.0	52.5	0.0875
2	11.525	1040.0	736.0	52.0	0.0875
3	11.527	1069.0	736.0	52.0	0.0875
4	11.525	1030.0	736.0	52.5	0.0875
5	11.524	1019.0	736.0	52.5	0.0875
6	11.512	1075.0	736.0	52.5	0.0875
7	11.513	1080.0	736.0	52.5	0.0875
8	11.506	1080.0	736.0	52.5	0.0875
Avg	11.521	1045.375	736.0	52.375	0.0875

TABLE LXI

EXPERIMENTAL MEASUREMENTS OF N-OCTANOL KINEMATIC VISCOSITY

Run	Cell Temperature, mV	Gauge Pressure, in Hg Vac	Atmospheric Pressure, mm Hg	Flow Time, seconds	Percent Deviation
		T = 1.458 mV		t	δ
1	1.486	19.3	743.7	1477.749	-0.340
2	1.460	18.4	743.7	1479.340	-0.233
3	1.451	17.9	743.7	1483.613	0.055
4	1.451	16.8	743.0	1482.359	-0.029
5	1.444	13.9	743.0	1490.900	0.547
Avg	1.458	17.26	743.42	1482.7922	
		T = 1.847 mV			
1	1.883	11.9	743.9	1031.914	-0.658
2	1.837	11.8	744.1	1035.563	-0.307
3	1.826	11.6	744.6	1039.042	0.028
4	1.848	11.5	744.8	1042.435	0.355
5	1.841	11.2	744.8	1044.791	0.582
Avg	1.847	11.6	744.44	1038.749	
		T = 2.030 mV			
1	2.014	9.5	742.3	958.110	-0.049
2	2.024	9.1	742.4	958.810	0.024
3	2.031	9.0	742.3	960.205	0.169
4	2.036	8.8	742.3	958.630	0.005
5	2.045	8.1	742.1	957.168	-0.148
Avg	2.030	8.9	742.28	958.5846	
		T = 2.527 mV			
1	2.527	4.8	741.2	721.552	0.149
2	2.540	4.3	741.2	721.101	0.086
3	2.526	4.0	741.3	720.270	-0.029
4	2.525	3.7	741.3	719.700	-0.108
5	2.518	3.3	741.4	719.781	-0.097
Avg	2.527	4.02	741.28	720.4808	

TABLE LXI (Continued)

Run	Cell Temperature, mV	Gauge Pressure, in Hg Vac	Atmospheric Pressure, mm Hg	Flow Time, seconds	Percent Deviation
		T = 2.865 mV			
1	2.861	2.5	740.6	591.255	0.229
2	2.861	2.2	740.6	591.008	0.187
3	2.864	2.0	740.6	590.068	0.028
4	2.869	2.5	740.6	587.931	-0.335
5	2.869	1.9	740.4	589.260	-0.109
Avg	2.865	2.22	740.56	589.9044	

TABLE LXII

EXPERIMENTAL MEASUREMENTS OF N-OCTANOL VISCOSITY WITH AN ARGON ATMOSPHERE

Run	Cell Temperature, mV	Gauge Pressure, mV	Atmospheric Pressure, mm Hg	Flow Time, seconds	Percent Deviation
		P = 4.777 mV			
1	1.485	4.778	739.5		
	1.474	4.779			
	1.480	4.776		1466.893	0.324
2	1.480	4.775	739.1		
	1.481	4.780			
	1.486	4.778		1462.735	0.039
3	1.484	4.779	738.9		
	1.482	4.778			
	1.486	4.779		1461.599	-0.039
4	1.477	4.775	738.4		
	1.479	4.778			
	1.487	4.775		1460.192	-0.135
5	1.486	4.775	738.2		
	1.490	4.774			
	1.490	4.774		1459.391	-0.190
Avg	1.483	4.777	738.82	1462.162	
		P = 7.941 mV			
1	1.489	7.950	735.8		
	1.488	7.944			
	1.478	7.941		1460.538	-0.138
2	1.475	7.939	736.0		
	1.480	7.939			
	1.480	7.939		1462.882	0.023
3	1.482	7.939	736.1		
	1.486	7.941			
	1.488	7.940		1463.331	0.053
4	1.484	7.941	736.3		
	1.483	7.942			
	1.484	7.942		1462.867	0.022

TABLE LXII (Continued)

Run	Cell Temperature, mV	Gauge Pressure, mV	Atmospheric Pressure, mm Hg	Flow Time, seconds	Percent Deviation
		P = 7.941 mV (Continued)			
5	1.488	7.940	736.2		
	1.485	7.939			
___	1.490	7.938	_____	1463.141	0.040
Avg	1.484	7.941	736.08	1462.5518	
		P = 12.040 mV			
1	1.451	12.065	745.0		
	1.499	12.060			
	1.469	12.050		1576.803	0.283
2	1.463	12.050	745.1		
	1.465	12.045			
	1.505	12.045		1563.911	-0.537
3	1.506	12.045	745.7		
	1.520	12.040			
	1.482	12.038		1577.139	0.305
4	1.560	12.034	745.9		
	1.549	12.030			
	1.608	12.029		1579.721	0.469
5	1.593	12.025	745.8		
	1.630	12.022			
___	1.646	12.022	____	1564.161	-0.521
Avg	1.530	12.040	745.5	1572.347	
		P = 11.907 mV			
1	1.480	11.890	749.4		
	1.478	11.890			
	1.442	11.894		1588.040	0.768
2	1.430	11.894	749.6		
	1.434	11.901			
	1.425	11.896		1563.236	-0.806

TABLE LXII (Continued)

Run	Cell Temperature, mV	Gauge Pressure, mV	Atmospheric Pressure, mm Hg	Flow Time, seconds	Percent Deviation
		P = 11.907 mV (Continued)			
3	1.430	11.901	749.8		
	1.435	11.908			
	1.430	11.911		1580.219	0.272
4	1.431	11.913	749.4		
	1.434	11.918			
	1.430	11.916		1583.729	0.494
5	1.437	11.921	749.0		
	1.452	11.925			
	1.484	11.934		1564.467	-0.728
Avg	1.443	11.907	749.44	1575.9382	

TABLE LXIII

EXPERIMENTAL MEASUREMENTS OF N-OCTANOL VISCOSITY WITH A HELIUM ATMOSPHERE

Run	Cell Temperature, mV	Gauge Pressure, mV	Atmospheric Pressure, mm Hg	Flow Time, seconds	Percent Deviation
		P = 4.698 mV			
1	1.481	4.696	736.3		
	1.485	4.695			
	1.490	4.695		1505.798	0.048
2	1.486	4.697	736.7		
	1.476	4.697			
	1.482	4.697		1506.0684	0.065
3	1.478	4.697	736.9		
	1.478	4.702			
	1.485	4.702		1504.578	-0.033
4	1.481	4.696	736.9		
	1.484	4.696			
	1.491	4.699		1505.219	0.010
5	1.493	4.699	737.0		
	1.494	4.704			
	1.494	4.704		1503.698	-0.091
Avg	1.485	4.698	736.76	150.0684	
		P = 7.735 mV			
1	1.455	7.759	740.4		
	1.470	7.751			
	1.462	7.749		1537.808	-0.138
2	1.463	7.749	740.9		
	1.470	7.745			
	1.467	7.745		1540.364	0.028
3	1.478	7.739	740.8		
	1.472	7.739			
	1.472	7.730		1539.349	-0.038

TABLE LXIII (Continued)

Run	Cell Temperature, mV	Gauge Pressure, mV	Atmospheric Pressure, mm Hg	Flow Time, seconds	Percent Deviation
		P = 7.735 mV (Continued)			
4	1.470	7.730	741.0		
	1.470	7.724			
	1.480	7.724		1541.099	0.076
5	1.472	7.719	741.2		
	1.470	7.716			
	1.469	7.713		1541.043	0.072
Avg	1.469	7.735	740.86	1539.9236	
		P = 12.296 mV			
1	1.438	12.274	741.4		
	1.438	12.280			
	1.438	12.280		1596.600	0.036
2	1.438	12.290	741.4		
	1.444	12.290			
	1.444	12.295		1596.490	0.029
3	1.443	12.295	741.1		
	1.445	12.299			
	1.443	12.299		1596.524	0.031
4	1.442	12.302	740.9		
	1.445	12.302			
	1.445	12.305		1595.711	-0.020
5	1.450	12.309	741.1		
	1.450	12.310			
	1.448	12.310		1594.820	-0.076
Avg	1.443	12.296	741.18	1596.029	

TABLE LXIV

EXPERIMENTAL MEASUREMENTS OF N-OCTANOL VISCOSITY WITH A HYDROGEN ATMOSPHERE

Run	Cell Temperature, mV	Gauge Pressure, mV	Atmospheric Pressure, mm Hg	Flow Time, seconds	Percent Deviation
		P = 4.947 mV			
1	1.420	4.937	749.6		
	1.426	4.937			
	1.436	4.944		1497.672	0.213
2	1.439	4.949	750.2		
	1.444	4.948			
	1.445	4.950		1495.587	0.074
3	1.449	4.954	750.5		
	1.450	4.952			
	1.450	4.946		1497.850	0.225
4	1.450	4.949	751.0		
	1.448	4.946			
	1.459	4.948		1491.054	-0.229
5	1.466	4.946	751.1		
	1.465	4.951			
	1.465	4.948		1490.250	-0.283
Avg	1.447	4.947	750.48	1494.4826	
		P = 7.903 mV			
1	1.431	7.895	754.3		
	1.431	7.900			
	1.435	7.899		1478.930	0.088
2	1.435	7.905	754.2		
	1.435	7.901			
	1.435	7.900		1477.900	0.019
3	1.442	7.905	754.2		
	1.449	7.903			
	1.450	7.905		1477.348	-0.019

TABLE LXIV (Continued)

Run	Cell Temperature, mV	Gauge Pressure, mV	Atmospheric Pressure, mm Hg	Flow Time, seconds	Percent Deviation
		P = 7.903 mV (Continued)			
4	1.459	7.907	753.9		
	1.461	7.905			
	1.457	7.906		1476.731	-0.061
5	1.457	7.907	753.6		
	1.461	7.903			
	1.470	7.904		1477.217	-0.028
Avg	1.447	7.903	754.04	1477.6252	
		P = 11.975 mV			
1	1.475	11.990	744.8		
	1.479	11.990			
	1.475	11.984		1504.248	-0.275
2	1.486	11.981	744.8		
	1.476	11.981			
	1.474	11.975		1509.084	0.045
3	1.480	11.975	744.6		
	1.483	11.972			
	1.489	11.972		1508.571	0.011
4	1.478	11.968	744.5		
	1.472	11.971			
	1.467	11.967		1510.281	0.125
5	1.480	11.968	744.2		
	1.482	11.965			
	1.488	11.965		1509.823	0.094
Avg	1.479	11.975	744.58	1508.4014	

TABLE LXV

EXPERIMENTAL MEASUREMENTS OF N-OCTANOL VISCOSITY WITH A NITROGEN ATMOSPHERE

Run	Cell Temperature, mV	Gauge Pressure, mV	Atmospheric Pressure, mm Hg	Flow Time, seconds	Percent Deviation
		P = 4.804 mV			
1	1.425	4.804	747.7		
	1.470	4.806			
	1.476	4.806		1526.978	-0.269
2	1.480	4.804	747.6		
	1.482	4.802			
	1.485	4.801		1531.761	0.043
3	1.486	4.805	747.6		
	1.479	4.805			
	1.481	4.810		1532.382	0.084
4	1.482	4.803	747.6		
	1.486	4.804			
	1.475	4.801		1532.170	0.070
5	1.476	4.801	747.3		
	1.466	4.802			
	1.467	4.806		1532.220	0.073
Avg	1.474	4.804	747.56	1531.1022	
		P = 8.007 mV			
1	1.466	8.011	744.8		
	1.472	8.006			
	1.476	8.011		1580.891	-0.600
2	1.516	8.005	744.7		
	1.481	8.008			
	1.520	8.010		1573.310	-1.077
3	1.535	8.003	744.5		
	1.520	8.005			
	1.523	8.008		1601.950	0.724

TABLE LXV (Continued)

Run	Cell Temperature, mV	Gauge Pressure, mV	Atmospheric Pressure, mm Hg	Flow Time, seconds	Percent Deviation
		P = 8.007 mV (Continued)			
4	1.520	8.006	744.5		
	1.536	8.005			
	1.547	8.005		1607.821	1.093
5	1.544	8.005	744.6		
	1.516	8.003			
	1.525	8.008		1588.230	-0.139
Avg	1.513	8.007	744.62	1590.4404	
		P = 11.912 mV			
1	1.407	11.908	752.9		
	1.402	11.910			
	1.410	11.910		1636.055	0.304
2	1.410	11.910	753.1		
	1.410	11.910			
	1.406	11.910		1628.439	-0.163
3	1.410	11.910	753.6		
	1.410	11.914			
	1.409	11.911		1626.964	-0.253
4	1.415	11.913	753.8		
	1.419	11.914			
	1.419	11.913		1632.547	0.089
5	1.415	11.914	753.9		
	1.420	11.916			
	1.509	11.917		1631.452	0.022
Avg	1.418	11.912	753.46	1631.0914	
		P = 11.853 mV			
1	1.457	11.850	753.9		
	1.450	11.851			
	1.450	11.851		1634.151	-0.826

TABLE LXV (Continued)

Run	Cell Temperature, mV	Gauge Pressure, mV	Atmospheric Pressure, mm Hg	Flow Time, seconds	Percent Deviation
		P = 11.853 mV (Continued)			
2	1.453	11.853	753.8		
	1.450	11.852			
	1.446	11.853		1653.799	0.367
3	1.449	11.856	753.9		
	1.444	11.857			
	1.457	11.860		1659.510	0.713
4	1.459	11.854	754.2		
	1.456	11.851			
	1.490	11.850		1657.354	0.583
5	1.462	11.845	754.3		
	1.472	11.856			
	1.465	11.860		1633.953	-0.838
Avg	1.457	11.853	754.02	1647.7534	

TABLE LXVI

EXPERIMENTAL MEASUREMENTS OF N-OCTANOL VISCOSITY WITH A METHANE ATMOSPHERE

Run	Cell Temperature, mV	Gauge Pressure, mV	Atmospheric Pressure, mm Hg	Flow Time, seconds	Percent Deviation
		P = 4.901 mV			
1	1.416	4.900	757.4		
	1.416	4.899			
	1.419	4.896		1407.108	0.232
2	1.420	4.900	757.5		
	1.424	4.900			
	1.425	4.900		1403.934	0.001
3	1.431	4.901	757.8		
	1.415	4.899			
	1.430	4.901		1403.054	-0.057
4	1.424	4.904	757.9		
	1.420	4.900			
	1.430	4.903		1402.683	-0.083
5	1.422	4.904	757.8		
	1.427	4.904			
	1.429	4.902		1402.469	-0.098
Avg	1.423	4.901	757.68	1403.8496	
		P = 7.773 mV			
1	1.429	7.772	751.5		
	1.426	7.775			
	1.435	7.775		1274.441	0.057
2	1.436	7.775	751.5		
	1.439	7.775			
	1.447	7.771		1274.559	0.066
3	1.450	7.775	751.5		
	1.450	7.775			
	1.450	7.774		1272.273	-0.114

TABLE LXVI (Continued)

Run	Cell Temperature, mV	Gauge Pressure, mV	Atmospheric Pressure, mm Hg	Flow Time, seconds	Percent Deviation
		P = 7.773 mV (Continued)			
4	1.454	7.775	751.5		
	1.455	7.770			
	1.456	7.772		1273.550	-0.013
5	1.460	7.770	751.5		
	1.442	7.768			
	1.444	7.767		1273.780	0.005
Avg	1.445	7.773	751.5	1273.7206	
		P = 11.670 mV			
1	1.432	11.673	749.6		
	1.431	11.671			
	1.439	11.670		1147.765	-0.048
2	1.441	11.675	749.4		
	1.445	11.674			
	1.452	11.671		1142.121	-0.540
3	1.453	11.671	749.4		
	1.446	11.670			
	1.450	11.669		1153.202	0.425
4	1.451	11.670	749.4		
	1.455	11.669			
	1.455	11.666		1153.162	0.422
5	1.464	11.664	748.8		
	1.462	11.665			
	1.472	11.666		1145.340	-0.259
Avg	1.450	11.670	749.32	1148.318	

TABLE LXVII

ANALYSIS OF ETHYLENE - PROPYLENE SAMPLE UNDER TEST DURING EQUIPMENT MALFUNCTION

Run	Ethylene Area	Propylene Area	Total Area	Ethylene Fraction	Propylene Fraction
1	432	12773	13205	0.0327	0.9673
2	411	12534	12945	0.0317	0.9683
3	412	12395	12807	0.0322	0.9678
4	417	12642	13059	0.0319	0.9681
5	407	12510	12917	0.0315	0.9685
6	427	12832	13259	0.0322	0.9678
7	406	12572	12978	0.0313	0.9687
8	388	11976	12364	0.0314	0.9686
9	378	11908	12286	0.0308	0.9692
10	401	11966	12376	0.0324	0.9676
11	424	12561	12985	0.0327	0.9673
12	406	12343	12749	0.0318	0.9682
13	419	12313	12732	0.0329	0.9671
14	380	11831	12211	0.0311	0.9689
15	362	11314	11676	0.0310	0.9690
Avg				0.0318	0.9682

VITA[2]

David Duane McCoy

Candidate for the Degree of

Doctor of Philosophy

Thesis: CRITICAL REGION BEHAVIOR AND EFFECT OF PRESSURE ON LIQUID VISCOSITY

Major Field: Chemical Engineering

Biographical:

Personal Data: Born in Boise, Idaho, December 9, 1940, the son of Mr. and Mrs. Stanley E. McCoy.

Education: Graduated from Emmett High School, Emmett, Idaho, in May, 1958; attended The University of Idaho, Moscow, Idaho, 1958-60; received the Degree of Associate of Science from Boise Junior College, Boise, Idaho, May, 1968; received the Degree of Bachelor of Science in Chemical Engineering at Oklahoma State University, Stillwater, Oklahoma, May, 1971; received the Degree of Master of Science in Chemical Engineering at Oklahoma State University, Stillwater, Oklahoma, May, 1973; completed requirements for the Doctor of Philosophy degree in Chemical Engineering at Oklahoma State University, Stillwater, Oklahoma in May, 1976.

Professional Experience: Employed by Kerr-McGee Corporation, Wynnewood, Oklahoma, as technical assistant from May, 1968 till January, 1969 and the summer of 1969; employed by Kerr-McGee Corporation, Cushing, Oklahoma, as a junior plant engineer during the summers of 1970 and 1971.

Membership in Scholarly or Professional Societies: Omega Chi Epsilon, Student Affiliate Member of the American Institute of Chemical Engineers, Associate Member of Sigma Xi.